Title

Klotho and the epigenetic regulation of the Wnt pathway by Jmjd3 in muscle stem cells

Author

McKee, Cynthia Marie

Publication Date

2022

Peer reviewed|Thesis/dissertation

UNIVERSITY OF CALIFORNIA

Los Angeles

Klotho and the epigenetic regulation of the Wnt pathway by Jmjd3 in muscle stem cells

A dissertation submitted in partial satisfaction of the requirements for the degree of Doctor of Philosophy in Molecular, Cellular, and Integrative Physiology

by

Cynthia Marie McKee

2022

ABSTRACT OF THE DISSERTATION

Klotho and the epigenetic regulation of the Wnt pathway by Jmjd3 in muscle stem cells

by

Cynthia Marie McKee

Doctor of Philosophy in Molecular, Cellular, and Integrative Physiology

University of California, Los Angeles, 2022

Professor James G. Tidball, Chair

Skeletal muscle is one of the most abundant tissues in the body because it supports fundamental processes of lifelike movement and breathing. Muscle stem cells, called satellite cells, support muscle development and life-long muscle repair through the activation of the β-catenin-mediated canonical Wnt pathway. Therefore, any changes in the number of satellite cells or in the activation of canonical Wnt signaling can impair myogenesis throughout life. In this dissertation research, we examined the role of the age-related molecule Klotho during early postnatal muscle development by testing the hypothesis that Klotho influences myogenesis through the epigenetic regulation of key genes required for satellite cell-mediated myogenesis. Regulatory pathways that influence muscle growth and repair, like Wnt/β-catenin signaling, are particularly interesting in the context of this work because activation of the Wnt/β-catenin pathway is the limiting step in myogenic differentiation. Through this work we identified a novel pathway that showed Klotho influenced myogenesis through the epigenetic regulation of

canonical *Wnt* genes mediated by the histone 3 lysine 27 (H3K27) demethylase Jmjd3. We showed muscle cells treated with Klotho had reduced *Jmjd3* expression and increased gene repressive H3K27 methylation (H3K27m2/3). Subsequent experiments revealed a reduction of canonical *Wnt* gene expression in muscle cells treated with Klotho and in whole muscles of mice that continuously express elevated *klotho*. We showed satellite cells are particularly responsive to Klotho during early postnatal development, a characteristic that did not occur in adult muscles. Our data revealed muscle cells treated with Klotho and siRNA targeting Jmjd3 did not have additive effects on *Wnt* gene expression indicating that Klotho and Jmjd3 operate in a similar pathway. Immunohistological analysis showed Klotho reduced the proportion of satellite cells with active β-catenin, suggesting Klotho's effects on myogenesis may be caused by reduced Wnt/β-catenin signaling. Next, we developed a mouse model with a satellite cell-specific mutation in the *Jmjd3* gene to test whether knocking down *Jmjd3* in satellite cells of developing muscle would mimic the effects of Klotho on myogenesis and the canonical Wnt pathway. We were surprised to find that muscle-specific Jmjd3 is essential for neonatal survival. Although *Jmjd3* mutant mice died within hours after birth, we confirmed *Jmjd3* mutant mice muscles had reduced expression of the canonical *Wnt* genes identified in prior experiments and immunohistological work showed the proportion of satellite cells with active β-catenin was reduced in the absence of Jmjd3. Collectively, this work showed elevated Klotho and reduced Jmjd3 modulated myogenesis through a similar epigenetic regulatory pathway that influenced β-catenin-mediated canonical Wnt signaling. Of note, our work revealed expression of muscle-specific *Jmjd3* is essential for survival and therefore should continue to be investigated in processes affecting myogenesis.

The dissertation of Cynthia Marie McKee is approved by:

Kenneth A. Dorshkind

Karen Marie Lyons

Thomas M. Vondriska

James G. Tidball, Committee Chair

University of California, Los Angeles

2022

DEDICATION

This dissertation is dedicated to Bear and to Saw.

TABLE OF CONTENTS

FIGURES AND TABLES

CHAPTER II

CHAPTER III

ACKNOWLEDGEMENTS

First, I would like to thank my research advisor and committee chair Dr. James Tidball for allowing me to pursue a complex project that was relatively new to the scope of the laboratory research. As part of a summer research program, I began my research experience in Dr. Tidball's lab in 2015, before officially starting my graduate work. That experience was a helpful introduction to my time at UCLA. Although I enjoyed my research rotations, I was delighted to return to Dr. Tidball's lab to conduct my graduate work. I appreciate the academic and research guidance I received from Dr. Tidball during my tenure in his lab. For example, Dr. Tidball tirelessly taught me technical writing skills, by going line-by-line through my fellowship applications, by including me in the grant writing process, and during the editing of our manuscript. On a personal note, I am grateful for the empathy Dr. Tidball showed me after my father passed away. This action highlighted the importance of always treating your team with kindness and respect.

It has been a privilege to have Dr. Kenneth Dorshkind, Dr. Karen Lyons, and Dr. Thomas Vondriska be a part of my doctoral committee. Their valuable input and thought-provoking questions during our meetings strengthened the rigor and scope of this project. Thank you to Dr. Vondriska and his team, Dr. Douglas J. Chapski, and Dr. Manuel Rosa-Garrido for your mentorship and collaboration.

To my current and former lab mates, it was an honor to work alongside you during this amazing time in my life. Particularly, thank you to Dr. Michelle Wehling-Henricks for supporting me as I navigated the trials and tribulations of this project as a Ph.D. trainee. Although Michelle has her own projects and significant responsibilities in the lab, she always made time to train me, answer my endless questions, and explain her answers in a way that left no ambiguity. Plus, she has great vegan recipe ideas! For all of that and more, I am forever grateful. To Suchita

Kumar, I am thankful that we had the time to work closely together and that we could talk through my crazy ideas. Your contribution to the project and the lab environment was vital. You are appreciated!

I also want to recognize the important professional mentors in my life that had a profound impact on the success I find today. First, Dr. Mark Frye has been an incredible leader and mentor who supported and guided me through the complexities of graduate school. His continuous encouragement reinforced the importance of self-trust, self-worth, and sharing my perspectives even if they were not the norm. Mark encouraged me to follow my heart and to do what was best for my personal and professional development. His advice, though not always easy to follow, is largely why I made it to this point. Next, Dr. Andrew Voss gave me a chance to join his lab when I had no experience, no scientific training, and no true understanding of what it meant to do research. Andy was my first research mentor, the one who sat me down to have a serious discussion about a career in science, and the one who shipped me off to UCLA as an undergraduate to learn techniques I could not learn at Cal Poly. Thank you, Andy, for seeing my potential and for challenging me to build a career in physiological science. I want to give a special shoutout to Dr. Bonnie Burns-Whitmore who held me up when I experienced personal difficulties that impacted my academics. The trust and faith you put in me will never be forgotten. Lastly, many thanks to Dr. Robert Talmadge for allowing me to finish my undergraduate research in his lab and for allowing me to pursue my research interests while also contributing to the larger-scale projects in his lab. Bob encouraged my scientific creativity and curiosity. I aspire to be a mentor like Bob, who lets his mentees fly while gently guiding their path.

It is also important to recognize the predoctoral research training programs that supported my undergraduate education and early career development. First, the Ronald E. McNair

Postbaccalaureate Achievement Program by the U.S. Department of Education prepares first-generation and underrepresented students for doctoral studies and scholarly activities. Second, the Lewis Stokes Alliances for Minority Participation (LSAMP) Research Apprentice program by the National Science Foundation that supports minorities in STEM fields. Finally, the Sally Casanova Scholars Pre-Doctoral Program was named after Dr. Sally Casanova and is awarded by California State University.

The work presented in Chapter II was completed under the guidance of James G. Tidball and is a version of "McKee CM, Chapski DJ, Wehling-Henricks M, Rosa-Garrido M, Kuro-o M, Vondriska TM, and Tidball JG. The anti-aging protein Klotho affects early postnatal myogenesis by downregulating Jmjd3 and the canonical Wnt pathway. *FASEB J.* 2022;00:e22192. doi:10.1096/fj.202101298R." The experimental design of this work was done by Cynthia M. McKee, Douglas J. Chapski, Manuel Rosa-Garrido, Michelle Wehling-Henricks, and James G. Tidball. Experiments and data analysis was completed by Cynthia M. McKee, Douglas J. Chapski, Michelle Wehling-Henricks, and James G. Tidball. The manuscript was prepared by Cynthia M. McKee and James G. Tidball and reviewed by the manuscript authors: Cynthia M. McKee, Douglas J. Chapski, Michelle Wehling-Henricks, Manuel Rosa-Garrido, Makoto Kuro-o, Thomas M. Vondriska, and James G. Tidball. A special thank you to Doug, Manuel, and Tom for your support and valuable collaboration.

The work presented in Chapter III was done under the guidance of James G. Tidball and is comprised of unpublished work and work that was used, in part for the grant proposal titled "Novel mechanisms regulating muscle growth and regeneration: elucidating the Klotho/Jmjd3/Wnt axis" funded by the National Institute of Arthritis and Musculoskeletal and Skin Diseases of the National Institutes of Health (R01AR075768). The experimental design of

this work was done by Cynthia M. McKee and James G. Tidball. Research experiments and data analysis presented in Chapter III were done by Cynthia M. McKee.

Research reported in this dissertation was supported by an F31 fellowship titled “Klotho and the epigenetic regulation of muscle stem cells” from the National Institute of Arthritis and Musculoskeletal and Skin Diseases of the National Institutes of Health (F31AR071782). This work was supported by the following fellowships awarded by the University of California, Los Angeles: T32 Predoctoral Training Grant from the National Institutes of Health for Molecular, Cellular, and Integrative Physiology, Eugene V. Cota-Robles Fellowship, Kenneth I. Shine Educational Endowment Award, and Competitive Edge.

Finally, I would like to share all of the love and gratitude in my heart with my friends and family for the support and belief that a girl from a small town on the northern border, who had her fair share of hills to climb could achieve what, at times, seemed to be impossible. Ron and Joanne, you are a force of encouragement and unconditional support. Thank you for being my educational inspiration and for helping me develop the tools to overcome my learning barriers. To my K-Star, thank you for being the rainbow to my clouds and the giggle behind my laughter. You kept me grounded these last few years and never let me forget who I am. Saw, you are the reason for all that I am and all that I will be. Never forget that you made the right choice in shipping me off to Cali. I appreciate you and Stan for always taking my calls and letting me talk through my thoughts. Bear, you are my fearless protector, my champion, and my guiding light. You are all of the things that are good in the world wrapped up in a beautiful package that I am honored to share this life and journey with. This work would not have been possible without you because, at the end of the day, you were there to make sure life was taken care of so I could follow my dreams. And for that I thank you.

VITA

Education

Ph.D. Candidate, Molecular, Cellular, and Integrative Physiology, UCLA	2015-2022
Bachelor of Science, Human Food and Nutrition, Cal Poly Pomona	2012-2015

Leadership & Professional Experience

Licensing Senior Associate, External R&D, Amgen	2022
Graduate Student Researcher, Lab of Dist. Prof. James Tidball, UCLA	2015-2022
Co-Managing Director, Nucleate Los Angeles	2021-2022
Fellow, MedTech Innovator	2021
Fellow, Pritzker Group Venture Capital	2018

Teaching Experience

Teaching Assistant, Science and Food, Physiological Sciences, UCLA	2017-2019
Certified STEM Tutor, Learning Resource Center, Cal Poly Pomona	2013-2015

Awards & Achievements

F31 NRSA Individual Predoctoral Fellowship, NIH	2018-2021
Kenneth I. Shine Educational Endowment Award	2018-2019
T32 Predoctoral NIH Training Grant: UCLA MCIP	2017-2018
Eugene V. Cota-Robles Graduate Student Fellow	2015-2022
MCIP Research Symposium, 1st place poster	2018
UCLA Anderson Knapp Venture Competition, 1st place	2018
UCLA Competitive Edge Summer Fellow	2015
Sally Casanova California Predoctoral Research Fellow	2014-2016
LSAMP Research Apprentice	2014-2015
Ronald E. McNair Scholar	2013-2015

Publications

1. **McKee CM**, Chapski DJ, Wehling-Henricks M, Rosa-Garrido M, Kuro-o M, Vondriska TM, and Tidball, JG. The anti-aging protein Klotho affects early postnatal myogenesis by down-regulating Jmjd3 and the canonical Wnt pathway. *FASEB J.* 2022;00:e22192. doi:10.1096/fj.202101298R

2. Miranda DR, Wong M, Romer SH, **McKee C**, Garza-Vasquez G, Medina AC, Bahn V, Steele AD, Talmadge RJ, Voss AA. Progressive Cl- channel defects reveal disrupted skeletal muscle maturation in R6/2 Huntington's mice. *J Gen Physiol*. 2017;149(1):55-74. doi:10.1085/jgp.201611603

CHAPTER I:

Introduction:

“Myogenesis and the importance of satellite cells for life-long muscle health”

Regulation of myogenesis is a tightly controlled and dynamic biological process

Skeletal muscle is the most abundant tissue in the body and supports organismal locomotion, posture and breathing. Adult skeletal muscle is remarkably adaptable to physiological requirements during growth, exercise, and in response to injury and it meets those demands with the aid of a population of muscle-derived stem cells, called satellite cells. [1] Satellite cells are regulated by muscle intrinsic factors, by factors excreted by other cells and by interactions with the extracellular matrix. [2] Those regulatory influences on satellite cells determine the state of cell activation, proliferation and differentiation during myogenesis. Therefore, life-long muscle homeostasis largely depends on establishing an adequate satellite cell population during development and the ability of satellite cells to respond to myogenic cues throughout life. [1-3]

Satellite cells of adult homeostatic muscle are in a quiescent state and ubiquitously express the paired box regulatory protein Pax7. [4] In response to myogenic cues, Pax7+ satellite cells activate and upregulate the myogenic transcription factor MyoD. [5] Pax7+/MyoD+ cells can proliferate producing two daughter cells. The progeny cells can re-enter quiescence by downregulating *Myod1* while maintaining *Pax7* expression or terminally differentiate by exiting the cell cycle, downregulating *Pax7* and upregulating terminal myogenic transcription factor myogenin. [6] Terminally differentiated mononuclear muscle cells can fuse to one another forming de novo multinucleated muscle fibers or fuse to an existing myofiber contributing to repair and myonuclear accretion. [7] These myogenic processes continue throughout life and disruptions in normal myogenesis can decrease the quality of life and in some cases result in premature death. [2,8] Therefore, the complex and tightly regulated sequence of events that occurs during early postnatal muscle development, when the adult satellite cell pool is established [9-11] may be particularly important for propagating an adequate satellite cell population capable of contributing to life-long muscle homeostasis. [12]

Myogenic transcription factors and early muscle development

Investigations of embryonic muscle development identified Myf5, MyoD, myogenin and Myf6/MRF4 as the four key myogenic regulatory factors expressed in muscle precursor cells in the myotome, the segment of the somite where embryonic pre-muscle tissue forms. [13] Those four skeletal muscle-specific transcription factors share a basic helix-loop-helix (bHLH) structure, overlapping DNA binding motifs and designated consensus sequences in the regulatory regions of muscle-specific genes. [14] Because these factors are uniquely expressed in muscle tissues and share sequence and functional similarities, muscle biologists have extensively reported on their function during myogenesis and the influence they have each other and downstream myogenic target genes. [15-25] Each of the bHLH myogenic factors has a unique expression pattern and they often accumulate in pairs during embryonic development suggesting functional redundancy within the gene family. Myf5 is first detectable at embryonic day 8 (E8) or 8-days post-conception prior to committed myogenic events in a mouse somite, [26] suggesting Myf5 directs precursor cells toward the myogenic lineage in the dermomyotome. [27,28] *Myog* and *Mrf4* transcripts are detectable by E8.5 - E9.5, [29,30] followed by the upregulation of *Myod1* at E10.5. [29] There is an extensive body of literature reporting some distinct functions of each transcription factor but also functional redundancy. [15-19]

The skeletal muscle of mice with a germline mutation in the genes coding *Myf5* or *Myod1* have no developmental skeletal muscle defects, [15,16] but *Myod1*mutant mice cannot adequately regenerate following muscle injury. [31] *Myod1* mutants express elevated levels of *Myf5* and *Myf5* mutants are born without distal ribs and die soon after birth. [15,16] Furthermore, mice with mutations in *Myod1*and *Myf5* genes survive to term but they are immobile, devoid of all skeletal muscle and die within 3-weeks following birth, suggesting MyoD and Myf5 share redundant functions and that one or both are required for skeletal muscle formation and the propagation of muscle cells during development. [17] The differential expression patterns in the somite suggest

each bHLH muscle transcription factor plays a distinct role in muscle cell lineage progression and migration during embryonic development, [28] while overlapping functionality in fetal and adult myogenesis supports regulatory mechanisms that are more complex. [22,25]

Mutations in the *Myog* gene causes severe muscle abnormalities in mice and, unlike the other single bHLH muscle transcription factors, is neonatally lethal. [18,19,32] When muscle masses are first obvious and distinguishable in the myotome at E12.5, *Myog* mutant tissue lacks basic structural proteins like myosin heavy chain and exhibited obvious fiber disorganization compared to their littermate controls. [19] *Myog*-null mutant mice upregulate a filament protein expressed in early myogenic cells called desmin. Prolonged desmin expression in myoblasts suggests that terminal differentiation was initiated but blocked from progressing in the absence of myogenin. [19]

Unlike germline *Myog*-null mice, *Myog*-null zebrafish are viable making zebrafish a good model to study the effects of myogenin loss during development and adulthood. Ganassi et al. [24] reported adult *Myog*-null zebrafish muscles were smaller than control muscles and had fewer myonuclei per fiber. Zebrafish muscle lacking *Myog* expressed lower levels of the genes coding for the late-stage myogenic fusion proteins *Mymk*, *Mymx* and *Mrf4* but had increased *Pax7* expression and more satellite cells per fiber. [24] Those data indicate the loss of myogenin during muscle development promotes proliferation, inhibits fusion and dysregulates fiber growth in adult muscle.

In vitro studies of cultured satellite cells isolated from adult rodent muscle lacking myogenin had no change in the mRNA levels of *Myf5*, *Myod1* or *Mrf4* under proliferation conditions but had significantly higher expression of the same genes under differentiation conditions. [33] The depletion of *Myog* in mice muscles after embryonic development had little effect on muscle

histological analysis, although *Myod1* and *Mrf4* transcripts were increased, [34] agreeing with prior *in vitro* studies. [33] The effects of myogenin on myogenesis was also studied in *mdx* mice, the model for Duchenne muscular dystrophy. [35] Dystrophic muscle undergoes continuous cycles of skeletal muscle degeneration and regeneration making it a good model to study muscle repair. [8,35] Knocking down *Myog* in adult dystrophic muscle had no effect on the regenerative pathway and unexpectedly reduced muscle fatigue likely by upregulating nNOS, [36] a pathway known to attenuate dystrophic pathology. [37] Collectively, the reports on *Myog*-null muscle, [19,24,33,34,36] suggests myogenin is essential for embryonic development but may not be required for adult myogenesis under specific conditions.

Unlike myogenin, the paired box regulatory proteins Pax3 and Pax7 have different requirements during development and in adult myogenesis. For example, Pax3 and Pax7 regulate the expansion, survival and self-renewal capacity of progenitor cells during embryogenesis, [11] but only Pax7 contributes to later stages of developmental myogenesis and all postnatal myogenic events. [4,38-40] Furthermore, the transcription factor activity of Pax3 and Pax7 are mechanistically different and their function depends on the stage of development; Pax3 is essential for regulating the early developmental cell migration and *Myod1* activation, [41-43] whereas Pax7 is primarily expressed in quiescent satellite cells and proliferating myoblasts in postnatal and mature muscle. [4,39]

Pax7-expressing cells are the primary contributors to early postnatal muscle growth

The majority of post-embryonic muscle growth is characterized by extensive Pax7+ cell activity. Pax7 transcripts and protein are abundant in both developmental myoblasts and adult satellite cells making Pax7 the most accepted biological marker for satellite cell identification. It is well understood that Pax7-expressing cells are the primary source of myonuclear accretion during fetal and early postnatal development in rodents and before the age of 18 years old in humans.

[44,45] Although there is an abundance of Pax7+ cells in developing muscle, that number dramatically decreases during the first weeks following birth. [6,46-48]

During the first 4-weeks following birth (P28), 80% of satellite cells in mice muscles were proliferative, [47,49] however by 6-weeks following birth less than 1% of satellite cells were still in the cell cycle and the adult satellite cell pool was established. [50,51] The reduction in proliferating satellite cells was accompanied by a short period of rapid growth between P28 and 6-weeks suggesting many of the proliferative satellite cells terminally differentiated contributing to increased fiber cross-sectional area in a very short period of time. The loss of *Pax7* caused severe muscle abnormalities and like *Myod1*/*Myf5* mutants, mutations in *Pax7* resulted in early postnatal death. [4,38,52] Early developmental investigations of Pax7 revealed reductions in total muscle mass, smaller limb muscle fiber diameter and thin diaphragm muscle in *Pax7*-null mice suggesting the postnatal muscle growth phase is mediated by Pax7+ cells. [4,38,52]

Similar to *Myog*-null mice, *Pax7*-null mutant pups had an abnormal gait and were unable to support themselves because of hindlimb splaying suggesting low levels of Pax7 influences skeletal muscle weakness. [4] Although 90-97% of *Pax7*-null mutant mice died soon after birth, [4,39,52] histological analysis at E18 or 7-days (P7) and 10-days (P10) following birth showed no abnormalities in fiber organization, but the population of Pax7+ satellite cells under the basal lamina was ablated. [4] Therefore, Pax7 is required for some but not all elements of skeletal muscle development and quiescent satellite cells may have different regulatory requirements compared to developmental muscle progenitors [48] but whether Pax7 is required for establishing the adult satellite cells population remains in question. [4,39,48]

While some have shown that abolishing Pax7 depletes satellite cell populations and resulted in premature death, [4,52] others believe that Pax7 is not essential for establishing the satellite cell

lineage or survival but may be required for the propagation and self-renewal potential of satellite cells in adult muscle. [39] Oustanina et al. report 5-10% of *Pax7*-null mutants can survive into adulthood, consistent with previous reports that 90-97% of *Pax7*-null mutants die soon after birth. [4,52] Following muscle injury of the surviving *Pax7*-null population, mononuclear myogenic cells did proliferate as measured by lineage tracing experiments. [39] However, *Pax7* mutants had elevated inflammation, more necrotic fibers and impaired regeneration to the extent that muscles never fully recovered following injury. [39] These data indicate Pax7 is required for the propagation and self-renewal capacity of satellite cells and normal muscle regeneration in adult muscle.

Postnatal muscle growth is a particularly dynamic and important period in determining life-long muscle function. Although muscle injury primarily occurs at later stages of life and the contributions of Pax7+ cells to muscle regeneration remain controversial, Lepper and colleagues hypothesized that inhibiting *Pax7* during postnatal development would significantly impact the regenerative capacity of developing muscle. Lepper et al. reported conditionally inactivating *Pax7* between P7-11 or P14-18 severely inhibits regeneration, whereas *Pax7* inhibition between P21-24 has little effect on regenerative capacity suggesting Pax7 is crucial for early postnatal myogenesis. [48] Furthermore, conditional mutants have more active myogenic cells and extended periods of myofiber fusion suggesting Pax7 is required for a state of quiescence. Additional lineage tracing experiments of uninjured muscle show that myofiber fusion sharply declines after P21 indicating a transition of myogenic progenitor cells into quiescent satellite cells, [48] consistent with more recent reports. [50,51]

Contributions of Pax7+ cells in adult muscle hypertrophy

Establishing the satellite cell lineage and the ability for satellite cells to self-renew relied on the expression of *Pax7* during neonatal development, [4,48,50,53] but questions remain whether satellite

cells are required for adult muscle growth, also known as muscle hypertrophy. [54,55] For example, McCarthy et al. used a Pax7-DTA conditional ablation mouse model to knockout 90% of Pax7-positive satellite cells in adult skeletal muscle. Following satellite cell ablation, they surgically removed the supporting gastrocnemius and soleus muscles producing synergistic overload on the plantaris muscle. The researchers found no differences in muscle mass or fiber cross-sectional area in overloaded muscles compared to sham-surgery controls, drawing the conclusion that satellite cells are not required for adult muscle hypertrophy. [54] However, this study agreed that satellite cells are required to form *de novo* fibers and to repair damaged fibers, as indicated by centralized nuclei. [54]

In a follow up study Egner et al. utilized the same Pax7-DTA model and induced synergistic overload on the plantaris muscle by surgically removing the distal half of the gastrocnemius and soleus muscles. [55] In contrast to McCarthy el al., Egner et al. reported increased cross-sectional area in overloaded muscles with satellite cells but no change in overloaded muscles with ablated satellite cells, contradicting previous reports. [54,55] Egner et al. argued that including *de novo* and regenerating myofibers, as McCarthy et al. did in their analysis, could skew the hypertrophic data resulting in false negative when comparing the cross-sectional area between the experimental groups. Therefore, Egner at al. excluded newly regenerated fibers as indicated by central nucleation and fibers positive for embryonic myosin heavy chain from the cross-sectional area data. [55] These data indicate synergistic overload does increase the cross-sectional area of muscle with intact satellite cells, but not in overloaded muscle without satellite cells.

Conditional *Pax7* ablation models are also used to examine muscle regrowth following muscle atrophy providing insights into whether satellite cells contribute to adult muscle growth. Jackson et al. ablated Pax7+ cells in adult mice muscles and subjected the mice to a 14-day hindlimb

suspension inducing muscle atrophy. [56] To test the hypothesis that satellite cells contribute to regrowth following atrophy, the researchers allowed a subset of control mice and Pax7-DTA mice to bare weight on their hindlimbs. Jackson et al. concluded that the contribution of satellite cells to muscle regrowth was minimal because there was no increase in muscle wet weights or individually isolated fiber width in reloaded Pax7-DTA muscles compared to controls. They also reported negligible satellite cell fusion by BrdU staining, very few regenerating fibers and no addition of myonuclei in the reloaded groups regardless of the presence or absence of satellite cells, indicating satellite cells play a minimal role in regrowth following atrophy. [56]

Although the contribution of satellite cells to muscle hypertrophy may conflict in the models described above, exercised-induced muscle hypertrophy relies on satellite cells as the primary contributor to muscle fiber growth in rodents and humans. Early investigations indicated that the robust increase in the number of satellite cells following exercise must contribute to nonregenerative muscle growth because fewer than 3% of fibers were damaged following acute resistance training. [57] More recent studies reported increased levels of *Pax7* transcripts and significantly more Pax7+ cells between 24-hours and 72-hours following resistance training compared to untrained muscle. [58,59] The increased number of Pax7+ cells was associated with larger muscle fibers and increased myonuclear density in healthy mice following prolonged physical activity but there was no change in satellite cell-ablated limb muscle. [60-62]

Unlike the voluntarily active limb muscles, the diaphragm is constantly activated in order to drive ventilation. Because the diaphragm is constantly activated, the muscle fiber composition is more oxidative and fatigue-resistant compared to the limb muscle. Like the limb muscles the diaphragm can also contract voluntarily and is subject to age-related and disease-related functional decline. Interestingly, when satellite cells were depleted from young and old diaphragm muscles prior to continuous voluntary wheel running, there was no change in the

cross-sectional area, fiber type distribution or extracellular matrix accumulation regardless of age or physical activity of the mice. [63] However, in the absence of satellite cells the myonuclear density was decreased by 7% in sedentary mice and 19% in exercised aged mice indicating prolonged reductions in satellite cells numbers in the diaphragm muscle may contribute to reduced myonuclear accretion over a lifespan. [63]

Hormones may also affect adult muscle hypertrophy but whether hormones, like testosterone induce muscle growth through satellite cell-mediated mechanisms is mostly unknown. Englund et al. recently tested the hypotheses that testosterone-induced hypertrophy was driven by satellite cell fusion and myonuclear accretion. [64] The group reported the number of Pax7+ cells increased in the soleus and plantaris muscles of mice following implantation of a testosterone-releasing pellet compared to control mice. [64] In addition, the total muscle weight and mean cross-sectional area increased with and without satellite cells in the soleus, plantaris and extensor digitorum longus muscles, [64] suggesting that testosterone-induced muscle hypertrophy is independent of satellite cells. However, myonuclear accretion in response to testosterone treatments was dependent on the presence pf Pax7+ cells, [64] suggesting that myonuclear accretion by satellite cell fusion and fiber hypertrophy are independently regulated, contradicting previous human studies correlating testosterone-induced satellite cell expansion and hypertrophy in young and old males. [65,66] Regardless of perturbations or environmental signaling cues that promote muscle hypertrophy, the evidence indicates Pax7-expressing cells play a critical role in the life-long stability of skeletal muscle.

Epigenetic regulation and myogenesis

Chromatin is located in the nucleus of a cells and is made up of genomic DNA tightly wound around histone proteins. Histone proteins are subject to a diverse set of posttranslational modifications including acetylation, methylation and phosphorylation that affect the ability for

transcriptional machinery to access the regulatory regions of a gene. For instance, trimethylation on lysine 4 of histone 3 (H3K4me3) is associated with gene accessibility and transcription by RNA polymerase II, whereas dimethylation and trimethylation on lysine 27 of histone 3 (H3K27me2/3) make gene regulatory regions inaccessible. [67] The epigenetic processes affecting gene accessibility or repression are conserved in all cell types and are controlled by the "histone code" of inherited epigenetic regulatory elements passed down to cell progeny. [68] The histone code designates cell commitment without changing the genetic sequence. [69,70] With each cell division, inherited epigenetic regulatory elements like H3K4me3 or H3K27me2/3 can modify the self-renewal capacity or cell lineage designation of each daughter cell. In skeletal muscle, satellite cells are subject to changes in epigenetic landscape during cell activation, cell division and in chronological aging during quiescence. [70,71]

Direct effects of epigenetic changes on satellite cell biology

The epigenetic changes in satellite cells occur in response to intrinsic regulatory factors like Pax7, Myf5, MyoD and myogenin and extrinsic factors produced by other cell types. [2,72] Fluctuations in energy and enzyme substrate availability directly influence the epigenetic landscape affecting normal myogenesis. [73,74] For instance, quiescent satellite cells slowly generate enzymatic substrates like nicotinamide adenine dinucleotide (NAD+) through the slow process of oxidative phosphorylation. NAD+ is an essential substrate for the histone deacetylase sirtuin 1 (Sirt1). [75] When satellite cells break quiescence and become activated, there is a metabolic shift from oxidative phosphorylation to glycolysis because of the robust energy requirement of activated and proliferative cells. Because glycolytic metabolism is favored in proliferative Pax7+ cells, the levels of NAD+ are reduced and do not fulfill the essential needs of Sirt1 to function as a H4K16 deacetylase. This caused acetyl groups to accumulate at H4K16 which reduced the downstream activation of muscle-specific genes associated with quiescent satellite cells. [74] Furthermore, a satellite cell-specific mutation in the Sirt1 gene caused

continuous expression of genes associated with myogenic activation and differentiation in uninjured muscle. [74]

Although some evidence indicates the importance H4K16 acetylation in maintaining quiescence, shifts in H3K27 methylation are required for later stages of myogenesis. Changes in H3K27 methylation is governed by two distinct and opposing enzymatic reactions. H3K27 methyltransferase Ezh2 and regulatory protein Jarid2 are part of the Polycomb Repressive Complex 2 (PRC2) which adds methyl groups to H3K27 causing gene repression. [76-78] Ezh2 and Pax7 are co-expressed in satellite cell and upon differentiation *Ezh2* and *Pax7* are downregulated identifying Ezh2 and elevated H3K27 methylation as regulatory checkpoints for terminal differentiation. Furthermore, a satellite cell-specific depletion of *Ezh2* reduced Pax7+ cells and overall muscle masses in postnatal muscle. [77,79] Knockdown of *Ezh2* in satellite cells prior to muscle injury delayed muscle regeneration and reduced the expansion of Pax7+ cells. [77,79] Although Jarid2 does not have an enzymatic function in the PRC2 complex, Jarid2 remains important for myogenesis because depleting *Jarid2* in Pax7-expressing cells blocks the β-catenin-mediated upregulation of MyoD required for satellite cell activation and differentiation. [78]

Utx is required for adult muscle regeneration

Contrasting the repressive nature of the PRC2 complex, Utx (KDM6A) and Jmjd3 (KDM6B) H3K27 demethylases permit transcriptional activation essential for differentiation. [80,81] The importance of H3K27 demethylation in myogenesis has been established using a satellite-cell specific depletion of *Utx* in an acute injury model. [82] Similar to the negative effects of the muscle-specific deletion of *Ezh2* on regeneration, depleting *Utx* prior to muscle injury in Pax7+ cells blocked regeneration, likely because *Myog* was downregulated. [82] Although some showed Utx as a key regulator of embryonic development and of myogenin *in vitro*, [83-85] others reported

Utx is not required for developmental myogenesis *in vivo* [82] and had no effect on myogenic transcription factor expression in pluripotent stem cells. [82,86]

The effects of Jmjd3 on myogenesis are unclear

Despite the in-depth understanding of Utx in myogenesis, less is known about the contributions of Jmjd3 to myogenesis. Similar to Pax7 and myogenin germline mutants, mutations in the *Jmjd3* gene are neonatally lethal. [87] Although, Faralli et al. reported that the reduced expression of Jmjd3 in satellite cells did not affect regeneration in adult muscle, [82] Rando and colleagues showed quiescent satellite cells of young muscle expressed high levels of *Jmjd3* and had less overall H3K27me3. [71] Alternatively, activated satellite cells of young muscle downregulated *Jmjd3*, upregulated *Ezh2* and had more H3K27me3 accumulation. [71] Together, these two studies suggest young muscle may be more susceptible to changes in Jmjd3 compared to mature, adult muscle.

Furthermore, ectopic expression of *Jmjd3* in human pluripotent stem cells induces *Pax7* expression and *Jmjd3* overexpression followed by *MyoD* overexpression upregulated *myogenin*. [86,88] Therefore, Jmjd3 could be required for establishing early Pax7+ cell populations and for myogenic differentiation in fetal muscle tissue, a timepoint in development when MyoD is available in proliferating myogenic cells. Furthermore, Jmjd3 can indirectly influence myogenesis because serves a distinct role in inflammatory cells which are upregulated following acute injury and required for whole tissue regeneration. [89-93] Therefore, Jmjd3 may also promote myogenic events through alternative, non-muscle pathways.

Molecular signaling pathways and myogenesis

Downstream of the epigenetic changes regulating myogenic transcription factor expression are the molecular signaling pathways that promote specific myogenic events. For example, Notch

signaling critically influences progenitor cell designation, [94] whereas the Wnt signaling pathway is essential for cell differentiation during embryonic development. [95] In adult myogenesis, Notch signaling regulates satellite cells self-renewal capacity, [96] whereas Wnt signaling influences proliferation and differentiation. [97,98] In fact, the transition from proliferative myoblasts to differentiated myogenic cells is dependent on the downregulation of Notch and the upregulation of Wnt, suggesting the progression of myogenesis is regulated my cross-talk between the two pathways. [99] Interestingly, age-related aberrant Notch and Wnt signaling is associated with the age-related decline in satellite cell function. [100-104]

Wnt signaling is essential for myogenesis

The Wnt signaling pathway is an indispensable, conserved mechanism used for intercellular communication in all multicellular animals. The binding of Wnt ligands to Frizzled receptors on the cell surface activates a Wnt cascade on the inside a cell affecting many biological processes in a variety of tissues including skeletal muscle. Activation of specific Wnt signaling cascades depends on the Wnt ligand-receptor interaction and is classified as either β-catenin-dependent canonical Wnt signaling or β-catenin-independent noncanonical signaling. [105] Some Wnts, like Wnt4 can activate both β-catenin-dependent and β-catenin-independent Wnt cascades, [106-109] while Wnt1, Wnt3a and Wnt5a primarily activate canonical Wnt signaling. [110]

In the absence of canonical Wnt activation by Wnt1, Wnt3a or other canonical Wnts, cytoplasmic β-catenin is bound to a degradation complex including a scaffolding protein Axin, glycogen synthase kinase 3 (GSK-3), adenomatous polyposis coli (APC), casein kinase 1 (CK1), and the ubiquitin ligase β-TrCP. [111] When canonical Wnts bind to the Frizzled receptor complex, the β-catenin degradation complex is inactivated subsequently releasing β-catenin and

recruiting Axin to the Fizzled receptor complex. [111,112] Free β-catenin translocates to the nucleus of a cell to activate myogenic Wnt target genes. [113]

Precise Wnt activation is required during the formation of embryonic tissue. In the somite different Wnts can activate myogenesis through canonical and noncanonical pathways. For example, canonical Wnt1 preferentially activates myogenesis through a Myf5-dependent pathway in the axial structures of newly formed somite, whereas noncanonical Wnt7a activates through a MyoD-dependent pathway in dorsal structures. [114] Wnt4, Wnt5a and Wnt6 equally activate *Myf5* and *Myod1* in the paraxial mesoderm. [114] Furthermore, *Wnt1* and *Wnt3a* mutant mice embryos lack the medial compartment of the dermomyotome shown by the reduced size of the Pax3 and Myf5 expression domains. [115] In addition, recombination of the β-catenin gene in Pax3-expressing cells abolished the development of embryonic myoblasts and blocked the progression of developmental myogenesis. [116] Conversely, transplanted cells expressing Wnt1 and Wnt3a promote Pax3 expression and the expansion of the dermomyotome in chick embryos. [111] Cultured somite cells treated with Wnt1, Wnt3 or Wnt4 but not Wnt7a upregulated *Myod1* and a gene coding for myosin heavy chain. [117,118] Together, these studies indicate an essential function of canonical Wnt signaling in muscle development before birth.

Wnt proteins are also essential for adult myogenesis because many Wnts are upregulated after muscle damage and modulate the expression of key myogenic transcription factors needed for muscle repair. [97,98] Muscle regeneration is triggered by injury-induced exercise, disease or toxicity. Following injury, circulating immune cells are recruited to the site of damage to remove waste products from impaired myofibers. Subsequent populations of immune cells secrete anti-inflammatory cytokines known to facilitate satellite cell proliferation and differentiation. [119]

Although Wnt signaling in healthy adult muscle is not well defined, [98] Wnt activation in regenerative muscle has been extensively studied. [99,107,108,110,120,121]

In response to injury, quiescent satellite cells activate following the downregulation of Wnt4. [107,108] Activated myoblasts proliferate and migrate to the site of injury, through the activation of noncanonical Wnt7a promoting muscle hypertrophy. [122] Simultaneous activation of the β-catenin target gene *Axin2* suggests canonical Wnt signaling is also activated during regeneration. [99,110] Although, canonical Wnt3a and Wnt5a are upregulated during muscle repair, [98] it is plausible that Wnt9a and Wnt10a also promote myogenesis because they are known activators of the canonical Wnt pathway. [123-126] Canonical Wnt signaling can also be modulated by the age-related protein, Klotho. [127,128] Interestingly, recent work investigating the effects of Klotho on myogenesis reveal augmented Wnt/β-catenin signaling when *klotho* is genetically manipulated, [129,130] providing some evidence that age-related signaling influences satellite cells biology in adult muscle, but does not give any evidence related to Klotho and Wnt signaling during developmental myogenesis.

Klotho promotes satellite cell population expansion and the regenerative capacity of muscle

Klotho is an age-related gene with high expression in the kidney, brain, ovaries, and skeletal muscle. [131] Klotho protein protects from oxidative stress, and influences proliferation and differentiation. [130-134] Two distinct transcripts arise from the single *klotho* gene through RNA splicing. The full-length gene encodes a single-pass transmembrane protein and the splice variant encodes a truncated secreted protein with hormone functions. [135] Full-length Klotho, also known as α-Klotho forms a co-receptor with FGFR1-4 when FGF growth hormones bind to their receptors eliciting an intracellular response. [131,136,137] The extracellular domain of α-Klotho can be cleaved, generating soluble Klotho which is released into circulation to act as a hormone,

thereby mimicking the truncated secreted form of Klotho generated by alternative splicing. [136,138,139]

The natural age-related decline of systemic Klotho affects all nine hallmarks of aging: epigenetic alternations, cellular senescence, altered intracellular communication, telomere attrition, nutrient sensing deregulation, mitochondrial dysfunction, stem cell exhaustion, loss of proteostasis and genomic instability. [140-142] Mutations in the *klotho* gene accelerate the age-related degeneration of susceptible tissues like skeletal muscle and overexpressing *klotho* promotes systemic tissue longevity and lifespan. [131,138] Because Klotho levels are highest in young tissues and Klotho deficiency is linked to all aspects of aging, it is plausible that Klotho also influences process of tissue development and regeneration.

Multiple investigations suggest Klotho can modulate stem cell biology. First, *klotho*-deficient mice have significant skin atrophy and fewer hair follicles than control mice. [131] Like skeletal muscle, skin and hair follicle microenvironments have a population of tissue resident stem cells that support turnover but are also subject to age-related functional decline. [128,143] Examination of the skin and hair follicles of *klotho*-deficient mice revealed fewer stem cells, increased cell senescence and aberrant Wnt signaling. [128] Second, *klotho* is epigenetically silenced at the pathological onset of dystrophic muscle when satellite cells are needed to aid in muscle regeneration. [144] The absence of *klotho* in dystrophic muscle was associated with fewer Pax7+ satellite cells, reduced muscle regeneration, severer pathology and shortened lifespan. But genetically increasing *klotho* expression in mdx mice dampened the severity of the disease, promoted the accumulation of satellite cells and increased the lifespan. [144,145] Third, myofibers isolated from *klotho*-deficient mice had fewer satellite cell clusters per myofiber, a characteristic that was rescued by treating fiber cultures with recombinant Klotho protein. [129] The negative effect of *klotho*-deficiency on satellite cell clusters reduced the regenerative capacity of injured

skeletal muscle because there was more fibrotic tissue and calcification in damaged *klotho*-deficient muscle compared to control muscle. [129] Finally, endogenous Klotho supports normal muscle repair because *klotho* expression increased 385% following acute injury when compared to non-injured muscle. [104,130] Furthermore, Klotho transgenic mice that overexpress the *klotho* gene had more Pax7+ cells as soon as 3-days following acute injury, which likely promoted the accelerated fiber growth observed at 7-days and 21-days. [130] Collectively, those studies [128-130,144,145] show that manipulating systemic levels of Klotho affects stem cells in multiple tissues.

Klotho's effects on Wnt signaling

Several reports indicate that Klotho influences the Wnt pathway in multiple tissues and cell types including skeletal muscle. [128-130,146-148] Previous investigators have shown that Klotho can bind to Wnt1, Wnt3a, Wnt4, Wnt5a and Wnt7a in renal cells *in vitro* and block β-catenin activation in the kidney *in vivo*. [128,146,148] Muscle fibers isolated from adult mice and treated with recombinant Klotho protein had reduced Wnt signaling, which was attributed to the binding of extracellular Wnt ligands. [129] Furthermore, the active form of β-catenin was downregulated in Pax7+ cells and on the surface of myofibers, which was reflected in the downregulation of β-catenin target genes 3-days following acute muscle injury. [130] The preceding work that reported Klotho modulated the Wnt pathway in muscle cell cultures [129] and in adult muscles [130] provides evidence that Klotho may also attenuate Wnt signaling in developmental myogenesis.

Conclusions

In summary, H3K27 methylation has been shown to be an important posttranslational modification regulating muscle development and regeneration. [76,82,83,86,149,150] Aberrant changes in epigenetic modifications are associated with the dysregulation of essential developmental pathways, muscle disease progression and early death. [87,144,151] Specifically, the silencing of the

H3K27 demethylase Jmjd3 is associated with reduced β-catenin signaling in pre-muscle embryonic tissue and caused certain perinatal death. [87,152] Thus, the effects of Jmjd3 on the Wnt pathways and downstream β-catenin signaling can have detrimental effects on muscle development and life-long muscle homeostasis. Several groups have explored the effects of Klotho on stem cells, muscle and the Wnt pathway. Mice lacking Klotho exhibit accelerated muscle aging [131] and serum Klotho is associated with changes muscle strength, endurance and daily activities in humans. [153,154] Furthermore, *klotho*-null mice have smaller myofibers and fewer satellite cells compared to healthy mice. [129] *Klotho* is upregulated following muscle injury [130] and in the absence of Klotho satellite cells are unable to contribute to muscle repair. [129,144] Conversely, mice with elevated Klotho have larger myofibers following acute muscle injury. [130] To date, the only known mechanism for Klotho's effects on Wnt-mediated myogenesis is by binding extracellular Wnt proteins, thereby inhibiting downstream β-catenin signaling. [129,130] Importantly, *klotho* is reduced in multiple terminal chronic diseases, including Duchenne muscular dystrophy and overexpressing *klotho* in dystrophic muscle reduces dystrophic pathology and prolongs life. [140,144,145] Together, this highlights the significance of investigating the potential epigenetic regulatory mechanisms influencing Klotho and the Wnt pathway during developmental myogenesis.

Specific aims

In this investigation, we examined the role of Klotho during early postnatal skeletal muscle development and Klotho's influence on the epigenetic state of satellite cells by addressing the following specific aims:

Aim 1: We tested whether Klotho influences muscle cell activation and differentiation though the suppression of the histone demethylase Jmjd3.

Aim 2: We determined if change in Jmjd3 expression in the presence of Klotho influenced the methylation state of lysine 27 on histone 3.

Aim 3: We investigated whether manipulating Klotho during postnatal skeletal muscle development affected Jmjd3 expression and localization in myogenic progenitor cells.

Aim 4: We tested whether a muscle-specific mutation of Jmjd3 would mimic the effects of Klotho on early postnatal muscle development.

References

1. Dhawan J, Rando TA. Stem cells in postnatal myogenesis: molecular mechanisms of satellite cell quiescence, activation and replenishment. *Trends Cell Biol*. Dec 2005;15(12):666-73. doi:10.1016/j.tcb.2005.10.007

2. Dumont NA, Wang YX, Rudnicki MA. Intrinsic and extrinsic mechanisms regulating satellite cell function. *Development*. May 2015;142(9):1572-81. doi:10.1242/dev.114223

3. Cornelison D. "Known Unknowns": Current Questions in Muscle Satellite Cell Biology. *Curr Top Dev Biol*. 2018;126:205-233. doi:10.1016/bs.ctdb.2017.08.006

4. Seale P, Sabourin LA, Girgis-Gabardo A, Mansouri A, Gruss P, Rudnicki MA. Pax7 is required for the specification of myogenic satellite cells. *Cell*. Sep 2000;102(6):777-86. doi:10.1016/s0092-8674(00)00066-0

5. Cornelison DD, Wold BJ. Single-cell analysis of regulatory gene expression in quiescent and activated mouse skeletal muscle satellite cells. *Dev Biol*. Nov 15 1997;191(2):270-83. doi:10.1006/dbio.1997.8721

6. Yin H, Price F, Rudnicki MA. Satellite cells and the muscle stem cell niche. *Physiol Rev*. Jan 2013;93(1):23-67. doi:10.1152/physrev.00043.2011

7. White RB, Biérinx AS, Gnocchi VF, Zammit PS. Dynamics of muscle fibre growth during postnatal mouse development. *BMC Dev Biol*. Feb 2010;10:21. doi:10.1186/1471-213X-10-21

8. Tidball JG, Wehling-Henricks M. Evolving Therapeutic Strategies for Duchenne Muscular Dystrophy: Targeting Downstream Events. *Pediatric Research*. 2004-12-01 2004;56(6):831-841. doi:doi:10.1203/01.PDR.0000145578.01985.D0

9. Gros J, Manceau M, Thomé V, Marcelle C. A common somitic origin for embryonic muscle progenitors and satellite cells. *Nature*. Jun 16 2005;435(7044):954-8. doi:10.1038/nature03572

10. Kassar-Duchossoy L, Giacone E, Gayraud-Morel B, Jory A, Gomès D, Tajbakhsh S. Pax3/Pax7 mark a novel population of primitive myogenic cells during development. *Genes Dev*. Jun 15 2005;19(12):1426-31. doi:10.1101/gad.345505

11. Relaix F, Rocancourt D, Mansouri A, Buckingham M. A Pax3/Pax7-dependent population of skeletal muscle progenitor cells. *Nature*. Jun 2005;435(7044):948-53. doi:10.1038/nature03594

12. Bachman JF, Chakkalakal JV. Insights into muscle stem cell dynamics during postnatal development. *FEBS J*. 2021;10.1111/febs.15856. doi:10.1111/febs.15856

13. Buckingham M, Bajard L, Chang T, et al. The formation of skeletal muscle: from somite to limb. *J Anat*. Jan 2003;202(1):59-68.

14. Olson EN, Klein WH. bHLH factors in muscle development: dead lines and commitments, what to leave in and what to leave out. *Genes Dev*. Jan 1994;8(1):1-8. doi:10.1101/gad.8.1.1

15. Braun T, Rudnicki MA, Arnold HH, Jaenisch R. Targeted inactivation of the muscle regulatory gene Myf-5 results in abnormal rib development and perinatal death. *Cell*. Oct 1992;71(3):369-82. doi:10.1016/0092-8674(92)90507-9

16. Rudnicki MA, Braun T, Hinuma S, Jaenisch R. Inactivation of MyoD in mice leads to up-regulation of the myogenic HLH gene Myf-5 and results in apparently normal muscle development. *Cell*. Oct 1992;71(3):383-90. doi:10.1016/0092-8674(92)90508-a

17. Rudnicki MA, Schnegelsberg PN, Stead RH, Braun T, Arnold HH, Jaenisch R. MyoD or Myf-5 is required for the formation of skeletal muscle. *Cell*. Dec 1993;75(7):1351-9. doi:10.1016/0092-8674(93)90621-v

18. Hasty P, Bradley A, Morris JH, et al. Muscle deficiency and neonatal death in mice with a targeted mutation in the myogenin gene. *Nature*. Aug 1993;364(6437):501-6. doi:10.1038/364501a0

19. Venuti JM, Morris JH, Vivian JL, Olson EN, Klein WH. Myogenin is required for late but not early aspects of myogenesis during mouse development. *J Cell Biol*. Feb 1995;128(4):563-76. doi:10.1083/jcb.128.4.563

20. Zammit PS, Golding JP, Nagata Y, Hudon V, Partridge TA, Beauchamp JR. Muscle satellite cells adopt divergent fates: a mechanism for self-renewal? *J Cell Biol*. Aug 02 2004;166(3):347-57. doi:10.1083/jcb.200312007

21. Zammit PS, Relaix F, Nagata Y, et al. Pax7 and myogenic progression in skeletal muscle satellite cells. *J Cell Sci*. May 2006;119(Pt 9):1824-32. doi:10.1242/jcs.02908

22. Cao Y, Kumar RM, Penn BH, et al. Global and gene-specific analyses show distinct roles for Myod and Myog at a common set of promoters. *EMBO J*. Feb 08 2006;25(3):502-11. doi:10.1038/sj.emboj.7600958

23. Olguin HC, Yang Z, Tapscott SJ, Olwin BB. Reciprocal inhibition between Pax7 and muscle regulatory factors modulates myogenic cell fate determination. *J Cell Biol*. Jun 04 2007;177(5):769-79. doi:10.1083/jcb.200608122

24. Ganassi M, Badodi S, Wanders K, Zammit PS, Hughes SM. Myogenin is an essential regulator of adult myofibre growth and muscle stem cell homeostasis. *Elife*. 2020;9:e60445. doi:10.7554/eLife.60445

25. Adhikari A, Kim W, Davie J. Myogenin is required for assembly of the transcription machinery on muscle genes during skeletal muscle differentiation. *PLoS One*. 2021;16(1):e0245618. doi:10.1371/journal.pone.0245618

26. Ott MO, Bober E, Lyons G, Arnold H, Buckingham M. Early expression of the myogenic regulatory gene, myf-5, in precursor cells of skeletal muscle in the mouse embryo. *Development*. Apr 1991;111(4):1097-107.

27. Buckingham M. Making muscle in mammals. *Trends Genet*. Apr 1992;8(4):144-8. doi:10.1016/0168-9525(92)90373-C

28. Sassoon DA. Myogenic regulatory factors: dissecting their role and regulation during vertebrate embryogenesis. *Dev Biol*. Mar 1993;156(1):11-23. doi:10.1006/dbio.1993.1055

29. Sassoon D, Lyons G, Wright WE, et al. Expression of two myogenic regulatory factors myogenin and MyoD1 during mouse embryogenesis. *Nature*. Sep 28 1989;341(6240):303-7. doi:10.1038/341303a0

30. Bober E, Lyons GE, Braun T, Cossu G, Buckingham M, Arnold HH. The muscle regulatory gene, Myf-6, has a biphasic pattern of expression during early mouse development. *J Cell Biol*. Jun 1991;113(6):1255-65. doi:10.1083/jcb.113.6.1255

31. Megeney LA, Kablar B, Garrett K, Anderson JE, Rudnicki MA. MyoD is required for myogenic stem cell function in adult skeletal muscle. *Genes Dev*. May 15 1996;10(10):1173-83. doi:10.1101/gad.10.10.1173

32. Nabeshima Y, Hanaoka K, Hayasaka M, Esumi E, Li S, Nonaka I. Myogenin gene disruption results in perinatal lethality because of severe muscle defect. *Nature*. Aug 05 1993;364(6437):532-5. doi:10.1038/364532a0

33. Meadows E, Cho JH, Flynn JM, Klein WH. Myogenin regulates a distinct genetic program in adult muscle stem cells. *Dev Biol*. Oct 15 2008;322(2):406-14. doi:10.1016/j.ydbio.2008.07.024

34. Knapp JR, Davie JK, Myer A, Meadows E, Olson EN, Klein WH. Loss of myogenin in postnatal life leads to normal skeletal muscle but reduced body size. *Development*. Feb 2006;133(4):601-10. doi:10.1242/dev.02249

35. Tanabe Y, Esaki K, Nomura T. Skeletal muscle pathology in X chromosome-linked muscular dystrophy (mdx) mouse. *Acta Neuropathol*. 1986;69(1-2):91-5. doi:10.1007/BF00687043

36. Meadows E, Flynn JM, Klein WH. Myogenin regulates exercise capacity but is dispensable for skeletal muscle regeneration in adult mdx mice. *PLoS One*. Jan 14 2011;6(1):e16184. doi:10.1371/journal.pone.0016184

37. Wehling M, Spencer MJ, Tidball JG. A nitric oxide synthase transgene ameliorates muscular dystrophy in mdx mice. *J Cell Biol*. Oct 2001;155(1):123-31. doi:10.1083/jcb.200105110

38. Relaix F, Montarras D, Zaffran S, et al. Pax3 and Pax7 have distinct and overlapping functions in adult muscle progenitor cells. *J Cell Biol*. Jan 02 2006;172(1):91-102. doi:10.1083/jcb.200508044

39. Oustanina S, Hause G, Braun T. Pax7 directs postnatal renewal and propagation of myogenic satellite cells but not their specification. *EMBO J*. Aug 2004;23(16):3430-9. doi:10.1038/sj.emboj.7600346

40. Kuang S, Chargé SB, Seale P, Huh M, Rudnicki MA. Distinct roles for Pax7 and Pax3 in adult regenerative myogenesis. *J Cell Biol*. Jan 2006;172(1):103-13. doi:10.1083/jcb.200508001

41. Tajbakhsh S, Rocancourt D, Cossu G, Buckingham M. Redefining the genetic hierarchies controlling skeletal myogenesis: Pax-3 and Myf-5 act upstream of MyoD. *Cell*. Apr 04 1997;89(1):127-38. doi:10.1016/s0092-8674(00)80189-0

42. Tremblay P, Dietrich S, Mericskay M, Schubert FR, Li Z, Paulin D. A crucial role for Pax3 in the development of the hypaxial musculature and the long-range migration of muscle precursors. *Dev Biol*. Nov 01 1998;203(1):49-61. doi:10.1006/dbio.1998.9041

43. Goulding M, Lumsden A, Paquette AJ. Regulation of Pax-3 expression in the dermomyotome and its role in muscle development. *Development*. Apr 1994;120(4):957-71.

44. Moss FP, Leblond CP. Satellite cells as the source of nuclei in muscles of growing rats. *Anat Rec*. Aug 1971;170(4):421-35. doi:10.1002/ar.1091700405

45. Verdijk LB, Snijders T, Drost M, Delhaas T, Kadi F, van Loon LJ. Satellite cells in human skeletal muscle; from birth to old age. *Age (Dordr)*. Apr 2014;36(2):545-7. doi:10.1007/s11357-013-9583-2

46. Schultz E. A quantitative study of the satellite cell population in postnatal mouse lumbrical muscle. *Anat Rec*. Dec 1974;180(4):589-95. doi:10.1002/ar.1091800405

47. Schultz E. Satellite cell proliferative compartments in growing skeletal muscles. *Dev Biol*. Apr 1996;175(1):84-94. doi:10.1006/dbio.1996.0097

48. Lepper C, Conway SJ, Fan CM. Adult satellite cells and embryonic muscle progenitors have distinct genetic requirements. *Nature*. Jul 2009;460(7255):627-31. doi:10.1038/nature08209

49. Shinin V, Gayraud-Morel B, Gomès D, Tajbakhsh S. Asymmetric division and cosegregation of template DNA strands in adult muscle satellite cells. *Nat Cell Biol*. Jul 2006;8(7):677-87. doi:10.1038/ncb1425

50. Bachman JF, Klose A, Liu W, et al. Prepubertal skeletal muscle growth requires Pax7-expressing satellite cell-derived myonuclear contribution. *Development*. 10 2018;145(20)doi:10.1242/dev.167197

51. Gattazzo F, Laurent B, Relaix F, Rouard H, Didier N. Distinct Phases of Postnatal Skeletal Muscle Growth Govern the Progressive Establishment of Muscle Stem Cell Quiescence. *Stem Cell Reports*. 09 08 2020;15(3):597-611. doi:10.1016/j.stemcr.2020.07.011

52. Mansouri A, Stoykova A, Torres M, Gruss P. Dysgenesis of cephalic neural crest derivatives in Pax7-/- mutant mice. *Development*. Mar 1996;122(3):831-8.

53. Seale P, Ishibashi J, Scimè A, Rudnicki MA. Pax7 is necessary and sufficient for the myogenic specification of CD45+:Sca1+ stem cells from injured muscle. *PLoS Biol*. May 2004;2(5):E130. doi:10.1371/journal.pbio.0020130

54. McCarthy JJ, Mula J, Miyazaki M, et al. Effective fiber hypertrophy in satellite cell-depleted skeletal muscle. *Development*. Sep 2011;138(17):3657-66. doi:10.1242/dev.068858

55. Egner IM, Bruusgaard JC, Gundersen K. Satellite cell depletion prevents fiber hypertrophy in skeletal muscle. *Development*. 08 2016;143(16):2898-906. doi:10.1242/dev.134411

56. Jackson JR, Mula J, Kirby TJ, et al. Satellite cell depletion does not inhibit adult skeletal muscle regrowth following unloading-induced atrophy. *Am J Physiol Cell Physiol*. Oct 2012;303(8):C854-61. doi:10.1152/ajpcell.00207.2012

57. Darr KC, Schultz E. Exercise-induced satellite cell activation in growing and mature skeletal muscle. *J Appl Physiol (1985)*. Nov 1987;63(5):1816-21. doi:10.1152/jappl.1987.63.5.1816

58. Bellamy LM, Joanisse S, Grubb A, et al. The acute satellite cell response and skeletal muscle hypertrophy following resistance training. *PLoS One*. 2014;9(10):e109739. doi:10.1371/journal.pone.0109739

59. Li P, Akimoto T, Zhang M, Williams RS, Yan Z. Resident stem cells are not required for exercise-induced fiber-type switching and angiogenesis but are necessary for activity-dependent muscle growth. *Am J Physiol Cell Physiol*. Jun 2006;290(6):C1461-8. doi:10.1152/ajpcell.00532.2005

60. Abou Sawan S, Hodson N, Babits P, Malowany JM, Kumbhare D, Moore DR. Satellite cell and myonuclear accretion is related to training-induced skeletal muscle fiber hypertrophy in young males and females. *J Appl Physiol (1985)*. 09 01 2021;131(3):871-880. doi:10.1152/japplphysiol.00424.2021

61. Masschelein E, D'Hulst G, Zvick J, et al. Exercise promotes satellite cell contribution to myofibers in a load-dependent manner. *Skelet Muscle*. 07 09 2020;10(1):21. doi:10.1186/s13395-020-00237-2

62. Englund DA, Murach KA, Dungan CM, et al. Depletion of resident muscle stem cells negatively impacts running volume, physical function, and muscle fiber hypertrophy in response to lifelong physical activity. *Am J Physiol Cell Physiol*. 06 2020;318(6):C1178-C1188. doi:10.1152/ajpcell.00090.2020

63. Murach KA, Confides AL, Ho A, et al. Depletion of Pax7+ satellite cells does not affect diaphragm adaptations to running in young or aged mice. *J Physiol*. 10 2017;595(19):6299-6311. doi:10.1113/JP274611

64. Englund DA, Peck BD, Murach KA, et al. Resident muscle stem cells are not required for testosterone-induced skeletal muscle hypertrophy. *Am J Physiol Cell Physiol*. 10 2019;317(4):C719-C724. doi:10.1152/ajpcell.00260.2019

65. Sinha-Hikim I, Roth SM, Lee MI, Bhasin S. Testosterone-induced muscle hypertrophy is associated with an increase in satellite cell number in healthy, young men. *Am J Physiol Endocrinol Metab*. Jul 2003;285(1):E197-205. doi:10.1152/ajpendo.00370.2002

66. Sinha-Hikim I, Cornford M, Gaytan H, Lee ML, Bhasin S. Effects of testosterone supplementation on skeletal muscle fiber hypertrophy and satellite cells in community-dwelling older men. *J Clin Endocrinol Metab*. Aug 2006;91(8):3024-33. doi:10.1210/jc.2006-0357

67. Kouzarides T. Chromatin modifications and their function. *Cell*. Feb 2007;128(4):693-705. doi:10.1016/j.cell.2007.02.005

68. Strahl BD, Allis CD. The language of covalent histone modifications. *Nature*. Jan 2000;403(6765):41-5. doi:10.1038/47412

69. Gottschling DE. Summary: epigenetics--from phenomenon to field. *Cold Spring Harb Symp Quant Biol*. 2004;69:507-19. doi:10.1101/sqb.2004.69.507

70. Moazed D. Mechanisms for the inheritance of chromatin states. *Cell*. Aug 2011;146(4):510-8. doi:10.1016/j.cell.2011.07.013

71. Liu L, Cheung TH, Charville GW, et al. Chromatin modifications as determinants of muscle stem cell quiescence and chronological aging. *Cell Rep*. Jul 2013;4(1):189-204. doi:10.1016/j.celrep.2013.05.043

72. Barreiro E, Tajbakhsh S. Epigenetic regulation of muscle development. *J Muscle Res Cell Motil*. 02 2017;38(1):31-35. doi:10.1007/s10974-017-9469-5

73. Rodgers JT, King KY, Brett JO, et al. mTORC1 controls the adaptive transition of quiescent stem cells from G0 to G(Alert). *Nature*. Jun 2014;510(7505):393-6. doi:10.1038/nature13255

74. Ryall JG, Dell'Orso S, Derfoul A, et al. The NAD(+)-dependent SIRT1 deacetylase translates a metabolic switch into regulatory epigenetics in skeletal muscle stem cells. *Cell Stem Cell*. Feb 05 2015;16(2):171-83. doi:10.1016/j.stem.2014.12.004

75. Imai S, Armstrong CM, Kaeberlein M, Guarente L. Transcriptional silencing and longevity protein Sir2 is an NAD-dependent histone deacetylase. *Nature*. Feb 17 2000;403(6771):795-800. doi:10.1038/35001622

76. Caretti G, Di Padova M, Micales B, Lyons GE, Sartorelli V. The Polycomb Ezh2 methyltransferase regulates muscle gene expression and skeletal muscle differentiation. *Genes Dev*. Nov 2004;18(21):2627-38. doi:10.1101/gad.1241904

77. Juan AH, Derfoul A, Feng X, et al. Polycomb EZH2 controls self-renewal and safeguards the transcriptional identity of skeletal muscle stem cells. *Genes Dev*. Apr 2011;25(8):789-94. doi:10.1101/gad.2027911

78. Adhikari A, Davie J. JARID2 and the PRC2 complex regulate skeletal muscle differentiation through regulation of canonical Wnt signaling. *Epigenetics Chromatin*. 08 2018;11(1):46. doi:10.1186/s13072-018-0217-x

79. Woodhouse S, Pugazhendhi D, Brien P, Pell JM. Ezh2 maintains a key phase of muscle satellite cell expansion but does not regulate terminal differentiation. *J Cell Sci*. Jan 2013;126(Pt 2):565-79. doi:10.1242/jcs.114843

80. Hong S, Cho YW, Yu LR, Yu H, Veenstra TD, Ge K. Identification of JmjC domain-containing UTX and JMJD3 as histone H3 lysine 27 demethylases. *Proc Natl Acad Sci U S A*. Nov 2007;104(47):18439-44. doi:10.1073/pnas.0707292104

81. Agger K, Cloos PA, Christensen J, et al. UTX and JMJD3 are histone H3K27 demethylases involved in HOX gene regulation and development. *Nature*. Oct 2007;449(7163):731-4. doi:10.1038/nature06145

82. Faralli H, Wang C, Nakka K, et al. UTX demethylase activity is required for satellite cell-mediated muscle regeneration. *J Clin Invest*. Apr 2016;126(4):1555-65. doi:10.1172/JCI83239

83. Wang C, Lee JE, Cho YW, et al. UTX regulates mesoderm differentiation of embryonic stem cells independent of H3K27 demethylase activity. *Proc Natl Acad Sci U S A*. Sep 2012;109(38):15324-9. doi:10.1073/pnas.1204166109

84. Welstead GG, Creyghton MP, Bilodeau S, et al. X-linked H3K27me3 demethylase Utx is required for embryonic development in a sex-specific manner. *Proc Natl Acad Sci U S A*. Aug 2012;109(32):13004-9. doi:10.1073/pnas.1210787109

85. Seenundun S, Rampalli S, Liu QC, et al. UTX mediates demethylation of H3K27me3 at muscle-specific genes during myogenesis. *EMBO J*. Apr 2010;29(8):1401-11. doi:10.1038/emboj.2010.37

86. Akiyama T, Wakabayashi S, Soma A, et al. Epigenetic Manipulation Facilitates the Generation of Skeletal Muscle Cells from Pluripotent Stem Cells. *Stem Cells Int*. 2017;2017:7215010. doi:10.1155/2017/7215010

87. Burgold T, Voituron N, Caganova M, et al. The H3K27 demethylase JMJD3 is required for maintenance of the embryonic respiratory neuronal network, neonatal breathing, and survival. *Cell Rep*. Nov 2012;2(5):1244-58. doi:10.1016/j.celrep.2012.09.013

88. Akiyama T, Wakabayashi S, Soma A, et al. Transient ectopic expression of the histone demethylase JMJD3 accelerates the differentiation of human pluripotent stem cells. *Development*. Oct 2016;143(20):3674-3685. doi:10.1242/dev.139360

89. De Santa F, Totaro MG, Prosperini E, Notarbartolo S, Testa G, Natoli G. The histone H3 lysine-27 demethylase Jmjd3 links inflammation to inhibition of polycomb-mediated gene silencing. *Cell*. Sep 2007;130(6):1083-94. doi:10.1016/j.cell.2007.08.019

90. Kruidenier L, Chung CW, Cheng Z, et al. A selective jumonji H3K27 demethylase inhibitor modulates the proinflammatory macrophage response. *Nature*. Aug 2012;488(7411):404-8. doi:10.1038/nature11262

91. Tidball JG, Dorshkind K, Wehling-Henricks M. Shared signaling systems in myeloid cell-mediated muscle regeneration. *Development*. Mar 2014;141(6):1184-96. doi:10.1242/dev.098285

92. Liu PS, Wang H, Li X, et al. α-ketoglutarate orchestrates macrophage activation through metabolic and epigenetic reprogramming. *Nat Immunol*. Sep 2017;18(9):985-994. doi:10.1038/ni.3796

93. Ishii M, Wen H, Corsa CA, et al. Epigenetic regulation of the alternatively activated macrophage phenotype. *Blood*. Oct 2009;114(15):3244-54. doi:10.1182/blood-2009-04-217620

94. Bray SJ. Notch signalling: a simple pathway becomes complex. *Nat Rev Mol Cell Biol*. Sep 2006;7(9):678-89. doi:10.1038/nrm2009

95. Cadigan KM, Nusse R. Wnt signaling: a common theme in animal development. *Genes Dev*. Dec 1997;11(24):3286-305. doi:10.1101/gad.11.24.3286

96. Wen Y, Bi P, Liu W, Asakura A, Keller C, Kuang S. Constitutive Notch activation upregulates Pax7 and promotes the self-renewal of skeletal muscle satellite cells. *Mol Cell Biol*. Jun 2012;32(12):2300-11. doi:10.1128/MCB.06753-11

97. Cossu G, Borello U. Wnt signaling and the activation of myogenesis in mammals. *EMBO J*. Dec 1999;18(24):6867-72. doi:10.1093/emboj/18.24.6867

98. Girardi F, Le Grand F. Wnt Signaling in Skeletal Muscle Development and Regeneration. *Prog Mol Biol Transl Sci*. 01 2018;153:157-179. doi:10.1016/bs.pmbts.2017.11.026

99. Brack AS, Conboy IM, Conboy MJ, Shen J, Rando TA. A temporal switch from notch to Wnt signaling in muscle stem cells is necessary for normal adult myogenesis. *Cell Stem Cell*. Jan 2008;2(1):50-9. doi:10.1016/j.stem.2007.10.006

100. Carlson ME, Hsu M, Conboy IM. Imbalance between pSmad3 and Notch induces CDK inhibitors in old muscle stem cells. *Nature*. Jul 24 2008;454(7203):528-32. doi:10.1038/nature07034

101. Carlson ME, Conboy MJ, Hsu M, et al. Relative roles of TGF-beta1 and Wnt in the systemic regulation and aging of satellite cell responses. *Aging Cell*. Dec 2009;8(6):676-89. doi:10.1111/j.1474-9726.2009.00517.x

102. Biressi S, Rando TA. Heterogeneity in the muscle satellite cell population. *Semin Cell Dev Biol*. Oct 2010;21(8):845-54. doi:10.1016/j.semcdb.2010.09.003

103. Brack AS, Conboy MJ, Roy S, et al. Increased Wnt Signaling During Aging Alters Muscle Stem Cell Fate and Increases Fibrosis. *Science*. 2007;317(5839):807-810. doi:10.1126/science.1144090

104. Sahu A, Mamiya H, Shinde SN, et al. Age-related declines in α-Klotho drive progenitor cell mitochondrial dysfunction and impaired muscle regeneration. *Nat Commun*. 11 2018;9(1):4859. doi:10.1038/s41467-018-07253-3

105. Nusse R. Wnt signaling and stem cell control. *Cell Res*. May 2008;18(5):523-7. doi:10.1038/cr.2008.47

106. Bernardi H, Gay S, Fedon Y, Vernus B, Bonnieu A, Bacou F. Wnt4 activates the canonical β-catenin pathway and regulates negatively myostatin: functional implication in myogenesis. *Am J Physiol Cell Physiol*. May 2011;300(5):C1122-38. doi:10.1152/ajpcell.00214.2010

107. Eliazer S, Muncie JM, Christensen J, et al. Wnt4 from the Niche Controls the Mechano-Properties and Quiescent State of Muscle Stem Cells. *Cell Stem Cell*. 11 2019;25(5):654-665.e4. doi:10.1016/j.stem.2019.08.007

108. Polesskaya A, Seale P, Rudnicki MA. Wnt signaling induces the myogenic specification of resident CD45+ adult stem cells during muscle regeneration. *Cell*. Jun 2003;113(7):841-52. doi:10.1016/s0092-8674(03)00437-9

109. Zhang Q, Pan Y, Ji J, Xu Y, Qin L. Roles and action mechanisms of WNT4 in cell differentiation and human diseases: a review. *Cell Death Discov*. Oct 12 2021;7(1):287. doi:10.1038/s41420-021-00668-w

110. Otto A, Schmidt C, Luke G, et al. Canonical Wnt signalling induces satellite-cell proliferation during adult skeletal muscle regeneration. *J Cell Sci*. Sep 2008;121(Pt 17):2939-50. doi:10.1242/jcs.026534

111. Stamos JL, Weis WI. The β-catenin destruction complex. *Cold Spring Harb Perspect Biol*. Jan 01 2013;5(1):a007898. doi:10.1101/cshperspect.a007898

112. Lustig B, Jerchow B, Sachs M, et al. Negative feedback loop of Wnt signaling through upregulation of conductin/axin2 in colorectal and liver tumors. *Mol Cell Biol*. Feb 2002;22(4):1184-93. doi:10.1128/mcb.22.4.1184-1193.2002

113. Schneider S, Steinbeisser H, Warga RM, Hausen P. Beta-catenin translocation into nuclei demarcates the dorsalizing centers in frog and fish embryos. *Mech Dev*. Jul 1996;57(2):191-8. doi:10.1016/0925-4773(96)00546-1

114. Tajbakhsh S, Borello U, Vivarelli E, et al. Differential activation of Myf5 and MyoD by different Wnts in explants of mouse paraxial mesoderm and the later activation of myogenesis in the absence of Myf5. *Development*. Nov 1998;125(21):4155-62.

115. Ikeya M, Takada S. Wnt signaling from the dorsal neural tube is required for the formation of the medial dermomyotome. *Development*. Dec 1998;125(24):4969-76.

116. Hutcheson DA, Zhao J, Merrell A, Haldar M, Kardon G. Embryonic and fetal limb myogenic cells are derived from developmentally distinct progenitors and have different requirements for beta-catenin. *Genes Dev*. Apr 2009;23(8):997-1013. doi:10.1101/gad.1769009

117. Wagner J, Schmidt C, Nikowits W, Christ B. Compartmentalization of the somite and myogenesis in chick embryos are influenced by wnt expression. *Dev Biol*. Dec 01 2000;228(1):86-94. doi:10.1006/dbio.2000.9921

118. Münsterberg AE, Kitajewski J, Bumcrot DA, McMahon AP, Lassar AB. Combinatorial signaling by Sonic hedgehog and Wnt family members induces myogenic bHLH gene expression in the somite. *Genes Dev*. Dec 01 1995;9(23):2911-22. doi:10.1101/gad.9.23.2911

119. Tidball JG. Regulation of muscle growth and regeneration by the immune system. *Nat Rev Immunol*. Mar 2017;17(3):165-178. doi:10.1038/nri.2016.150

120. Murphy MM, Keefe AC, Lawson JA, Flygare SD, Yandell M, Kardon G. Transiently active Wnt/β-catenin signaling is not required but must be silenced for stem cell function during muscle regeneration. *Stem Cell Reports*. Sep 09 2014;3(3):475-88. doi:10.1016/j.stemcr.2014.06.019

121. Rudolf A, Schirwis E, Giordani L, et al. β-Catenin Activation in Muscle Progenitor Cells Regulates Tissue Repair. *Cell Rep*. 05 2016;15(6):1277-90. doi:10.1016/j.celrep.2016.04.022

122. Bentzinger CF, von Maltzahn J, Dumont NA, et al. Wnt7a stimulates myogenic stem cell motility and engraftment resulting in improved muscle strength. *J Cell Biol*. Apr 14 2014;205(1):97-111. doi:10.1083/jcb.201310035

123. Tanaka S, Terada K, Nohno T. Canonical Wnt signaling is involved in switching from cell proliferation to myogenic differentiation of mouse myoblast cells. *J Mol Signal*. Oct 2011;6:12. doi:10.1186/1750-2187-6-12

124. Zhang W, Xu Y, Zhang L, et al. Synergistic effects of TGFβ2, WNT9a, and FGFR4 signals attenuate satellite cell differentiation during skeletal muscle development. *Aging Cell*. Jun 2018:e12788. doi:10.1111/acel.12788

125. Narita T, Sasaoka S, Udagawa K, et al. Wnt10a is involved in AER formation during chick limb development. *Dev Dyn*. Jun 2005;233(2):282-7. doi:10.1002/dvdy.20321

126. Cawthorn WP, Bree AJ, Yao Y, et al. Wnt6, Wnt10a and Wnt10b inhibit adipogenesis and stimulate osteoblastogenesis through a β-catenin-dependent mechanism. *Bone*. Feb 2012;50(2):477-89. doi:10.1016/j.bone.2011.08.010

127. Kuro-o M, Matsumura Y, Aizawa H, et al. Mutation of the mouse klotho gene leads to a syndrome resembling ageing. *Nature*. Nov 1997;390(6655):45-51. doi:10.1038/36285

128. Liu H, Fergusson MM, Castilho RM, et al. Augmented Wnt signaling in a mammalian model of accelerated aging. *Science*. Aug 2007;317(5839):803-6. doi:10.1126/science.1143578

129. Ahrens HE, Huettemeister J, Schmidt M, Kaether C, von Maltzahn J. Klotho expression is a prerequisite for proper muscle stem cell function and regeneration of skeletal muscle. *Skelet Muscle*. 07 2018;8(1):20. doi:10.1186/s13395-018-0166-x

130. Welc SS, Wehling-Henricks M, Kuro-O M, Thomas KA, Tidball JG. Modulation of Klotho expression in injured muscle perturbs Wnt signalling and influences the rate of muscle growth. *Exp Physiol*. Jan 2020;105(1):132-147. doi:10.1113/EP088142

131. Kuro-o M, Matsumura Y, Aizawa H, et al. Mutation of the mouse klotho gene leads to a syndrome resembling ageing. 10.1038/36285. *Nature*. 11/06/print 1997;390(6655):45-51.

132. Kuro-o M. Klotho as a regulator of oxidative stress and senescence. *Biol Chem*. Mar 2008;389(3):233-41. doi:10.1515/BC.2008.028

133. Yamamoto M, Clark JD, Pastor JV, et al. Regulation of oxidative stress by the anti-aging hormone klotho. *J Biol Chem*. Nov 2005;280(45):38029-34. doi:10.1074/jbc.M509039200

134. Fan J, Sun Z. The Anti-aging Gene Klotho Regulates Proliferation and Differentiation of Adipose-derived Stem Cells. *Stem Cells*. Feb 2016;34(6):1615-1625. doi:10.1002/stem.2305

135. Shiraki-Iida T, Aizawa H, Matsumura Y, et al. Structure of the mouse klotho gene and its two transcripts encoding membrane and secreted protein. *FEBS Lett*. Mar 1998;424(1-2):6-10. doi:10.1016/s0014-5793(98)00127-6

136. Kurosu H, Ogawa Y, Miyoshi M, et al. Regulation of fibroblast growth factor-23 signaling by klotho. *J Biol Chem*. Mar 2006;281(10):6120-3. doi:10.1074/jbc.C500457200

137. Kurosu H, Choi M, Ogawa Y, et al. Tissue-specific expression of betaKlotho and fibroblast growth factor (FGF) receptor isoforms determines metabolic activity of FGF19 and FGF21. *J Biol Chem*. Sep 2007;282(37):26687-95. doi:10.1074/jbc.M704165200

138. Kurosu H, Yamamoto M, Clark JD, et al. Suppression of aging in mice by the hormone Klotho. *Science*. Sep 2005;309(5742):1829-33. doi:10.1126/science.1112766

139. Chen CD, Podvin S, Gillespie E, Leeman SE, Abraham CR. Insulin stimulates the cleavage and release of the extracellular domain of Klotho by ADAM10 and ADAM17. *Proc Natl Acad Sci U S A*. Dec 2007;104(50):19796-801. doi:10.1073/pnas.0709805104

140. Kuro-o M. Klotho in health and disease. *Curr Opin Nephrol Hypertens*. Jul 2012;21(4):362-8. doi:10.1097/MNH.0b013e32835422ad

141. Bian A, Neyra JA, Zhan M, Hu MC. Klotho, stem cells, and aging. *Clin Interv Aging*. 2015;10:1233-43. doi:10.2147/CIA.S84978

142. López-Otín C, Blasco MA, Partridge L, Serrano M, Kroemer G. The hallmarks of aging. *Cell*. Jun 06 2013;153(6):1194-217. doi:10.1016/j.cell.2013.05.039

143. Li L, Clevers H. Coexistence of quiescent and active adult stem cells in mammals. *Science*. Jan 29 2010;327(5965):542-5. doi:10.1126/science.1180794

144. Wehling-Henricks M, Li Z, Lindsey C, et al. Klotho gene silencing promotes pathology in the mdx mouse model of Duchenne muscular dystrophy. *Hum Mol Genet*. 2016;25(12):2465-2482. doi:10.1093/hmg/ddw111

145. Wehling-Henricks M, Welc SS, Samengo G, et al. Macrophages escape Klotho gene silencing in the mdx mouse model of Duchenne muscular dystrophy and promote muscle growth and increase satellite cell numbers through a Klotho-mediated pathway. *Hum Mol Genet*. 2018;27(1):14-29. doi:10.1093/hmg/ddx380

146. Satoh M, Nagasu H, Morita Y, Yamaguchi TP, Kanwar YS, Kashihara N. Klotho protects against mouse renal fibrosis by inhibiting Wnt signaling. *Am J Physiol Renal Physiol*. Dec 2012;303(12):F1641-51. doi:10.1152/ajprenal.00460.2012

147. Komaba H, Kaludjerovic J, Hu DZ, et al. Klotho expression in osteocytes regulates bone metabolism and controls bone formation. *Kidney Int*. 09 2017;92(3):599-611. doi:10.1016/j.kint.2017.02.014

148. Zhou L, Li Y, Zhou D, Tan RJ, Liu Y. Loss of Klotho contributes to kidney injury by derepression of Wnt/β-catenin signaling. *J Am Soc Nephrol*. Apr 2013;24(5):771-85. doi:10.1681/ASN.2012080865

149. Jin W, Peng J, Jiang S. The epigenetic regulation of embryonic myogenesis and adult muscle regeneration by histone methylation modification. *Biochem Biophys Rep*. Jul 2016;6:209-219. doi:10.1016/j.bbrep.2016.04.009

150. Wang AH, Zare H, Mousavi K, et al. The histone chaperone Spt6 coordinates histone H3K27 demethylation and myogenesis. *EMBO J*. Apr 2013;32(8):1075-86. doi:10.1038/emboj.2013.54

151. Burgold T, Spreafico F, De Santa F, et al. The histone H3 lysine 27-specific demethylase Jmjd3 is required for neural commitment. *PLoS One*. Aug 2008;3(8):e3034. doi:10.1371/journal.pone.0003034

152. Ohtani K, Zhao C, Dobreva G, et al. Jmjd3 controls mesodermal and cardiovascular differentiation of embryonic stem cells. *Circ Res*. Sep 2013;113(7):856-62. doi:10.1161/CIRCRESAHA.113.302035

153. Semba RD, Cappola AR, Sun K, et al. Relationship of low plasma klotho with poor grip strength in older community-dwelling adults: the InCHIANTI study. *Eur J Appl Physiol*. Apr 2012;112(4):1215-20. doi:10.1007/s00421-011-2072-3

154. Crasto CL, Semba RD, Sun K, Cappola AR, Bandinelli S, Ferrucci L. Relationship of low-circulating "anti-aging" klotho hormone with disability in activities of daily living among older community-dwelling adults. *Rejuvenation Res*. Jun 2012;15(3):295-301. doi:10.1089/rej.2011.1268

CHAPTER II:

"The anti-aging protein Klotho affects early postnatal myogenesis by down-regulating Jmjd3 and the canonical Wnt pathway"

Cynthia M. McKee[1], Douglas J. Chapski[2], Michelle Wehling-Henricks[3], Manuel Rosa-Garrido[2], Makoto Kuro-o[4], Thomas M. Vondriska[2], and James G. Tidball.[1,3,5] The anti-aging protein Klotho affects early postnatal myogenesis by down-regulating Jmjd3 and the canonical Wnt pathway. *FASEB J.* 2022;00:e22192. doi:10.1096/fj.202101298R

(In press, 20 January 2022)

[1]Molecular, Cellular & Integrative Physiology Program
University of California
Los Angeles, CA 90095

[2]Departments of Anesthesiology, Medicine, Physiology
David Geffen School of Medicine at UCLA
650 Charles Young Dr.
Los Angeles CA 90095

[3]Department of Integrative Biology and Physiology
University of California
Los Angeles, CA 90095

[4]Division of Anti-Aging Medicine
Center for Molecular Medicine
Jichi Medical University
3311-1 Yakushiji
Shimotsuke, Tochigi 329-0498, Japan

[5]Department of Pathology and Laboratory Medicine
David Geffen School of Medicine at UCLA
650 Charles Young Dr.
University of California
Los Angeles, CA 90095

Correspondence:

James G. Tidball
Molecular, Cellular & Integrative Physiology Program
University of California
Los Angeles, CA 90095-1606
Phone: 310-206-3395
Email: jtidball@physci.ucla.edu

ABBREVIATIONS

AEC - 3-amino-9-ethylcarbazole
BAM – Binary Sequence Alignment/Map
BP – Biological processes
ChIP - Chromatin immunoprecipitation
ChIP-Seq - Chromatin immunoprecipitation with sequencing
DAVID - Database for Annotation, Visualization and Integrated Discovery
EFmKL46 - Human elongation factor-1alpha promoter
Ezh2 - Enhancer of zeste 2 polycomb repressive complex 2 subunit
GO - Gene Ontology
H3K27 – Histone 3 lysine 27
H3K27me2/3 – Di-methylated or tri-methylated histone 3 lysine 27
H3K27me3 – Tri-methylated histone 3 lysine 27
Jarid2 - Jumonji, AT rich interactive domain 2
Jmjd3 - Jumonji domain-containing 3, histone lysine demethylase
KEGG - Kyoto Encyclopedia of Genes and Genomes
KL – Klotho
αKL – alpha Klotho
sKL – Soluble KL
KL Tg / KL Tg+ – Klotho transgene
Macs - Model-based analysis of ChIP-Seq
Myog - Myogenin
Myod1 – Myogenic differentiation 1
Pax7 – Paired-box protein 7
PRC2 - Polycomb repressive complex 2
SAM – Sequence Alignment/Map
TSS – Transcriptional start site
UTX - Ubiquitously-transcribed X chromosome tetratricopeptide, histone lysine demethylase
Wnt - Wingless-type MMTV integration site family, member

ABSTRACT

Modulating the number of muscle stems cells, called satellite cells, during early postnatal development produces long-term effects on muscle growth. We tested the hypothesis that high expression levels of the anti-aging protein Klotho in early postnatal myogenesis increase satellite cell numbers by influencing the epigenetic regulation of genes that regulate myogenesis. Our findings show that elevated *klotho* expression caused a transient increase in satellite cell numbers and slowed muscle fiber growth, followed by a period of accelerated muscle growth that leads to larger fibers. Klotho also transcriptionally down-regulated the H3K27 demethylase Jmjd3, leading to increased H3K27 methylation and decreased expression of genes in the canonical Wnt pathway, which was associated with a delay in muscle differentiation. In addition, Klotho stimulation and Jmjd3 down-regulation produced similar but not additive reductions in the expression of Wnt4, Wnt9a and Wnt10a in myogenic cells, indicating that inhibition occurred through a common pathway. Together, our results identify a novel pathway through which Klotho influences myogenesis by reducing expression of Jmjd3, leading to reductions in the expression of Wnt genes and inhibition of canonical Wnt signaling.

INTRODUCTION

The life-long health and function of skeletal muscle can be strongly influenced by a population of muscle stem cells that reside in muscle. These cells, called satellite cells, experience extensive and complex regulation by numerous factors intrinsic to muscle cells, by factors produced by other cells and by interactions with the extracellular matrix.[1] Each of those regulatory influences has direct, immediate effects on satellite cells that determine their state of activation, proliferation and differentiation during muscle development. However, the responses of satellite cells to those signals also have long-term influences on muscle mass and regenerative capacity that can affect the vitality of organisms.[1-3]

Although establishing and maintaining a sufficient population of satellite cells is necessary for normal muscle homeostasis and health throughout life, the period of early postnatal development may be particularly important in determining the life-long function of muscle. The first 28 days following birth (P28) in mice is an especially dynamic period influencing satellite cell numbers and fate. During that period, ~80% of rodent satellite cells are actively proliferating [4,5] but by 6 to 8-weeks of age, fewer than 1% of satellite cells are in the cell cycle[6,7] and the satellite cell pool number is established.[8] Measurements of changes in satellite cell numbers during muscle development and maturation indicate that growth of muscle fibers in mice until ~P21 may be influenced by the number of satellite cells present.[9,10] In addition, the adult numbers of satellite cells and muscle fiber nuclei are largely established in mice by ~P28 [9], although the numbers can be modified in mature organisms by exercise, injury or disease.[11,12] Furthermore, reductions of satellite cell numbers at ~P28 that are caused by limb irradiation produce smaller muscle fibers and fewer myonuclei in mice which persist until the mice are at least 14 months old.[13,14] Thus, factors that regulate satellite cell number and differentiation early in life may have long-term influences on muscle mass and function because maintaining a sufficient pool of satellite cells is necessary for successful muscle regeneration throughout life.[15]

Satellite cell numbers increase when quiescent, non-proliferative satellite cells that express the Pax7 transcription factor become activated to a proliferative population that expresses Pax7 and the transcription factor MyoD. MyoD plays a central role in regulating early stages of muscle differentiation.[16-18] Those Pax7+/MyoD+ cells can continue to proliferate or they can return to a Pax7+/MyoD- quiescent state, or they can withdraw from the cell cycle and express myogenin.[19] Myogenin, also a transcription factor, regulates terminal differentiation of myogenic cells and their fusion into mature muscle fibers.[20,21] Thus, any factor that increases cycling of Pax7+/MyoD+ myogenic cells or inhibits the transition of proliferative myogenic cells to post-mitotic cells could expand satellite cell numbers during early postnatal development.

Several observations suggest that the anti-aging protein Klotho could potentially influence the large, rapid increase of Pax7+ satellite cells in early postnatal myogenesis. First, stimulation of myogenic cells *in vitro* with recombinant Klotho more than doubles their proliferation during a 48-hour period.[12] Also, Klotho hypomorphic mice show large reductions in the number of Pax7+ myogenic cells at P14.[22] In addition, elevated expression of Klotho in dystrophic muscle causes large increases in satellite cells that persist into late stages of pathology, showing a positive relationship between Klotho expression levels and satellite cell numbers.[12] Finally, Klotho expression in healthy skeletal muscle is greatest during early postnatal development (P14) and then rapidly declines [12] over a time course that resembles the reduction of numbers of proliferative satellite cells in postnatal development.[4-7,10]

In this investigation, we test the hypothesis that high levels of Klotho expression in early postnatal myogenesis increase satellite cell numbers, in part, through effects on the epigenetic regulation of genes that regulate myogenesis. We explore a potential role for Klotho in affecting epigenetic regulatory mechanisms that control the transition of myogenic cells from a

proliferative population to a post-mitotic, terminally-differentiated population. For example, changes in expression of enzymes that affect the methylation of lysine 27 on histone 3 (H3K27) located at the regulatory region of specific genes have large influences on myogenic cell proliferation and differentiation. H3K27 methylation can be increased by the polycomb repressive complex 2 (PRC2) which includes the methyltransferase Ezh2 and the regulatory protein Jarid2, leading to gene repression.[23,24] Deletion or inhibition of either Ezh2 or Jarid2 in myogenic cells reduces Pax7+ cell numbers and disrupts satellite cell activation and differentiation.[25] Conversely, UTX (KDM6A) and Jmjd3 (KDM6B) demethylate H3K27 to allow transcriptional activation that is essential for muscle terminal differentiation.[26,27] UTX is an important, positive regulator of myogenin expression *in vitro* [28] and deletion of *Utx* in satellite cells inhibits the expression of myogenin following muscle injury.[29] Perturbing Jmjd3 expression also affects the expression of myogenic transcription factors; the transient, ectopic expression of Jmjd3 in pluripotent stem cells induces expression of Pax7.[30,31] Thus, if Klotho modifies the expression or activity of any of the key epigenetic regulatory enzymes that control myogenesis, the high levels of Klotho expression that occur in early postnatal muscle could play important roles in influencing the numbers and development of satellite cells.

METHODS

Ethical Approval

All experiments involving the use of animals were performed according to the National Institutes of Health Guide for the Care and Use of Laboratory Animals. All protocols were approved by the Chancellor's Animal Research Committee at the University of California, Los Angeles (Animal Welfare Assurance number A-3196).

Mice

C57 BL/6 (wild-type/Wt mice) were purchased from The Jackson Laboratory (Jax Labs, Bar Harbor, ME, USA) and transgenic mice overexpressing Klotho (KL Tg+) were generously gifted by Dr. Makoto Kuro-o. The *klotho* transgene is under the control of the constitutively expressed human elongation factor-1alpha promotor (EFmKL46). Mice over-expressing Klotho were back-crossed on to the C57 BL/6 background and were genotyped at weaning to ensure the presence of the *klotho* transgene. Mice were housed in a specific pathogen-free facility under 12-hour light and dark cycles. Only male mice were used in these studies. Mice were euthanized by inhalation of isoflurane and weighed prior to muscle collection. Individual muscles were collected, weighed and flash-frozen for subsequent RNA isolation or histological analysis. Experimental group size ranges from 4-5 mice per group.

Muscle fiber cross-sectional area

Frozen quadriceps muscles were cross-sectioned at the midbelly and stained for 10 minutes with hematoxylin followed by three, double-distilled H_2O rinses. Fiber cross-sectional area measurements were taken for no fewer than 500 fibers for each section analyzed. Fibers were sampled from five or more separate locations within the muscle cross-section and digitally measured using ImageJ.[32,33] Classification of small and large fibers was determined by setting

three standard deviations from the mean cross-sectional area for the control group and quantifying the percent of fibers that fell within those ranges.[34,35]

RNA isolation and quantitative PCR

Whole muscle tissue was mechanically homogenized (Dupont, Wilmington, DE, USA) in Trizol (Invitrogen, Waltham, MA, USA). RNA was extracted with chloroform and precipitated with isopropanol. RNA was DNase-treated and purified with RNeasy Mini Kit (Qiagen, Hilden, Germany) according to manufacturer's protocol. Total RNA was quantified by spectrophotometry (Beckman, Brea, CA, USA) at 260 nm absorbance. RNA samples used for analysis had a concentration greater than or equal to 0.2 µg/µl and absorbance ratio of 1.8 or higher. RNA quality was determined by the clear separation of 28S and 18S ribosomal RNA by electrophoresis. 2 µg of total RNA was reverse transcribed with Super Script Reverse Transcriptase II (Invitrogen, Waltham, MA, USA) using Oligo$(dT)_{12\text{-}18}$ Primers (Invitrogen, Waltham, MA, USA) for product extension. cDNA was used to measure the expression for the genes of interest using SYBR Green qPCR Master Mix (Bio-Rad, Hercules, CA, USA) or iTaq Universal SYBR Green Supermix (Bio-Rad, Hercules, CA, USA). Real-time quantitative PCR was performed on an iQ5 thermocycler system with optical system software (Bio-Rad, Hercules, CA, USA) or on a QuantStudio 5 system (Thermo Fisher, Waltham, MA, USA). To increase scientific rigor and because genes used to normalize qPCR data can vary with age, disease or treatments,[36-38] we empirically determined that Srp14, Hprt1 and Rnps1 were suitable reference genes based on methods previously described.[39] The normalization factor for each sample was calculated using the geometric mean of the Ct-values measured from the reference genes. The highest relative expression value for each gene was set to 1 and all other expression values were scaled accordingly. QPCR primer sequences are listed in Table 2.1.

Table 2.1.

Gene	Forward	Reverse
Axin2	GACGCACTGACCGACGATTC	CTGCGATGCATCTCTCTCTGG
Ccnd1	CGAGGAGCTGCTGCAAATG	GGGTTGGAAATGAACTTCACATC
Ezh2	CTGCTGAGCGTATAAAGACAC	CTTAGAGGAGCTGGACGT
Fzd3	GGAACGCTGCAGAGAGTATCAC	GGAATCCCAACTATGAGAGCC
Fzd9	TGTGTTGGTACCCCTATCTTGC	CTTCTCCAGCTTCTCCGTATTG
Hprt1	GCAAACTTTGCTTTCCCTGG	ACTTCGAGAGGTCCTTTTCACC
Jarid2	GGTCTGCTCAGGACTTACGG	TTGGGTTTGGTTTCCTTGAC
Jmjd3	AGTGAGGAAGCCGTATGCTG	AGCCCCATAGTTCCGTTTGTG
Klotho	GTCTCGGGAACCACCAAAAG	CTATGCCACTCGAAACCGTC
Myod1	GAGCGCATCTCCACAGACAG	AAATCGCATTGGGGTTTGAG
Myog	CCAGTACATTGAGCGCCTAC	ACCGACTCCAGTGCATTGC
Pax7	CTCAGTGAGTTCGATTAGCCG	AACGGTTCCCTTTGTCGC
Rnsp1	AGGCTCACCAGGAATGTGAC	CTTGGCCATCAATTTGTCCT
Srp14	AGAGCGAGCAGTTCCTGAC	CGGYGCTGATCTTCCTTTTC
Wnt4	GAGAAGTTTGACGGTGCCAC	GTCCTCATCTGTATGTGGCTTG
Wnt9a	GACTTCCACAACAACCTCGTG	AGGAGCCAGACACACCATG
Wnt10a	CGAATGAGACTCCACAACAACCG	CGTGGCATTTGCACTTACGC
Utx	GGTGCTTTATGTCGATCCCAG	CAGCATTGGACAAAGTGCAGG

Table 2.1. Primers sequences used for PCR.

Production of Pax7 antibody

Hybridoma cells expressing antibodies to Pax7 were purchased from the Developmental Studies Hybridoma Bank (DSHB, University of Iowa). Cells were cultured in ventilated T-75

flasks with complete medium consisting of Iscove's Modified Dulbecco's Medium (Sigma, St. Louis, MO, USA) supplemented with sodium bicarbonate, 1% penicillin-streptomycin (Gibco, Waltham, MA, USA), and 20% fetal bovine serum (FBS) according to the DSHB culturing protocol. Complete medium was added every other day until day 6 in culture at which time serum-free complete medium was added to cultures to maintain a cell density between 5 x 10^5 to 1 x 10^6 cells/ml. After 14 days in culture, cells were split evenly into non-ventilated flasks and diluted with equal volumes serum-free complete medium. After 14 days of culturing, Pax7 conditioned medium was collected and sterile filtered prior to antibody purification. Anti-Pax7 was affinity purified from conditioned medium and eluted with 0.1 M glycine. Antibody concentration was determined by measuring absorbance at 280 nm with a spectrophotometer (Beckman, Brea, CA, USA). Antibody specificity was determined by western blot and immunohistochemistry.

Immunohistochemistry

Quadriceps muscles were dissected and rapidly frozen in isopentane cooled in liquid nitrogen. Frozen, OCT embedded cross-sections were cut at a thickness of 10 μm. Sections were air-dried for 30 minutes and fixed with 4% paraformaldehyde (PFA) or ice-cold acetone for 10 minutes and washed for 15 minutes in phosphate-buffered saline (PBS). Prior to labeling with antibodies for Pax7, sections were subject to 40 minutes of antigen retrieval in sodium citrate buffer containing 0.05% Tween-20 (pH 6.0) and heated in a water bath to 95 - 100°C. Endogenous peroxidases were quenched for 10 minutes with 0.3% H_2O_2. Sections were treated with blocking buffer from a mouse-on-mouse immunohistochemistry kit (M.O.M Kit; Vector Laboratories, Burlingame, CA, USA) supplemented with 0.3 M glycine for 1 hour. Sections were incubated with mouse anti-dystrophin (1:30; RRID:AB_442081), anti-Pax7 (1:500), or anti-MyoD (1:50; RRID:AB_395255) primary antibodies in a humidified chamber, overnight at 4°C. Sections were subsequently incubated with the M.O.M. kit biotin-conjugated anti-mouse IgG

(1:200) for 30 minutes, followed by 15 minutes of PBS washes and a 30-minute incubation with M.O.M. kit ABC reagents. Immunolabeling was visualized with the peroxidase substrate 3-amino-9-ethylcarbazole (AEC kit; Vector Laboratories, Burlingame, CA, USA), causing a dark red reaction product. Following development, sections labeled for dystrophin were stained with hematoxylin as described above. The number of myonuclei per fiber was determined by counting the number of myonuclei stained for hematoxylin within dystrophin-stained fibers and the total number of fibers within a field of view. The number of immunolabeled cells per 100 fibers was determined by counting the number of immunolabeled cells and the total number of muscle fibers in muscle cross-sections.

Immunofluorescence

For sections immunolabeled with two or more antibodies, tissue was fixed with 4% PFA for 10 minutes, subjected to a 40-minute antigen retrieval and a 1 hour blocking incubation (M.O.M. kit) with 0.3 M glycine. Sections were co-labeled with anti-Pax7 (1:500) or anti-Pax7 (1:50; RRID:AB_2159836) and goat anti-Klotho (1:10; RRID:AB_2296612), chicken anti-laminin (1:200; RRID:AB_2134058), rabbit anti-Jmjd3 (1:200; RRID:AB_10987745), rabbit anti-H3K27me3 (1:1000; RRID:AB_2616029), or antibodies probing the active, non-phosphorylated (Ser45) β-catenin (1:1500; RRID:AB_2650576). Sections were incubated with primary antibodies overnight in a humidified chamber at 4°C. Sections were subsequently washed and incubated for 30 minutes with horse anti-mouse Dylight-594 (1:200; RRID:AB_2336412) and horse anti-rabbit Dylight-488 (1:100; RRID:AB_2336403), anti-chicken IgY H&L Alexa-488 (1:200; RRID:AB_2827653), or biotinylated anti-goat secondary (1:200; RRID:AB_2336123) followed by avidin-Dylight 488 (1:500, RRID:AB_2336405). Sections were mounted with Prolong Gold Antifade Mountant containing DNA stain DAPI (#P36931; Invitrogen, Waltham, MA, USA). For data expressed as percent of Pax7+ cells beneath the basal lamina, cells were determined to be Pax7 and DAPI positive and then determined to be beneath the anti-laminin labeled basal

lamina or outside the anti-laminin labeled basal lamina. For data expressed as percent co-labeled, cells were determined to be Pax7 and DAPI positive then determined to be Klotho, Jmjd3, H3K27me3 or β-catenin positive. Data are expressed as the percentage of total Pax7+ satellite cells that are under laminin or as the total Pax7+ satellite cells that also express Jmjd3, H3K27me3 or active β-catenin (Jmjd3+ Pax7+, H3K27me3+ Pax7+ or β-catenin+ Pax7+/ total Pax7+).

Cell culture and *in vitro* treatments

C2C12 myoblasts were seeded on 60 mm culture plates at 100,000 cells per dish or in 6-well plates at 40,000 cell per well. Myoblasts were maintained in growth medium (Dulbecco's Modified Eagle Medium (DMEM) containing 10% FBS, penicillin and streptomycin) at 37°C and in 5% CO_2. Culture medium was refreshed every other day unless otherwise stated. Myogenic cells were serum-starved to induce differentiation and collected at the 1-day, 5-days or 7-days following differentiation.

Klotho stimulation of myoblasts *in vitro*

C2C12 myoblasts were seeded and cultured as outline above. Cultures were stimulated with 10 μg/ml heparin (Sigma, St. Louis, MO, USA) or heparin and 1 μg/ml Klotho (R&D Systems, Minneapolis, MN, USA) in growth medium at 24- and 48-hours post-plating. Following 48 hours of stimulation cells were collected in Trizol reagent for RNA isolation.

Klotho stimulation with subsequent siRNA knock-down of Jmjd3

C2C12 myoblasts were seeded in 6-well dishes, cultured in antibiotic-free DMEM containing 10% heat-inactivated FBS at 37°C and 5% CO_2. After 24 hours in culture, cells were rinsed three times with 1 ml of DPBS and cultured in Opti-MEM (Gibco, Waltham, MA, USA). Cells

were transfected with 50 pmol/ml of Stealth siRNA oligos targeting Kdm6b/Jmjd3 (#1320001; Invitrogen, Waltham, MA, USA) or Stealth siRNA medium GC control oligos (#12935300; Invitrogen, Waltham, MA, USA) using RNAiMAX reagent (Invitrogen, Waltham, MA, USA) for 6 hours according to the manufacturer's protocol. Following transfection, cells were collected for RNA or protein analysis.

Jmjd3 over-expression in myogenic cells

C2C12 myoblasts were cultured in 6-well dishes, as described above. After 24 hours in culture, the cells were rinsed three times with 1 ml of DPBS and cultured in Opti-MEM. Cells were transfected with pCS2-Jmjd3-F expression plasmid (RRID:Addgene_17440) or a pCS2 control vector using Lipofectamine 3000 Transfection Reagent (Invitrogen, Waltham, MA, USA) for 6 hours according to the manufacturer's protocol. Following transfection, myoblasts were cultured in differentiation medium for 72-hours and RNA and protein were collected for analysis.

GSK-J4 treatment of C2C12 myoblasts

C2C12 myoblasts were seeded on 6-well plates and treated with 1.2 mM of GSK-J4 [40,41] (Cayman Chemical, Ann Arbor, MI, USA) at 24- and 48-hours post-plating. Following 48 hours of treatment, cells were collected for RNA analysis.

Western blot following differentiation

C2C12 myoblasts were cultured to specified confluency and subject to differentiation. Cells were washed three times with ice-cold DPBS and collected in reducing sample buffer (80 mM Tris-HCl, pH 6.8, 0.1 M DTT, 70 mM SDS and 10% glycerol) supplemented with proteinase inhibitor cocktail (#P8340; Sigma, St. Louis, MO, USA), 0.2 M Na_3VO_4, and 5 M NaF and passed through a 23-gauge needle five or more times. Cell lysates were boiled 3 minutes and centrifuged at 12,000 g for 1 minute at 4°C. A portion of the supernatant fraction was used to

determine total protein concentration by filter paper assay. Protein homogenates containing 30 μg of total protein were separated on a 10% SDS-PAGE gel and transferred by electrophoresis to a nitrocellulose membrane for 3 hours in transfer buffer (0.2 M glycine, 25 mM Tris base and 20% methanol). Equal loading and efficiency of transfer was verified by staining with Ponceau S solution (#P-7170; Sigma, St. Louis, MO, USA). Nitrocellulose membranes were incubated in blocking buffer containing 0.1% Tween-20, 0.2% gelatin, and 3% dry milk overnight at 4°C. Membranes were probed with anti-Jmjd3 (1:100), anti-Klotho (1:50), or anti-myogenin (1:100) for 3 hours at room temperature or overnight at 4°C, washed six times for 10 minutes in wash buffer (0.05% Tween-20, 0.2% gelatin, and 3% dry milk) or in wash buffer containing 25 mM Tris, pH 7.4, 0.15 M NaCl (TBS) containing 0.05% Tween-20 (0.05% TBST) and overlayed with ECL horseradish peroxidase anti-rabbit IgG (1:100,000; RRID:AB_772206) or ECL horseradish peroxidase anti-mouse IgG (1:10,000; RRID:AB_772210) for 1 hour at room temperature. Membranes were washed six times for 10 minutes in wash buffer prior to development. Membranes were developed with FemtoGlow Western Plus (#FWPD02; Michigan Diagnostics, Royal Oak, MI, USA) and imaged on a SynGene PXi imager (Bangalore, Karnataka, India) using GeneSys V1.5.4.0 software. Relative quantities of Jmjd3 and myogenin proteins were determined using ImageJ software and normalized to input protein.

Western blot following Jmjd3 inhibition with Klotho and siRNA

After 48 hours of Klotho treatment followed by a 6-hour transfection with siRNA targeting Jmjd3, C2C12 cells were washed three times with ice-cold DPBS and collected in reducing sample buffer supplemented with proteinase inhibitor cocktail, 0.2 M Na_3VO_4, and 5 M NaF and passed through a 23-gauge needle five or more times. Cell lysates were then prepared and analyzed by western blotting as described above, using anti-Jmjd3 (1:100) or rabbit anti-desmin (1:50; RRID:AB_476910). Primary antibodies were applied to the blots for 3 hours at room

temperature. Prior to incubation with Wnt-related antibodies probing for rat anti-Wnt4 (1:200; RRID:AB_2215448), rabbit anti-Wnt9a (1:500; RRID:AB_2772907), or rabbit anti-Wnt10a (1:500; RRID:AB_1277809), membranes were incubated overnight at 4°C in blocking buffer containing 25 mM Tris pH 7.4, 0.15 M NaCl, 0.1% Tween 20 and 3-5% dry milk. The following day, membranes were washed in 0.1% TBST wash buffer three to six times for 10 minutes and probed with primary antibodies in a humidified chamber overnight at 4°C. Following primary incubation, membranes were washed in 0.1% TBST three to six times. Membranes probed with anti-Wnt4 were overlaid with ECL horseradish peroxidase anti-rat IgG (1:10,000; RRID:AB_772207) for 1 hour at room temperature. Membranes probed with anti-Wnt9a or anti-Wnt10a were overlaid with ECL horseradish peroxidase anti-rabbit IgG for 1 hour at room temperature. All membranes were washed three to six times in 0.1% TBST, developed with FemtoGlow Western Plus, and imaged on a SynGene PXi imager (Bangalore, Karnataka, India).

Chromatin immunoprecipitation on Klotho treated myoblasts

C2C12 myoblasts were seeded at 2.0 x 10^5 on 100 mm culture dishes and maintained in growth medium and treated with Klotho as outlined above. Following 48 hours of stimulation cells were washed with DPBS, released with 0.05% trypsin EDTA (Gibco, Waltham, MA, USA) and quenched with growth medium. Cells were fixed in 1% formaldehyde on an end-to-end rotator (Barnstead/Thermolyne) for 10 minutes at room temperature. 1% formaldehyde solution was quenched with 2 M glycine for a final concentration of 125 mM glycine and incubated on rotation for 10 minutes. Cells were washed 3 times with cold DPBS prior to lysing. Subsequent steps were done following the ChIP-IT High Sensitivity Kit (Active Motif, Carlsbad, CA, USA) manufacturer's protocol. Cells were lysed in chromatin prep buffer (Active Motif, Carlsbad, CA, USA) containing proteinase inhibitor cocktail and 100 mM phenylmethylsulfonyl fluoride (PMSF)

and incubated on ice for 10 minutes. The lysate was transferred to an ice-cold Dounce homogenizer for mechanical dissociation. The homogenate was then centrifuged at 2350 rpm for 3 minutes at 4°C. The pellet fraction was resuspended in ChIP buffer containing proteinase inhibitor cocktail and PMSF, transferred to a 1.5 ml sonication tube (Active Motif, Carlsbad, CA, USA) and incubated on ice for 10 minutes. Chromatin was sheared by sonication (Active Motif, Carlsbad, CA, USA) at 20 amp for cycles of 15 seconds on and 15 seconds off to reach a fragment side of approximately 200 bp. DNA fragments were electrophoresed on a 2.0% agarose gel and digitally visualized (SynGene, Bangalore, Karnataka, India) with gel red staining. ~17 □g of chromatin were incubated with ChIP-verified anti-H3K27me2/3 (RRID:AB_2793246) or IgG negative control antibodies on end-to-end rotation overnight at 4°C. The following day, Protein G agarose beads were washed and added to each sample for chromatin immunoprecipitation (ChIP). The chromatin-bead mixtures were incubated for 3.5 hours on an end-to-end rotator at 4°C. Each sample was loaded on to a ChIP filtration column, washed and dried by centrifugation at 1250 g for 3 minutes at room temperature. ChIP DNA was eluted twice with 50 μl of Elution Buffer AM4. ChIP-DNA was reverse cross-linked and purified with the ChIP-IT DNA Isolation Kit (Active Motif, Carlsbad, CA, USA) per manufacturer's protocol. Briefly, eluted ChIP DNA was mixed with Proteinase K and incubated in a thermomixer (Eppendorf, Hamburg, Germany) set to at 900 rpm and 55°C for 30 minutes, followed by 80°C for 2 hours. DNA was diluted with DNA Purification Binding Buffer with 10 μl of 3 M sodium acetate for pH adjustment yielding a bright yellow reaction mixture. Each sample was placed in a DNA purification column and washed with DNA Purification Wash Buffer. Purified DNA was eluted in 40 μl of DNA Purification Elution Buffer and stored at -20°C prior to DNA sequencing.

Chromatin immunoprecipitation-sequencing (ChIP-Seq) analysis

DNA quality control and sequencing were done at the UCLA Technology Center for Genomics and Bioinformatics at the University of California, Los Angeles. Single-end DNA sequencing was performed on an Illumina (San Diego, CA, USA) HiSeq3000 instrument with ~39 to 45 million reads per sample and a read length of 50 base-pairs (bp). Raw fastq files were aligned to the mm10 genome using Bowtie2 [42] with default parameters, achieving an alignment rate between 95-98%. Resulting SAM files were converted to BAM format and sorted using Samtools.[43] Broad peaks were called using Model-based analysis of ChIP-Seq [44] (macs2 callpeak function) with the sorted ChIP and input alignments (BAM files) as the treatment and control files, respectively, and specifying the following parameters: --broad --broad-cutoff 0.1 -g mm --nomodel. We calculated peaks found after Klotho treatment but not in Control condition, and quantified read density around peak centers (+/- 1kb) using computeMatrix from DeepTools [45] with the --skipZeros parameter and the output of bamCoverage [45] as inputs. The resulting matrix was then used with plotHeatmap [45] for visualization. Genomic regions and functional analyses were done using R on peaks falling within -3000 bp to +300 bp from the transcription start site (TSS) of genes defined by the Bioconductor [46,47] package TxDb.Mmusculus.UCSC.mm10.ensGene.[48] We used R to identify gene promoters that overlap with H3K27me2/3 peaks and quantify the percent overlap. Promoters with H3K27me2/3 peak occupancy after Klotho treatment only are shown in Table 2.2 and by definition have 0% H3K27me2/3 overlap in the vehicle-treated control condition. Gene Ontology (GO) analysis and Kyoto Encyclopedia of Genes and Genomes (KEGG) [49] was done using the Database for Annotation, Visualization and Integrated Discovery (DAVID) [50,51] which uses a modified Fisher's Exact test to examine statistical significance of enrichment for each term. KEGG results were verified using the KEGG.db package from Bioconductor and a hypergeometric test to measure statistical significance for each term. Raw ChIP-seq were uploaded to the National Center for Biotechnology Information's Gene Expression Omnibus and are available under accession number GSE189109.

Statistics

Data are presented as the mean ± standard error of the mean (SEM). Non-parametric student's t-test was used when determining differences between two groups and one-way analysis of variance (ANOVA) with Dunnett's multiple comparison test when comparing more than one group to one control group or Tukey's Post Hoc was used when comparing more than two groups. Groups were determined to be significantly different at $p < 0.05$.

RESULTS

Klotho modulates muscle development during early postnatal growth

Klotho expression in skeletal muscle declines from early postnatal development until maturity, which suggests that Klotho may affect muscle development in young animals.[12] Our findings show that *klotho* mRNA expression is highest in wild-type mice at 14 days after birth (P14), declines during the mid-stage of postnatal development at 28 days after birth (P28) and is further reduced in 3-months-old adult muscles (Fig. 2.1A). Immunohistological observations at P14 show that Klotho protein is located in Pax7-expressing cells (Pax7+), on the surface of some myofibers and in other cells in the interstitium (Fig. 2.1B). However, by 3-months of age, the proportion of Pax7+ cells that expressed Klotho significantly declined (Fig. 2.1C, D), confirming that the reductions of Klotho mRNA levels in muscle that occurred between P14 and 3-months of age (Fig. 2.1A) were mirrored by reductions in the proportion of Pax7+ cells that expressed detectible levels of Klotho protein. Because Klotho protein is expressed in Pax7+ cells and muscle fibers during development and *klotho* expression declines during postnatal muscle growth, we tested whether modifying *klotho* expression would affect muscle growth in young mice (Supplemental Fig. 2.1). QPCR data confirmed that the *klotho* transgene (KL Tg) produced elevated levels of *klotho* mRNA during skeletal muscle development and in adult skeletal muscle (Supplemental Fig. 2.1A). However, expression of the transgene had only slight effects on reducing total body mass or the mass of individual muscles at P14 and no effect on body or muscle mass at P28 or at 3-months old (Supplemental Fig. 2.1B-H).

Despite the small effects of KL Tg expression on muscle mass in young mice, we observed significant effects on muscle fiber growth. The mean cross-sectional area of quadriceps muscle fibers was reduced by more than 30% in KL Tg+ mice during early postnatal development (Fig. 2.1E-H). However, fiber size did not differ between KL Tg+ and wild-type mice at P28 (Fig. 2.1I-L) and the fiber size of KL Tg+ mice exceeded wild-type fibers by more than 24% at 3-months of

age (Fig. 2.1M-P). These changes in fiber cross-sectional areas represented a ~4-fold increase in wild-type muscles and a ~10-fold increase in KL Tg+ fibers between P14 and 3-months of age (Fig. 2.1G, O). Collectively, these data show that increased expression of *klotho* during early postnatal growth delays muscle development, but subsequently the transgene accelerates muscle growth.

We also tested whether the differences in muscle fiber cross-sectional area between transgenic and control mice were reflected by differences in myonuclei per fiber by assaying whether transgene expression affected the number of hematoxylin-stained myonuclei in anti-dystrophin stained sections. Our measurements show that at P14, when transgenic muscle fibers have smaller CSA (Fig. 2.1G), there are fewer myonuclei per fiber (Fig. 2.1Q-S). At 3 months, when transgenic muscle fibers have greater CSA (Fig. 2.1O), there are more myonuclei per fiber (Supplemental Fig. 2.1).

Klotho increases numbers of activated satellite cells during postnatal development

Because the number of satellite cells that are present in muscle in the first weeks of postnatal muscle development can influence the growth of muscle fibers, [9,10] we tested whether KL Tg expression affected numbers of quiescent or activated satellite cells that expressed Pax7. We found that elevated levels of KL Tg expression increased the number of Pax7+ cells at P14 and P28, but not at 3-months of age (Fig. 2.2A-C). Notably, the reduction of Pax7+ cells in wild-type muscles that occurred between P14 and 3-months coincided with the reduction of *klotho* expression that occurred between P14 and 3-months (Fig. 2.1A). Similarly, the presence of the transgene increased the number of activated myoblasts indicated by elevated numbers of MyoD+ cells at P14, P28 and at 3-months (Fig. 2.2D-F). We also tested whether KL Tg expression affected the proportion of Pax7+ cells that are located underneath the basal lamina, using double-immunohistochemistry for Pax7 and laminin (Fig. 2.2G-I). These data show that at

P14 the proportion of Pax7+ cells that are beneath the basal lamina is reduced by the KL Tg, although transgene expression at that age increased the numbers of Pax7+ cells (Fig. 2.2C), supporting our interpretation that expression of the transgene in young neonatal animals increases the numbers of activated, Pax7+ cells.

Klotho reduces the expression of the H3K27 demethylase *Jmjd3* in myogenic cells *in vitro*

We tested whether the effects of Klotho on early myogenesis could result from influences on the expression of epigenetic regulatory factors that may contribute to silencing or activating myogenic genes. In particular, we assayed whether Klotho stimulation of myoblasts *in vitro* affected the expression of proteins that control the methylation of H3K27 because H3K27 methylation is a well-established, negative regulator for the expression of myogenic transcription factors that include *Pax7*, *Myod1* and *Myog*.[28,52,53] QPCR analysis showed that Klotho stimulation significantly reduced the expression of *Jmjd3*, an H3K27 demethylase (Fig. 2.3A). However, the expression of *Utx* (another H3K27 demethylase), *Jarid2* (which promotes the methylation of H3K27) and *Ezh2* (an H3K27 methyltransferase) were not affected at the mRNA level by Klotho stimulation (Fig. 2.3B-D).

Jmjd3 promotes muscle differentiation *in vitro*

Our findings showing that Klotho affects muscle development and decreases *Jmjd3* expression suggested the possibility that some of Klotho's effects on myogenesis could be mediated by its down-regulation of Jmjd3. Several observations support that possibility. First, qPCR data show that *Jmjd3* expression increased at the onset of muscle differentiation and then remained elevated for at least 7-days (Fig. 2.4A). In addition, western blots showed more Jmjd3 protein in myotubes than in myoblasts (Fig. 2.4B) and the increase in Jmjd3 in myotubes coincided with a shift in expression of Klotho isoforms. Western blot probing for full-length, transmembrane

αKlotho (αKL) and truncated, soluble Klotho (sKL) showed sKL is the dominant form of Klotho in myoblasts and αKL is highly upregulated in myotubes (Fig. 2.4B). We also observed that the down-regulation of sKL and up-regulation of Jmjd3 during myogenesis coincided with a small increase in *Myod1* expression (Fig. 2.4C) and a greater than 680-fold increase in *Myog* expression (Fig. 2.4D), linking elevations of Jmjd3 levels in myogenesis with increased terminal differentiation of myogenic cells.

We then assayed whether Jmjd3 may have influenced these changes in expression of myogenic transcription factors by treating myoblasts with siRNA that targeted the gene sequence encoding the catalytic domain of the Jmjd3 demethylase protein. *Jmjd3* down-regulation in siRNA treated myoblasts was confirmed by qPCR (Fig. 2.4E). Although *Pax7* mRNA (Fig. 2.4F) and *Myod1* mRNA (Fig. 2.4G) levels were unaffected by Jmjd3 inhibition, *Myog* transcripts were reduced by more than 50% (Fig. 2.4H). We also assayed whether increased expression of Jmjd3 affected the expression of myogenic transcription factors by transfecting myoblasts with a pCS2-Jmjd3-F expression plasmid or a pCS2-control plasmid. Over-expression of *Jmjd3* (Fig. 2.4I) produced no change in the expression of *Pax7* (Fig. 2.4J) or *Myod1* mRNAs (Fig. 2.4K) but increased *Myog* by nearly 2-fold (Fig. 2.4L). Similarly, transfection of myoblasts with the Jmjd3 expression plasmid increased Jmjd3 protein relative to total protein compared to myoblasts transfected with control plasmid and likewise increased myogenin protein in Jmjd3 overexpressing myoblasts (Fig. 2.4M-O). Together, these observations indicate that Jmjd3 positively modulates myogenesis as muscle cells transition from proliferative, MyoD+ myoblasts into differentiated, myogenin-expressing cells.

Klotho treatment of myoblasts promotes H3K27 methylation and reduces expression of Wnt-family genes

Our observations showing that Klotho is a negative regulator of *Jmjd3* expression and that Jmjd3 is a positive regulator of *Myog* expression suggested that Klotho could possibly affect myogenesis by influencing the H3K27 methylation at myogenic regulatory genes, especially myogenin. We tested whether Klotho influences the methylation state of H3K27 in myoblasts using chromatin immunoprecipitation followed by DNA sequencing (ChIP-seq) but found no evidence of changes in H3K27 di- and tri-methylation of nucleosomes occupying *Myog*. However, a heat map showing H3K27me2/3 ChIP-seq peaks that appear after Klotho treatment but not in control samples (Fig. 2.5A), demonstrated significant enrichment of H3K27me2/3 signal around multiple, other loci. Prominent among those loci, Klotho-stimulated myoblasts had more H3K27me2/3 silencing marks at the promoter regions of genes classified by KEGG as part of the renin-angiotensin system, Jak-STAT signaling, sugar and lipid metabolism, pluripotent stem cell regulation, the Hippo signaling pathway and the Wnt signaling pathway (Fig. 2.5B). Gene Ontology (GO) analysis for the biological process (BP) terms of genes with increased H3K27 methylation following Klotho stimulation were associated with regulation of developmental processes, stem cell regulatory processes, ion and metabolic homeostasis, the Ras signaling pathway and the canonical Wnt signaling pathway (Fig. 2.5C). The accumulation of H3K27me2/3 silencing marks at the promoter regions of Wnt family genes in Klotho treated samples could be developmentally important because silencing those genes could disrupt normal myogenesis.[54-57] QPCR analysis showed significant reductions in expression of 3 Wnt ligands (*Wnt4, Wnt9a, Wnt10a*) and 2 Wnt receptors (*Fzd3* and *Fzd9*) in cells stimulated with Klotho (Fig. 2.5D-H), confirming that increased H3K27 methylation at these Wnt-family genes is associated with their suppression in muscle cells.

Inhibition of H3K27 demethylases reduces expression of Wnt4 and Wnt10a in myogenic cells

Because our data showed that Klotho reduces *Jmjd3* expression and promotes the accumulation of H3K27 di- and tri-methylation at the promoter of Wnt family members, we examined whether the reductions in Wnt transcript levels were directly related to the inhibition of H3K27 demethylase activity. QPCR data from myoblasts treated with GSK-J4, a pharmacological inhibitor targeting H3K27 demethylases, showed that expression of *Wnt4* (Fig. 2.6A) and *Wnt10a* (Fig. 2.6C) were reduced by the treatment, although *Wnt9a*, *Fzd3* and *Fzd9* (Fig. 2.6B, D, E) were unaffected.

Klotho stimulation and Jmjd3 knock-down do not have additive, inhibitory effects on the expression of Wnt4, Wnt9a or Wnt10a

We next addressed whether inhibition of *Jmjd3* expression and Klotho stimulation would produce additive, inhibitory effects on the expression of Wnt family genes or Wnt target genes in myoblasts, which would indicate that they inhibited expression through separate pathways. Our qPCR data showed that treatments with recombinant Klotho and siRNA for Jmjd3 each reduced *Jmjd3* expression compared to controls, although siRNA for Jmjd3 was more effective at reducing *Jmjd3* transcripts (Fig. 2.7A). We also found that expression of each Wnt transcript assayed (*Wnt4, Wnt9a, Wnt10a*) was significantly reduced by siRNA for *Jmjd3* but adding Klotho treatment to the inhibition with siRNA did not produce more inhibition than achieved with siRNA alone (Fig. 2.7B-D). These findings indicate that transcriptional inhibition of these genes by blocking H3K27 demethylation through siRNA for Jmjd3 is not further enhanced by activating Klotho. Unlike the influence of siRNA for *Jmjd3* on Wnt genes, no effects on the expression of the Wnt receptors Fzd3 and Fzd9 were observed (Fig. 2.7E,F); however, *Fzd9* expression was reduced by Klotho treatment alone (Fig. 2.7F). Thus, Klotho may inhibit *Fzd9* through a pathway not regulated by Jmjd3. We also tested whether the reductions in Wnt ligand mRNA correlated with changes in downstream target molecules by assaying for mRNA levels of *Axin2*, a negative

regulator of the Wnt pathway [58] and *Ccnd1* which encodes cyclin D1, a positive regulator of cell cycle progression.[59,60] Similar to our findings with *Fzd9*, expression of *Axin2* and *Ccnd1* was reduced by Klotho but not by Jmjd3 siRNA (Fig. 2.7G,H), which may indicate Klotho inhibition of these genes was independent of Jmjd3.

We next assayed whether reductions in Jmjd3 and Wnt gene expression that occurred in Klotho or Jmjd3 siRNA treated myoblasts were detectible by western blot at the protein level (Fig. 2.7I). Both Klotho and Jmjd3 siRNA produced clear reductions in Jmjd3 protein when administered separately or combined, compared to the control group (Fig. 2.7I). Although treatment effects on Wnt4 protein levels were less apparent (Fig. 2.7I), Wnt10a protein was reduced by Jmjd3 siRNA treatment, by Klotho stimulation and by the combined treatment groups compared to controls (Fig. 2.7I). Wnt9a protein was undetectable in the control and treatment groups.

Klotho modulates Jmjd3 and H3K27 methylation in satellite cells

We tested whether our observations that stimulation with recombinant Klotho decreased *Jmjd3* expression and elevated H3K27 methylation in myoblasts *in vitro* reflected the actions of Klotho during muscle development *in vivo*. QPCR analysis on whole quadriceps muscles show *Jmjd3* expression is reduced at P14 and P28 but not at 3-months of age in KL Tg+ mice, compared to wild-type mice (Fig. 2.8A). Furthermore, we observed that Jmjd3 is present in Pax7+ cells (Fig. 2.8B) and the proportion of Pax7+ cells expressing detectible Jmjd3 protein was reduced in KL Tg+ muscles at P14 (Fig. 2.8C, D) and at P28 (Fig. 2.8D) but not at 3-months (Fig. 2.8D). Next, we probed for H3K27me3 in Pax7+ cells to determine whether the reduction in Jmjd3 reflects changes in H3K27 methylation and observed that H3K27me3 was located in Pax7+ and Pax7- cells in developing muscle tissue (Fig. 2.8E, F). However, the proportion of Pax7+ cells that contained detectible H3K27me3 was greater in KL Tg+ mice compared to wild-type at P14 (Fig.

2.8E-G) and P28 (Fig. 2.8G) but not at 3-months (Fig. 2.8G). We emphasize that the absence of detectible anti-H3K27me3 binding to some satellite cell nuclei does not indicate that those cells were devoid of H3K27 methylation; the observation shows that the quantity of H2K27 marks in those cells was lower than the detection limits of the technique. These findings indicate that Klotho activation reduces Jmjd3 levels, and consequently increases H3K27me3, in developing muscle *in vivo* through 28 days.

Klotho reduces the expression of Wnt4, Wnt9a, and Wnt10a during early postnatal muscle growth

Because *Jmjd3* expression was reduced in KL Tg+ muscle during early postnatal development and accompanied by elevated H3K27 methylation, we assayed for corresponding reductions in the expression of Wnt pathway genes that we found to experience increased H3K27 methylation in Klotho-stimulated myoblasts. Similar to our *in vitro* findings, we found that KL Tg expression decreased expression of *Wnt4*, *Wnt9a* and *Wnt10a* in P14 mice (Fig. 2.9A-C). However, only *Wnt4* expression was reduced in KL Tg+ muscles at P28 or 3-months. We also observed that *Fzd9* expression was decreased at P14 resembling the effect of Klotho stimulation of myoblasts *in vitro*, but not affected at other ages tested (Fig. 2.9E). Also similar to our *in vitro* findings, KL Tg expression did not reduce expression of *Fzd3* or *Ccnd1* (Fig. 2.9D,E); instead the transgene produced elevations in expression of both at P28, showing that Klotho-driven reduction of Jmjd3 is not an important regulator of the expression of either gene. Although KL Tg expression reduced the expression of *Axin2* in muscles, the effect occurred only in 3-month-old mice (Fig. 2.9F) when the transgene did not influence *Jmjd3* expression (Fig. 2.8A), which also suggests that the transgene does not influence *Axin2* expression in muscle via Klotho suppression of Jmjd3 function, resembling our observation on myoblasts *in vitro*.

Klotho represses Wnt-signaling in Pax7-expressing cells during postnatal development and early adulthood

Our results pertaining to the effects of Klotho on developmental myogenesis and the inhibition of the expression of Wnt ligands, Wnt receptors and Wnt target genes suggest that muscle growth during development is influenced by fluctuating levels of Klotho. Because myogenesis is driven in part by canonical Wnt-signaling, [54] we assayed for activation of the Wnt-signaling pathway in Pax7+ cells during development and in early adulthood, using an antibody to detect activated β-catenin which medicates canonical Wnt-signaling.[61,62] Our findings show that ~25 to 35% of Pax7+ cells expressed detectible levels of activated β-catenin during early postnatal development in wild-type muscle (Fig. 2.10A, C) but the KL Tg significantly reduced the proportion of Pax7+ cells with activated β-catenin to less than 20% (Fig. 2.10B, C). However, we also observed that active β-catenin in wild-type, Pax7+ cells declines between P28 and 3-months and elevated levels of Klotho continue to inhibit Wnt-signaling during early adulthood (Fig. 2.10C), indicating that Klotho influences Wnt-signaling in myogenic cells from early postnatal development until maturity.

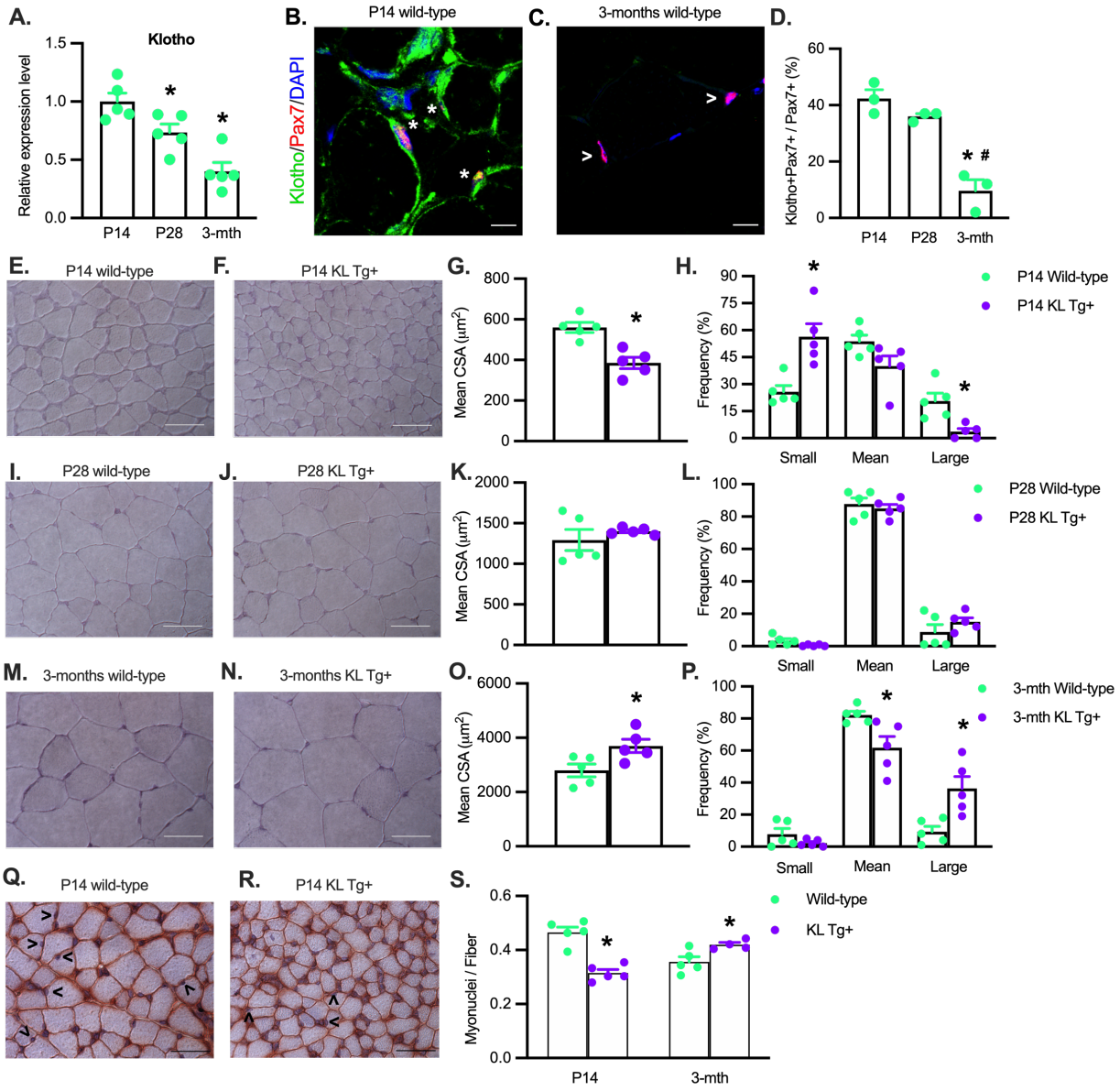

Figure 2.1. Expression of a *klotho* transgene affects muscle development. (A) QPCR data showing relative mRNA expression of *klotho* in quadriceps muscle lysates of P14, P28 and 3-months Wt mice. N = 5 per time point. * indicates significantly different from P14 at $p < 0.05$ analyzed by one-way ANOVA followed by Dunnett's multiple comparisons test. Error bar represents SEM. (B, C) Sections of P14 and 3-months Wt quadriceps muscles labeled with anti-Pax7 (red), anti-Klotho (green) and DNA labeled with DAPI (blue). * indicates Pax7+ cells that are also Klotho+. Open arrowhead (>) indicates Pax7+ single-labeled cells. Bars = 10 μm. (D) Ratio of Klotho+/Pax7+ cells to total Pax7+ cells in sections of quadriceps muscles. (E, F) Representative images of Wt (E) and KL Tg+ (F) quadriceps muscle at P14 stained with hematoxylin. Bar = 50 μm. (G) Mean cross-sectional area for quadriceps muscle fibers from P14 Wt and KL Tg+ mice. (H) Frequency distribution of fiber cross-sectional areas for quadriceps muscles at P14 from Wt and KL Tg+ mice. N = 5. (I, J) Representative images of Wt (I) and KL Tg+ (J) quadriceps muscle at P28 stained with hematoxylin. Bar = 50 μm. (K) Mean cross-sectional area for quadriceps muscle fibers from P28 Wt and KL Tg+ mice. (L) Frequency distribution of fiber cross-sectional areas for quadriceps muscles at P28 from Wt and KL Tg+ mice. (M, N) Representative images of Wt (M) and KL Tg+ (N) quadriceps at 3-months stained with hematoxylin. Bar = 50 μm. (O) Mean cross-sectional area for quadriceps muscle from 3-months Wt and KL Tg+ mice. (P) Frequency distribution of fiber cross-sectional areas for quadriceps muscles at 3-months from Wt and KL Tg+ mice. For G, K and O, * indicates significantly different from the mean cross-sectional area of age-matched Wt fibers at $p < 0.05$ analyzed by *t*-test. Error bar represents SEM. N = 5. For H, L and P, * indicates

significantly different from age-matched Wt fibers of the same sized group at $P < 0.05$ analyzed by *t*-test. Error bar represents SEM. N = 5. (Q, R) Representative images of Wt (Q) KL Tg+ (R) quadriceps at P14 stained with anti-dystrophin and hematoxylin. Open arrowhead (>) indicates myonuclei. Bar = 50 μm. (S) Numbers of myonuclei per fiber in quadriceps from Wt and KL Tg+ mice at P14 and 3-months. * indicates significantly different from age-matched Wt fibers at $p < 0.05$ analyzed by *t*-test. Error bar represents SEM. N = 5.

Figure 2.2.

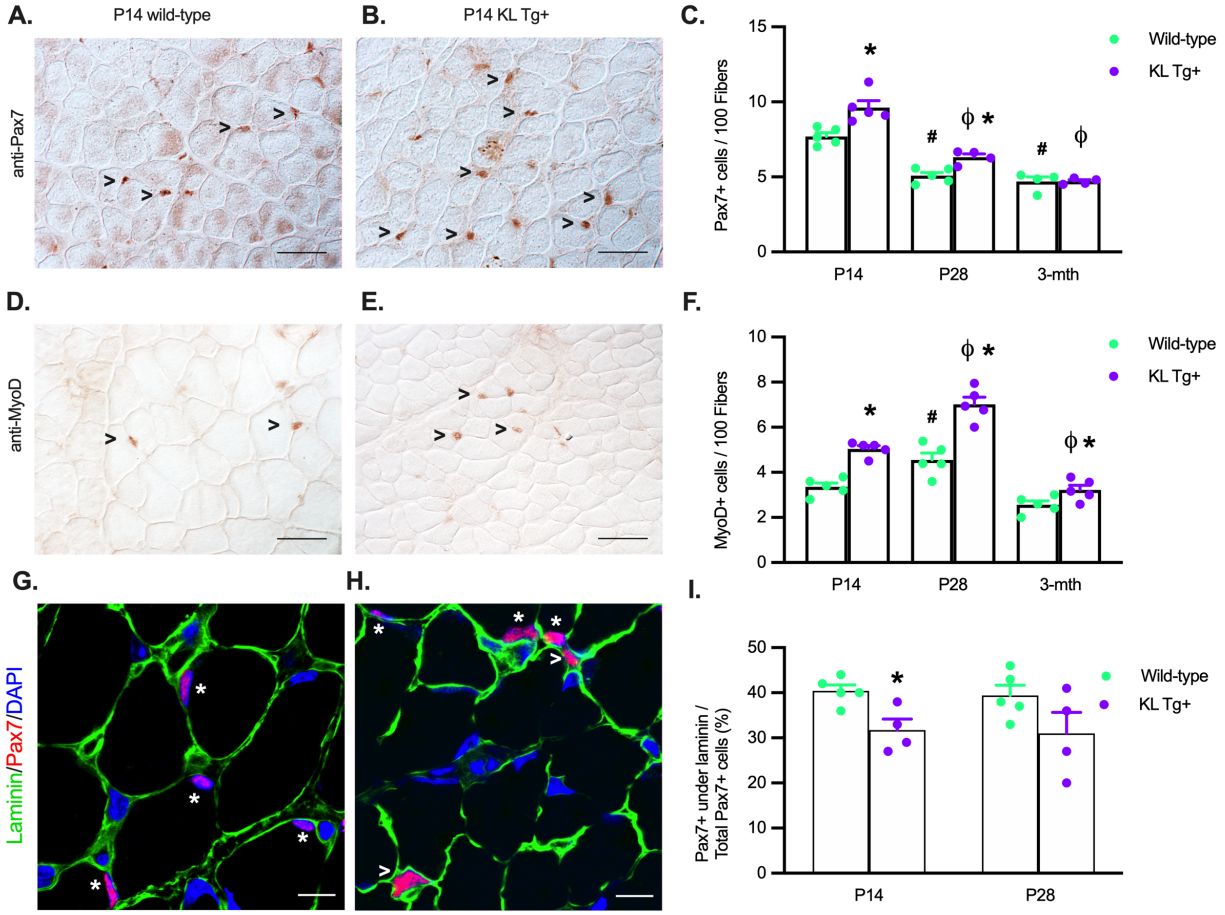

Figure 2.2. ***Klotho*** **transgene expression increases numbers of satellite cells and activated myoblasts during early postnatal development** (A, B) Representative images of Wt (A) and KL Tg+ (B) quadriceps muscle at P14 immunolabeled for Pax7 (reddish-brown nuclei). (C) Numbers of Pax7+ cells per 100 fibers in quadriceps from Wt and KL Tg+ at P14, P28 and 3-months mice. (D, E) Representative images of Wt (D) and KL Tg+ (E) quadriceps muscle at P14 immunolabeled for MyoD (reddish-brown nuclei). (F) Numbers of MyoD+ cells per 100 fibers in quadriceps from Wt and KL Tg+ at P14, P28 and 3-months mice. For A, B, D and E, open arrowheads (>) indicate Pax7+ (A, B) or MyoD+ (D, E) labeled cells. Bar = 50 μm. For C and F, * indicates significantly different from age-matched Wt control at $P < 0.05$ analyzed by *t*-test. # indicates significantly different from P14 Wt at $p < 0.05$ analyzed by one-way ANOVA with Tukey's multiple comparisons test. ϕ indicates significantly different from P14 KL Tg+ at $p < 0.05$ analyzed by one-way ANOVA with Tukey's multiple comparisons test. Error bar represents SEM. N = 4 or 5. (G, H) Representative images of Wt (G) and KL Tg+ (H) quadriceps muscle at P14 immunolabeled for Pax7 (red), laminin (green) and DNA labeled with DAPI (blue). * indicates Pax7+ cells under the basal lamina. Open arrowheads (>) indicate Pax7+ cells outside of laminin. Bars = 10 μm. (I) Ratio of Pax7+ cells under the basal lamina to total Pax7+ cells in sections of quadriceps muscles from P14 and P28 Wt and KL Tg+ mice. * indicates significantly different from age-matched Wt control at $P < 0.05$ analyzed by *t*-test. Error bar represents SEM. N = 4 or 5.

Figure 2.3.

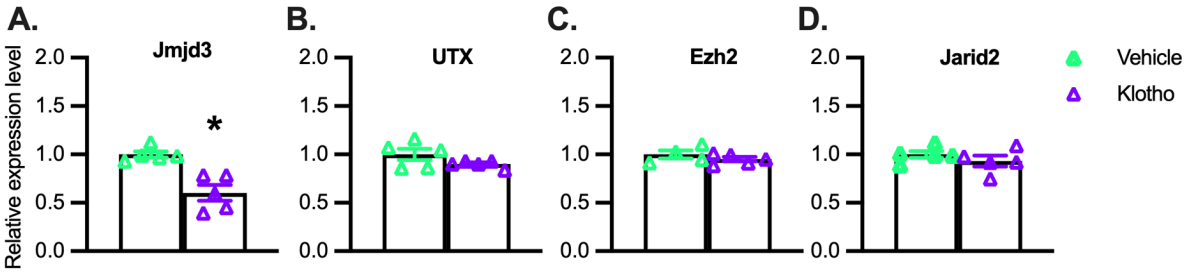

Figure 2.3. ***Klotho*** **reduces** ***Jmjd3*** **expression in myogenic cells** ***in vitro*****.** QPCR data showing relative expression of *Jmjd3* (A), *Utx* (B), *Ezh2* (C) and *Jarid2* (D) in cultured myoblasts treated with recombinant Klotho for 48-hrs. * indicates significantly different from vehicle treated cells at $p < 0.05$ analyzed by *t*-test. Error bar represents SEM. N = 4 or 5 for each data set.

Figure 2.4.

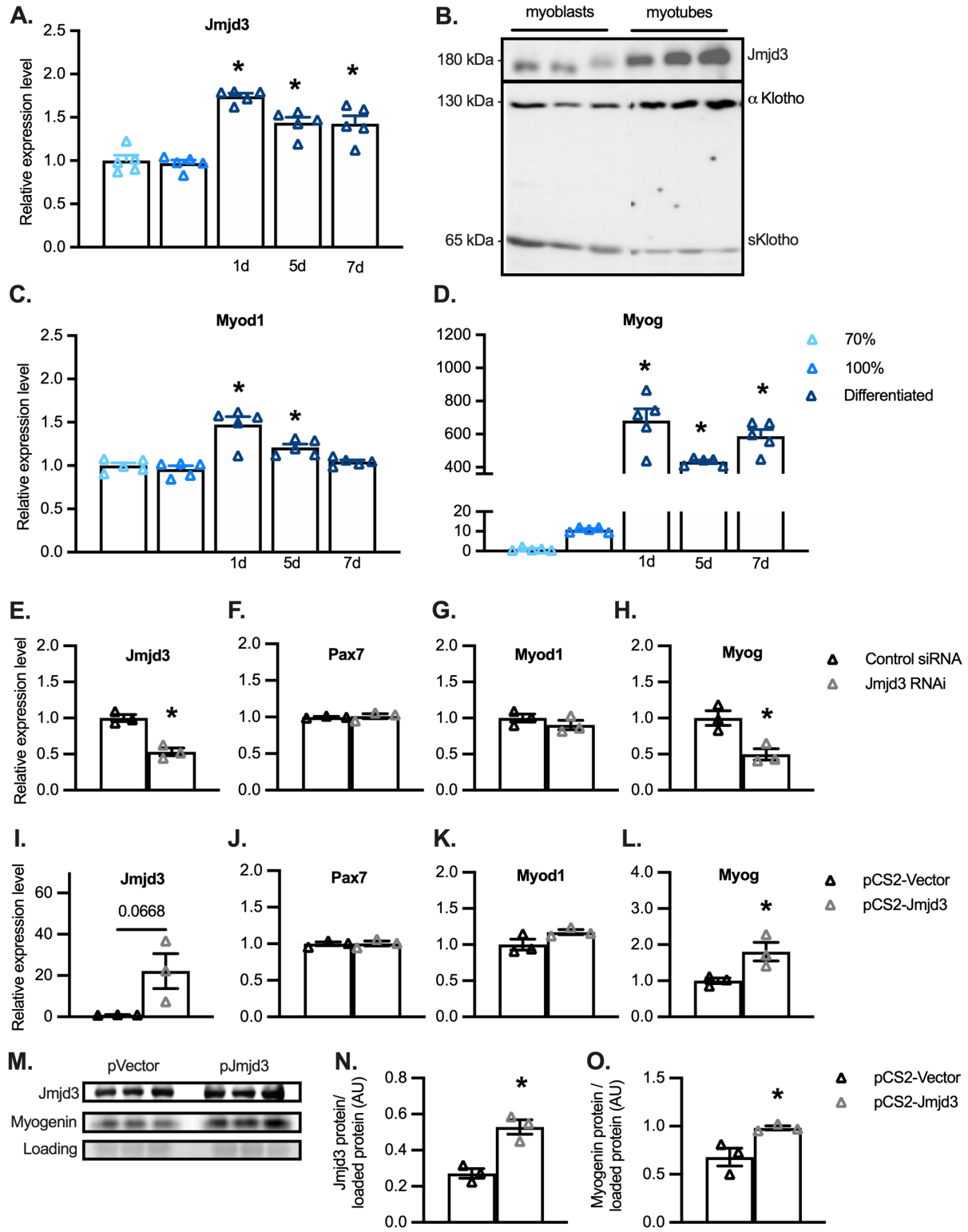

<u>Figure 2.4.</u> Jmjd3 promotes muscle differentiation *in vitro.* (A) QPCR data showing relative expression of *Jmjd3* in sub-confluent (70%) and confluent (100%) myoblasts and in myogenic cells at 1-day, 5-days and 7-days following the onset of differentiation. * indicates significantly different from 70% confluent myoblast control group at $p < 0.05$

analyzed by one-way ANOVA with Dunnett's multiple comparison test. Error bar represents SEM. N = 5 for each data set. (B) Western blot showing relative expression of Jmjd3 and KL in sub-confluent myoblasts and differentiated myotubes. (C, D) QPCR data showing relative expression of *Myod1* (C) and *Myog* (D) in myogenic cell cultures. * indicates significantly different from 70% confluent myoblast control group at $p < 0.05$ analyzed by one-way ANOVA with Dunnett's multiple comparison test. Error bar represents SEM. N = 5 for each data set. (E-H) QPCR data showing relative expression for *Jmjd3* (E), *Pax7* (F), *Myod1* (G), and *Myog* (H) in cultured myoblast cells transfected with control siRNA or siRNA targeting Jmjd3. * indicates significantly different from cells transfected with control siRNA at $p < 0.05$ analyzed by *t*-test. Error bar represents SEM. N = 3 for all data sets. (I-L) QPCR data showing relative expression for transcripts of *Jmjd3* (I), *Pax7* (J), *Myod1* (K), and *Myog* (L) in cultured myoblasts transfected with control pCS2-vector plasmid or pCS2-Jmjd3-F expression plasmid for 6-hrs followed by 72-hrs in differentiation conditions. * indicates significantly different from cells transfected with control pCS2-vector plasmid at $P < 0.05$ analyzed by *t*-test. Error bar represents SEM. N = 3 for all data sets. (M) Western blot showing relative levels of Jmjd3 and myogenin in myogenic cells transfected with control pCS2-vector plasmid or pCS2-Jmjd3-F expression plasmid for 6-hrs followed by 72-hrs in differentiation conditions. (N, O) Quantification of total Jmjd3 protein (N) or myogenin protein (O) relative to protein loaded per gel lane. * indicates significantly different from cells transfected with control pCS2-vector plasmid at $P < 0.05$ analyzed by *t*-test. Error bar represents SEM. N = 3 for all data sets.

Figure 2.5.

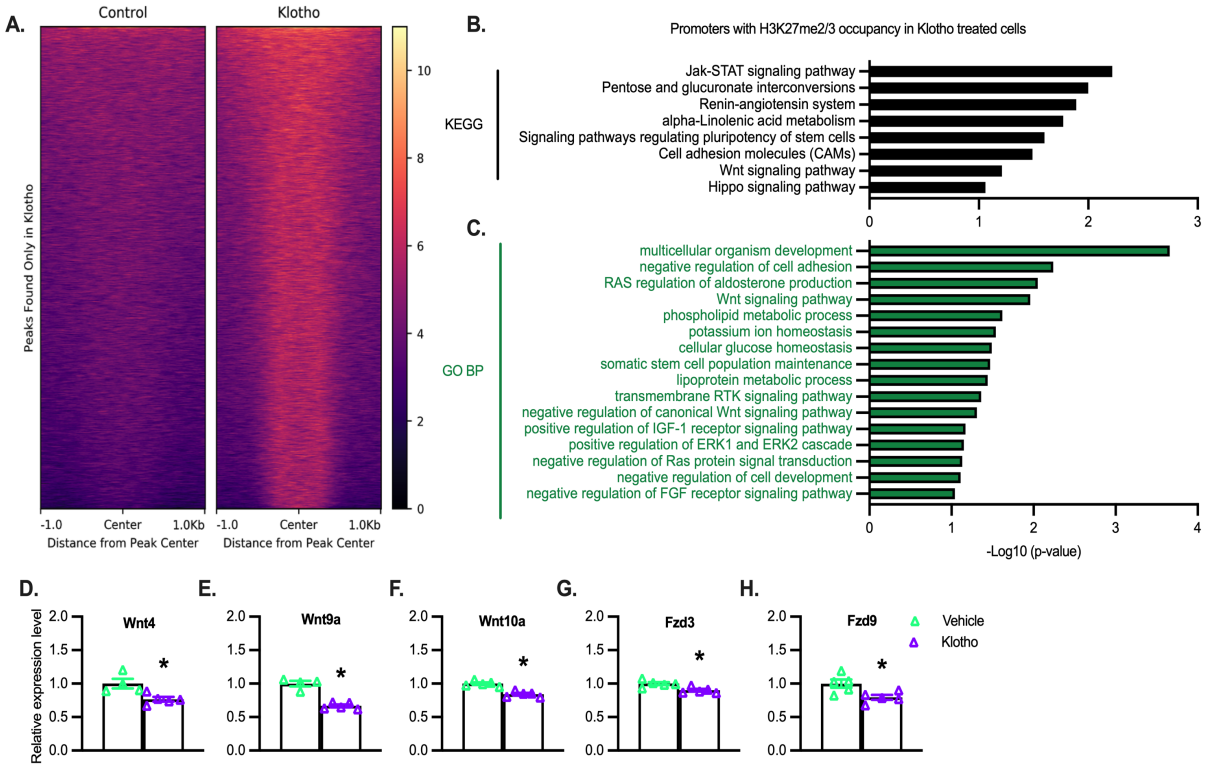

<u>Figure 2.5.</u> Klotho treatment of myoblasts increases H3K27 methylation and reduces expression of Wnt-family genes. (A) H3K27me2/3 ChIP-seq heatmap centered around peaks observed after Klotho treatment that are not observed in the Control, showing higher read density in the Klotho condition. Color scale indicates low (black) to high (pale yellow) read density. (B) KEGG analysis of genes with promoter H3K27me2/3 occupancy in the presence of recombinant Klotho. -$\log_{10}$(p-value) indicates significance of hypergeometric test result based on the number of gene promoters identified in each category relative to total number of genes within each term. N = 1 for each ChIP and input sample. (C) GO Biological Process analysis of genes with promoter H3K27me2/3 occupancy in the presence of recombinant Klotho treatment. N = 1 for each ChIP and input sample. Data graphed as -$\log_{10}$(p-value) based on the number of gene promoters identified in each category relative to total number of genes within each term. (D-H) QPCR data showing relative expression of *Wnt4* (D), *Wnt9a* (E), *Wnt10a* (F), *Fzd3* (G) and *Fzd9* (H) in cultured myoblasts treated with recombinant Klotho for 48-hrs. * indicates significantly different from vehicle treated cells at $p < 0.05$ analyzed by *t*-test. Error bar represents SEM. N = 4 or 5 for each data set

Table 2.2.

Symbol	Chr:Start-End	Gene ID	H3K272/3 Peak(s) in KL-treated cells	Promotor overlap (%)
Wnt4	chr4:137277489-137299726	ENSMUSG00000036856	chr4:137274634-137274877; chr4:137276224-137277069	33
Wnt9a	chr11:59306928-59333552	ENSMUSG00000000126	chr11:59304349-59305664	40
Wnt10a	chr1:74791516-74804179	ENSMUSG00000026167	chr1:74789946-74790493	17
Fzd3	chr14:65201026-65262463	ENSMUSG00000007989	chr14:65261701-65263591	43
Fzd9	chr5:135248938-135251230	ENSMUSG00000049551	chr5:135252831-135253153	10
Frzb	chr2:80411970-80447625	ENSMUSG00000027004	chr2:80446165-80447428	3
Wisp3	chr10:39150971-39163794	ENSMUSG00000062074	chr10:39164763-39165022; chr10:39166089-39167811	29
Csnk2a2	chr8:95446096-95488820	ENSMUSG00000046707	chr8:95491364-95492299	14
Pp2cb	chr8:33599621-33619794	ENSMUSG00000009630	chr8:33597564-33598858	39
Sfrp2	chr3:83766321-83774316	ENSMUSG00000027996	chr3:83766030-83766774	18
Csnk1e	chr15:79417856-79443919	ENSMUSG00000022433	chr15:79444679-79446189	46
Nkd2	chr13:73818534-73847631	ENSMUSG00000021567	chr13:73848780-73850045	38

Nkd1	chr8:88521344-88594887	ENSMUSG00000031661	chr8:88520969-88524273	20
Shisa2	chr14:59625281-59631658	ENSMUSG00000044461	chr14:59625308-59626307	8

Table 2.2. Wnt-related genes whose promoters (3000 bp upstream to 300 bp downstream of TSS) overlap with H3K27me2/3 peaks in Klotho-stimulated C2C12 myoblasts. Promoter overlap percentage indicates percent of a given promoter overlapping with H3K27me2/3 peak(s) in the Klotho-treated condition. Notably, all listed promoters have 0% overlap with H3K27me2/3 peaks in the vehicle-treated control condition, which suggests that these Wnt-related promoters have preferential heterochromatic mark deposition under Klotho stimulation. Column names indicate: gene symbol, gene location (chr:start-end), Ensemble gene ID, location of broad peaks, and promotor overlap (%) with H3K27me2/3 peaks in C2C12 cells treated with recombinant Klotho for 48-hrs.

Figure 2.6.

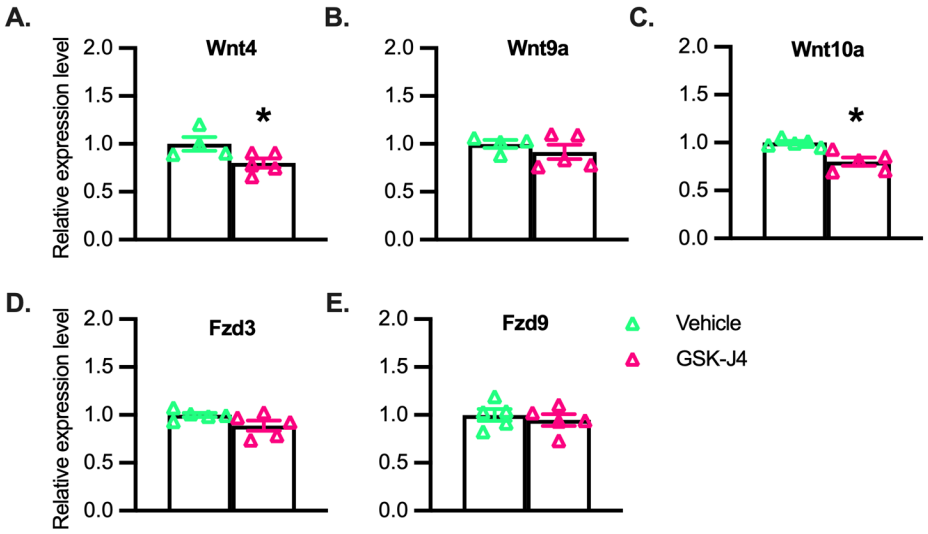

Figure 2.6. Inhibition of H3K27 demethylases reduces expression of *Wnt4* and *Wnt10a* in myogenic cells. (A-E) QPCR data showing relative expression of *Wnt4* (A), *Wnt9a* (B), *Wnt10a* (C), *Fzd*3 (D) and *Fzd9* (E) in cultured myoblasts treated with 1.2 mM of GSK-J4 for 48-hrs. * indicates significantly different from vehicle treated cells at $p < 0.05$ analyzed by *t*-test. Error bar represents SEM. N = 4 or 5 for each data set.

Figure 2.7.

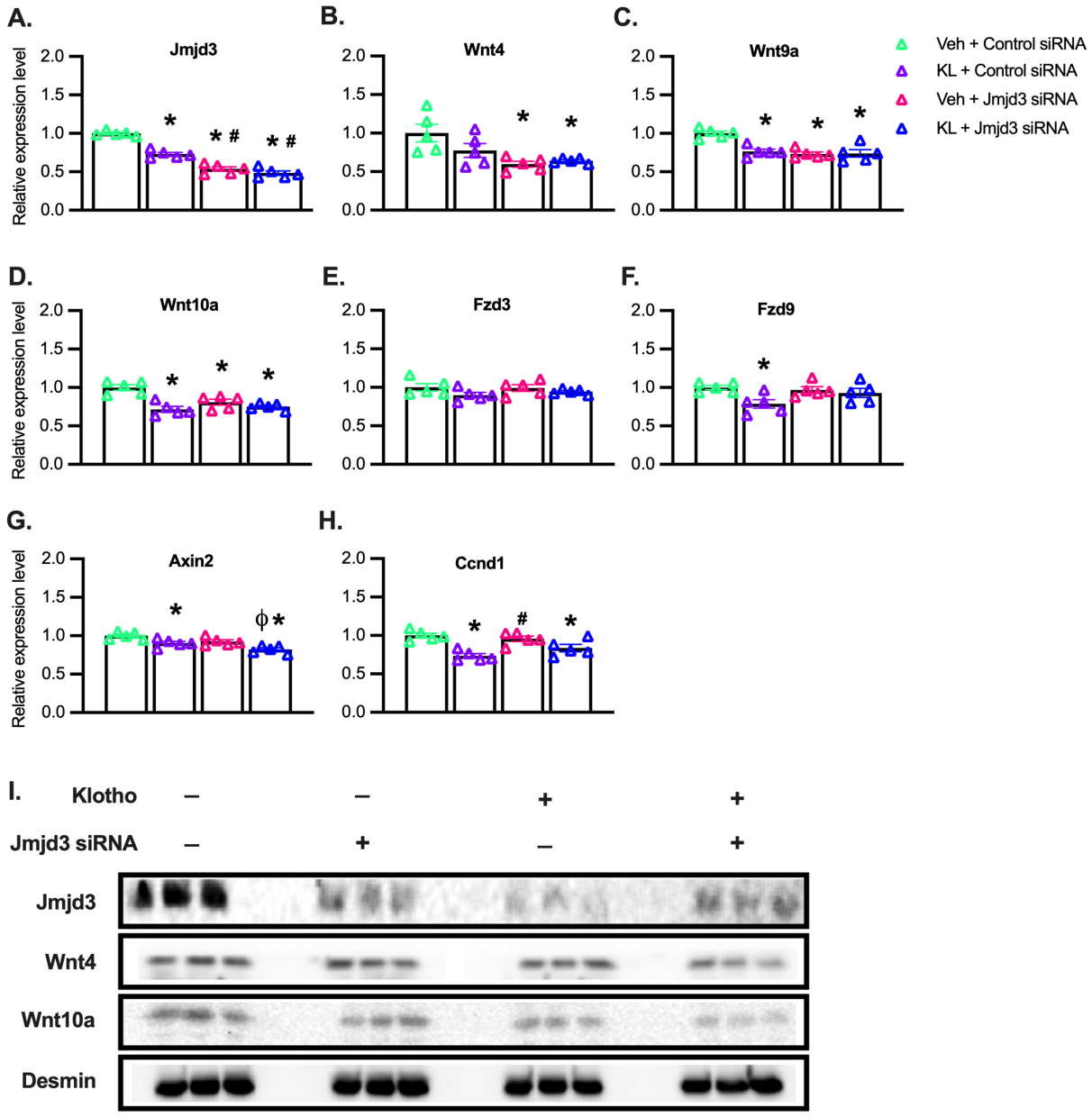

Figure 2.7. Klotho stimulation and Jmjd3 knock-down do not have additive, inhibitory effects on the expression of *Wnt4*, *Wnt9a* and *Wnt10a*. (A-I) Myoblasts were treated with vehicle and control siRNA (Veh + Control siRNA), Klotho and control siRNA (KL + Control siRNA), vehicle and Jmjd3 siRNA (Veh + Jmjd3 siRNA) or Klotho and Jmjd3 siRNA (KL + Jmjd3 siRNA). (A-H) QPCR data showing relative expression of *Jmjd3* (A), *Wnt4* (B), *Wnt9a* (C), *Wnt10a* (D), *Fzd3* (E), *Fzd9* (F), *Axin2* (G) and *Ccnd1* (H) in KL + Control siRNA, Veh + Jmjd3 siRNA or KL + Jmjd3 siRNA treated myoblasts compared to vehicle treated controls. For all bar charts, * indicates significantly different from Veh + Control siRNA treated cells at $p < 0.05$ analyzed by one-way ANOVA with Tukey's multiple comparisons test. # indicates significantly different from KL + Control siRNA treated cells at $p < 0.05$ analyzed by one-way ANOVA with Tukey's multiple comparisons test. ϕ indicates significantly different from Veh + Jmjd3 siRNA treated cells at $p < 0.05$ analyzed by one-way ANOVA with Tukey's multiple comparisons test. Error bar represents SEM. N = 5 for all qPCR data sets. (I) Western blot analysis showing effects of Klotho, Jmjd3 RNAi or Jmjd3 RNAi with Klotho on Jmjd3 (180 kDa), Wnt4 (50 kDa), Wnt10a (46 kDa) and loading control desmin (60 kDa). Wnt9a protein was undetected in all groups. N = 3 for all groups.

Figure 2.8.

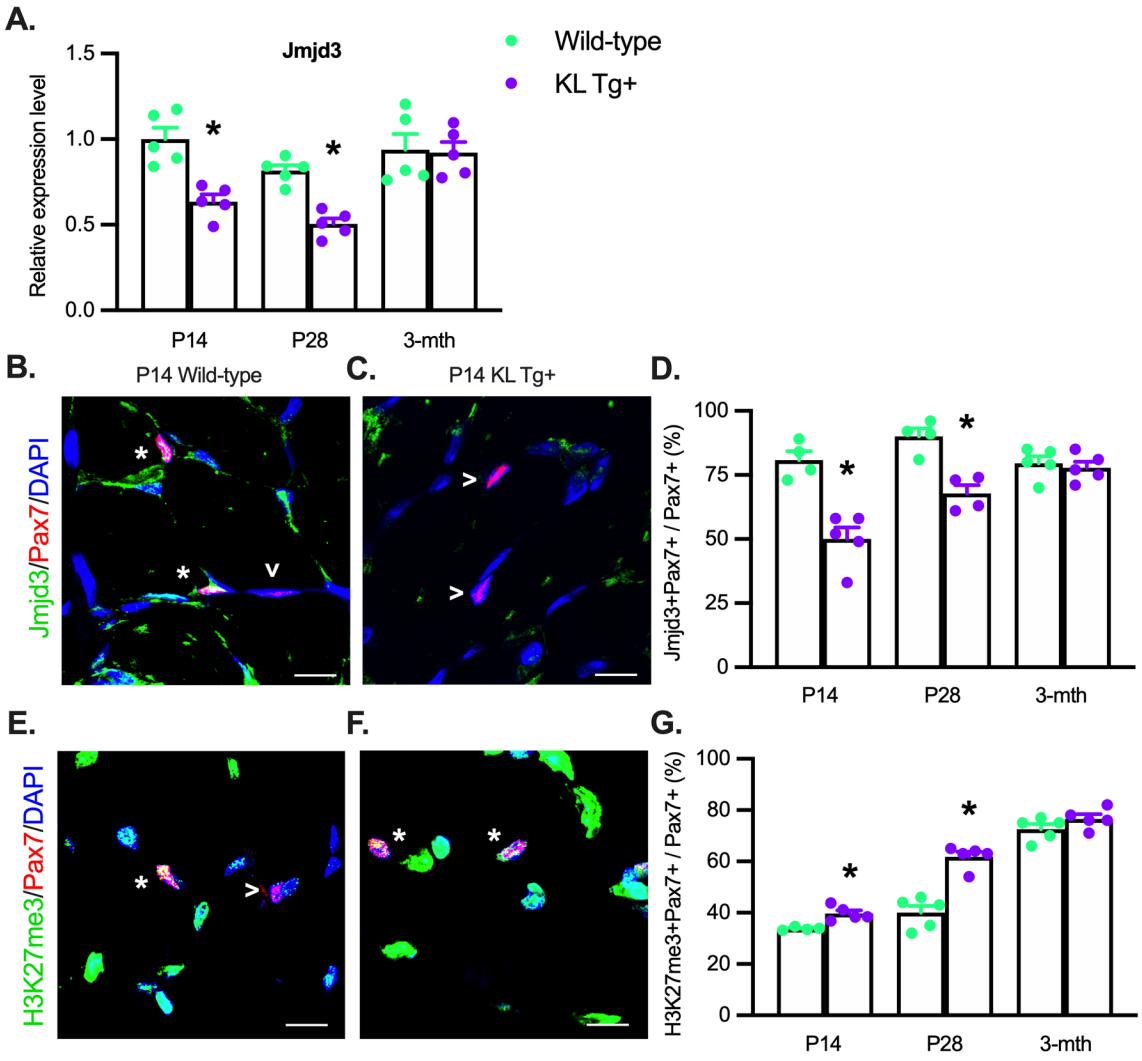

Figure 2.8. ***Klotho*** **transgene expression reduces** ***Jmjd3*** **transcripts and localization in Pax7+ cells and increases H3K27 methylation Pax7+ cells in early postnatal development.** (A) QPCR analysis showing *Jmjd3* in quadriceps muscle lysates of Wt and KL Tg+ mice. (B, C) Representative images of quadriceps muscle sections from P14 Wt (B) and KL Tg+ (C) mice showing immunofluorescent double-labeling for Pax7 and Jmjd3. * indicates Pax7+ cells that were also Jmjd3+. Open arrowheads (>) indicate Pax7+ single-labeled cells. (D) Ratio of Jmjd3+/Pax7+ cells to total Pax7+ cells in sections of quadriceps muscles. (E, F) Representative images of P14 Wt (E) and KL Tg+ (F) showing immunofluorescent double labeling for Pax7 and trimethylated H3K27 (H3K27me3) in quadriceps muscle cross-sections. * indicates Pax7+ cells that were also H3K27me3+. Open arrowheads (>) indicate Pax7+ single-labeled cells. (G) Ratio of H3K27me3+/Pax7+ cells to total Pax7+ cells in quadriceps muscles sections. For all bar charts, * indicates significantly different from age-matched Wt at $p < 0.05$ analyzed by *t*-test. Error bar represents SEM. N = 4 or 5 for each data set.

Figure 2.9.

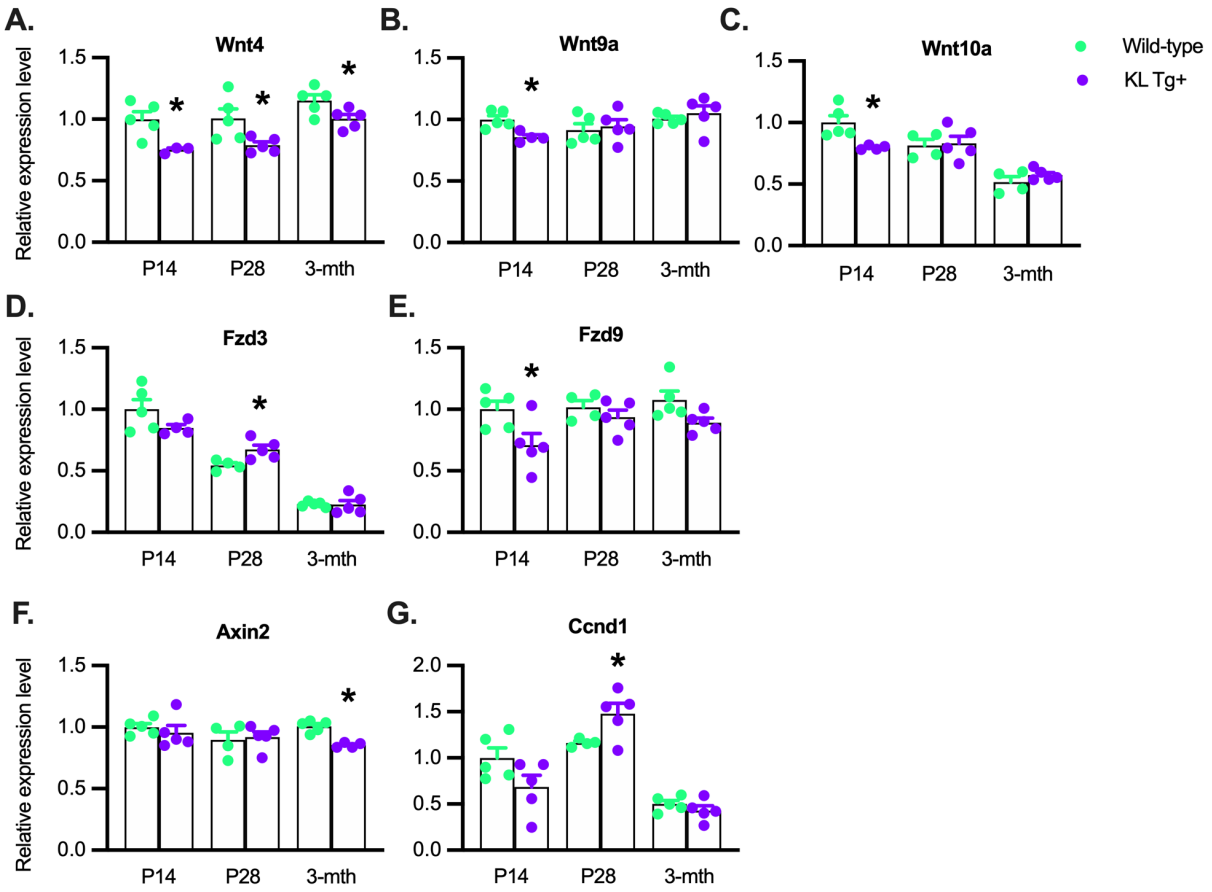

Figure 2.9. ***Klotho*** **transgene expression reduces the expression of Wnt4, Wnt9a and Wnt10a during early postnatal muscle growth.** (A-G) QPCR data showing relative expression for transcripts of *Wnt4* (A), *Wnt9a* (B), *Wnt10a* (C), *Fzd3* (D), *Fzd9* (E), *Axin2* (F) and *Ccnd1* (G) in quadriceps muscles of Wt and KL Tg+ mice. * indicates significantly different from age-matched Wt at $P < 0.05$ analyzed by *t*-test. Error bar represents SEM. N = 3-5 for each data set.

Figure 2.10.

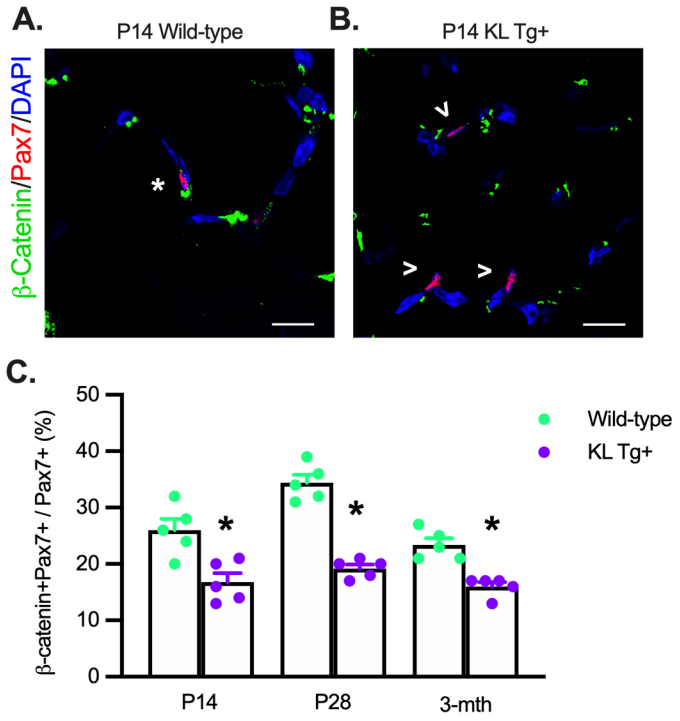

Figure 2.10. ***Klotho*** **transgene expression reduces Wnt-signaling in Pax7+ cells during early postnatal muscle growth.** (A, B) Sections of Wt (A) and KL Tg+ (B) quadriceps muscle at P14 labeled with anti-Pax7 (red), anti- β-catenin (green) and DNA labeled with DAPI (blue). * indicates Pax7+ cells also expressing active β-catenin+. Open arrowheads (>) indicate Pax7+ single-labeled cells. Bar = 10 μm. (C) Ratio of Pax7+ cells that showed activated β-catenin relative to total Pax7+ cells in Wt and KL Tg+ quadriceps muscles. * indicates significantly different from age-matched Wt at $p < 0.05$ analyzed by *t*-test. Error bar represents SEM. N = 5 for each data set.

Supplemental Figure 2.1.

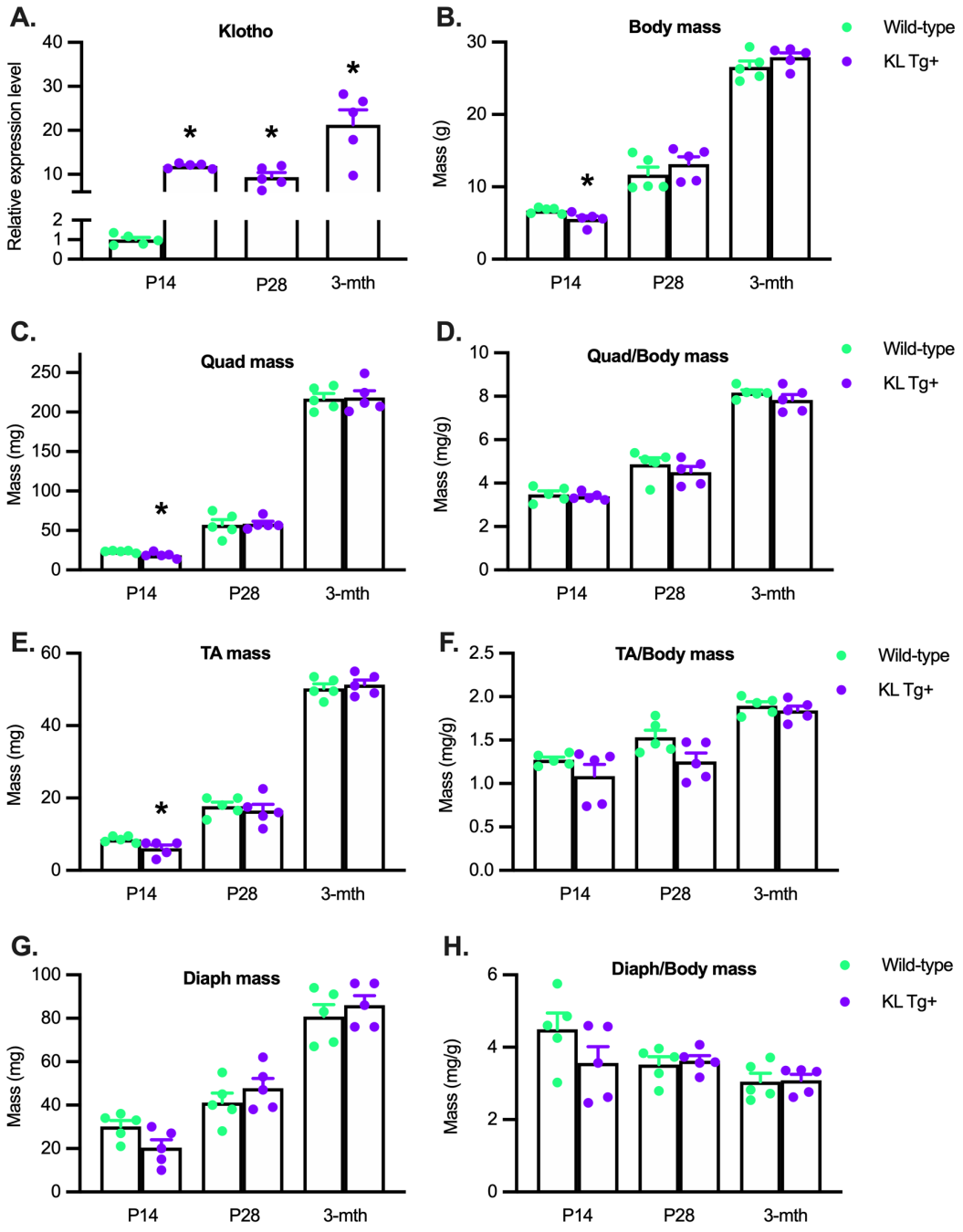

<u>Supplemental Figure 2.1.</u> Expression of a *klotho* transgene affects body mass and hindlimb muscle mass. (A) QPCR data showing relative expression of *klotho* in quadriceps muscle lysates of P14 Wt and P14, P28 and 3-months KL Tg+ mice show expression of a *klotho* transgene increases *klotho* transcripts throughout development. * indicates significantly different from P14 Wt at $p < 0.05$ analyzed by one-way ANOVA followed by Dunnett's multiple comparisons test. Error bar represents SEM. N = 5 for each data set. (B) Body mass (g) of Wt and KL Tg+ mice at P14, P28 and 3-months. (C) Quadriceps mass (mg) of Wt and KL Tg+ mice. (D) Quadriceps mass normalized to body mass (mg/g) of Wt and KL Tg+ mice. (E) TA mass (mg) of Wt and KL Tg+ mice. (F) TA mass normalized to body mass (mg/g) of Wt and KL Tg+ mice. (G) Diaphragm mass (mg) of Wt and KL Tg+ mice. (H) Diaphragm mass normalized to body mass (mg/g) of Wt and KL Tg+ mice. For B-H, * indicates significantly different from age-matched Wt at $p < 0.05$ analyzed by *t*-test. Error bar represents SEM. N = 5 for each data set.

DISCUSSION

The function of *klotho* as an anti-aging gene has been validated in many organs and tissues in which its age-related loss contributes to senescence. For example, the progressive decline in Klotho in aging skeletal muscle diminishes mitochondrial function in myogenic cells and reduces the regenerative capacity of muscle.[63] In addition, the accelerated, epigenetic silencing of *klotho* expression in dystrophic muscle contributes to losses of muscle function, reductions in satellite cell numbers and increases in muscle fibrosis, all of which are characteristics of aging muscle.[12] Because of those associations between reductions of *klotho* expression in aging and diseased muscle and physiological changes associated with aging, we were surprised to learn that the period of most rapid reduction of *klotho* expression occurs in the first few weeks of postnatal muscle development, [12] suggesting that Klotho may play a significant, regulatory role in development, as well as aging. The findings of our investigation show that increases in *klotho* expression during postnatal muscle growth cause transient increases in satellite cell numbers and affect the rate of muscle fiber growth in young mice. Furthermore, our results identify a novel pathway through which Klotho can influence myogenesis by reducing expression of the histone demethylase Jmjd3 in muscle, leading to reductions in the expression of Wnt family genes and inhibition of canonical Wnt signaling in satellite cells.

The transient increase in Pax7+ cells in postnatal muscle that was caused by expression of the *klotho* transgene indicates that Klotho stimulates the expansion of populations of activated myogenic cells, but does not influence satellite cell activation. Furthermore, those increases in numbers of myogenic cells is attributable to increased proliferation because Klotho stimulation of activated myogenic cells increases the proportion that contain nuclear Ki67, a marker of cell proliferation, without affecting apoptosis or necrosis.[12] At P14, when over 80% of satellite cells are activated, [4,5] we found that elevated Klotho production caused the greatest expansion of Pax7+ cell numbers. However, our data show that the transgene had no effect on numbers of

Pax7+ cells at 3-months of age, when fewer than 1% of satellite cells are in the cell cycle.[7] The amplification of satellite cell numbers during the first 3 weeks of postnatal development can have long-term consequences on muscle growth, because the majority of those cells fuse with existing fibers to become myonuclei and the adult number of myonuclei is established by P21.[9] Although the Klotho-mediated amplification of Pax7+ cell proliferation in early postnatal development was short-lived, we found that muscle fibers in Klotho transgenic mice were over 24% larger in diameter than fibers in wild-type muscles at 3-months of age, which corresponds to ~24 years of age for humans. This long-term increase in muscle fiber size that extends into adulthood is converse to the consequence of ablating satellite cells from early postnatal muscle. Experimental depletion of ~70% of satellite cells from P28 mouse muscles significantly reduced subsequent growth of muscle fibers.[10] These observations indicate that the developmental significance of the relatively high levels of Klotho expression that occur in muscles of early postnatal mice is to amplify the numbers of activated myogenic cells, which then increase muscle growth at subsequent stages of development. They also show that the transient delivery of exogenous factors to growing muscles during early postnatal growth could lead to larger muscle fibers in adulthood.

Because of the well-established importance of epigenetic regulatory factors for controlling the proliferation and differentiation of myogenic cells, we assayed whether the influence of Klotho on myogenesis could be mediated by changes in the expression of enzymes that are involved in epigenetic modification of myogenic genes. Although Klotho did not affect expression of some of the best characterized epigenetic regulatory factors involved in myogenesis, we observed a strong down-regulation of Jmjd3 in myoblasts stimulated with Klotho *in vitro* and in muscles expressing the *klotho* transgene *in vivo.* Jmjd3 plays a significant role in removing silencing histone marks from genes that regulate development from the earliest stages of embryogenesis through to differentiation of specific cell lineages in adult organisms. In the early mesodermal

lineage, from which skeletal muscle eventually arises, Jmjd3 influences mesoderm differentiation and Jmjd3 mutation in embryonic stem cells increases H3K27 methylation at the promoter of the mesodermal regulator, *Brachyury*, leading to reductions in Wnt-induced mesodermal differentiation.[64] Although a role for Jmjd3 in affecting myogenesis has not been identified in previous investigations, the forced expression of ectopic Jmjd3 in human pluripotent stem cells can induce their expression of muscle specific genes, including Pax7.[30] That observation suggested the possibility that Jmjd3 may also regulate development of committed myogenic cells, which our data now verify. Notably, the down-regulation of *Jmjd3* expression and the reduced proportion of Pax7+ cells that expressed detectible Jmjd3 in Klotho transgenic muscles occurred in young muscles, but not in adult muscles. This indicates that the regulatory roles of Klotho modulation of Jmjd3 may be complementary to the role of another H3K27 demethylase, UTX, in adult myogenesis. Although no defects in developmental myogenesis were observed in mice in which *Utx* was ablated in satellite cells, myogenesis in adult muscle following acute injury was impaired in the mutants, leading to slower muscle growth and regeneration following injury.[29]

Our findings that Klotho reduced the expression of *Wnt* genes in muscle *in vivo* and *in vitro* and that the inhibitory effects on *Wnt4*, *Wnt9a*, *Wnt10a* and *Fzd9* expression generally declined as postnatal development proceeded, indicates that the effects of Klotho on early postnatal myogenesis occur, in part, through inhibition of Wnt signaling. The reduced expression of *Wnt* genes specifically in early postnatal development is important because signaling initiated by Wnt binding to receptors in the Fzd family has powerful influences on myogenesis. For example, signaling through the canonical, β-catenin-dependent Wnt pathway is required for satellite cell differentiation [54] and pharmacological activation of the canonical pathway enhances muscle differentiation.[54,65-67] Wnt4, Wnt9a and Wnt10a can increase β-catenin activity leading to

activation of the canonical pathway.[68-73] Similarly, Wnt ligation of Fzd9 can increase activation of the canonical pathway.[74-76] Numerous observations support the conclusion that Wnt4, Wnt9a and Wnt10a can promote muscle differentiation. The expression of each is elevated at the onset of muscle differentiation, coinciding with increases in β-catenin activation [56,57] and over-expression of Wnt4 in differentiating muscles increased expression of target genes in the canonical pathway.[57] In addition, over-expression of either Wnt4 or Wnt9a increased muscle differentiation *in vitro*.[56,57] Although inhibition of Wnt signaling by Klotho could also potentially occur through Jmjd3-independent mechanisms that have not been identified, our findings show that the primary pathway activated by Klotho for inhibition of at least some Wnt family members involves Jmjd3. We found that the magnitude of inhibition of expression of Wnt4, Wnt9a and Wnt10a in Klotho treated cells was not further increased by Jmjd3 siRNA treatments, indicating that reductions in the expression of those Wnt family members by Klotho and Jmjd3 siRNA occurred predominantly through a common pathway.

The negative regulation of the expression of Wnt family members by Klotho introduces a novel, epigenetic mechanism through which Klotho can influence Wnt function and myogenesis. Previous investigators have shown that Klotho can bind to Wnt1, Wnt3a, Wnt4, Wnt5a and Wnt7a [77,78] and have shown that the binding can inhibit activity of at least Wnt3a in a cell free system.[77] Furthermore, Klotho treatment of isolated muscle fibers *in vitro* diminished Wnt signaling, which was attributed to Klotho binding to extracellular Wnt.[22] However, our findings show that Klotho can influence Wnt function and myogenesis through an epigenetic pathway. There are important, physiological differences between Wnt inhibition by binding soluble Klotho in the extracellular space versus the novel mechanism we propose. First, Wnt inhibition achieved by maintaining gene silencing of Wnt family members would provide a mechanism for long-term inhibition that does not require continuous secretion of Klotho. In addition, the mechanism that we propose would suppress expression of specific Wnt receptors only in cells

that express Klotho receptors. This would provide more specific targeting of the inhibitory influence than achieved by Klotho acting only as an extracellular Wnt antagonist.

Although our findings show that Klotho decreases the expression of Wnt family members in myogenic cells, which is associated with increases in myogenic cell proliferation and reductions in their differentiation, there may be other less direct pathways through which increases in Klotho influence Wnt-mediated regulation of myogenesis that we have not identified in this investigation. For example, because Wnt4 is a secreted ligand that can act through autocrine or paracrine pathways, there may be non-muscle cell types *in vivo* in which Wnt4 expression is reduced by Klotho, leading to less activation of the canonical Wnt pathway in muscle cell through a paracrine effect. Nevertheless, as shown by previous investigators, [56] knock-down of Wnt4 expression in myoblasts is sufficient to significantly reduce their differentiation, expression of myogenin and their subsequent growth as myotubes, following fusion. Thus, the reduction of Wnt expression in myogenic cells that are stimulated with Klotho or in which Jmjd3 expression is reduced is sufficient to explain the reductions in myogenin expression, muscle differentiation and fiber growth that we report in our investigation.

The most parsimonious interpretation of our findings in light of current knowledge of the role of Wnt signaling in muscle differentiation is that Klotho acts on myogenic cells after their activation, leading to inhibition of Wnt expression and diminished signaling through the canonical Wnt pathway. That disruption in Wnt signaling slows myogenic cell differentiation which produces a transient amplification of myogenic cell numbers. In addition to expanding numbers of myogenic cells by delaying their differentiation, the pro-mitotic influence of Klotho on activated myogenic cells would further increase their numbers.[12] In natural, postnatal myogenesis this regulatory influence of Klotho would be limited, in part, by the decline in Klotho production in young mice as development proceeds. However, as our findings show, when reductions in *klotho*

expression in muscle are prevented by expression of a *klotho* transgene, the influences of Klotho on the numbers of Pax7+ cells and on the level of expression of Jmjd3 and specific members of the Wnt family still occur only in early postnatal myogenesis. That observation shows that additional, unidentified mechanisms are in place that limit the influences of Klotho in early postnatal muscle development, in addition to changes in *klotho* expression. Those mechanisms are subject to continuing studies.

REFERENCES

1. Dumont NA, Wang YX, Rudnicki MA. Intrinsic and extrinsic mechanisms regulating satellite cell function. *Development*. May 2015;142(9):1572-81. doi:10.1242/dev.114223

2. Dhawan J, Rando TA. Stem cells in postnatal myogenesis: molecular mechanisms of satellite cell quiescence, activation and replenishment. *Trends Cell Biol*. Dec 2005;15(12):666-73. doi:10.1016/j.tcb.2005.10.007

3. Cornelison D. "Known Unknowns": Current Questions in Muscle Satellite Cell Biology. *Curr Top Dev Biol*. 2018;126:205-233. doi:10.1016/bs.ctdb.2017.08.006

4. Schultz E. Satellite cell proliferative compartments in growing skeletal muscles. *Dev Biol*. Apr 1996;175(1):84-94. doi:10.1006/dbio.1996.0097

5. Shinin V, Gayraud-Morel B, Gomès D, Tajbakhsh S. Asymmetric division and cosegregation of template DNA strands in adult muscle satellite cells. *Nat Cell Biol*. Jul 2006;8(7):677-87. doi:10.1038/ncb1425

6. Moss FP, Leblond CP. Satellite cells as the source of nuclei in muscles of growing rats. *Anat Rec*. Aug 1971;170(4):421-35. doi:10.1002/ar.1091700405

7. Ontell M, Feng KC, Klueber K, Dunn RF, Taylor F. Myosatellite cells, growth, and regeneration in murine dystrophic muscle: a quantitative study. *Anat Rec*. Feb 1984;208(2):159-74. doi:10.1002/ar.1092080203

8. Gattazzo F, Laurent B, Relaix F, Rouard H, Didier N. Distinct Phases of Postnatal Skeletal Muscle Growth Govern the Progressive Establishment of Muscle Stem Cell Quiescence. *Stem Cell Reports*. 09 08 2020;15(3):597-611. doi:10.1016/j.stemcr.2020.07.011

9. White RB, Biérinx AS, Gnocchi VF, Zammit PS. Dynamics of muscle fibre growth during postnatal mouse development. *BMC Dev Biol*. Feb 2010;10:21. doi:10.1186/1471-213X-10-21

10. Bachman JF, Klose A, Liu W, et al. Prepubertal skeletal muscle growth requires Pax7-expressing satellite cell-derived myonuclear contribution. *Development*. 10 2018;145(20): dev167197. doi:10.1242/dev.167197

11. Kurosaka M, Naito H, Ogura Y, Kojima A, Goto K, Katamoto S. Effects of voluntary wheel running on satellite cells in the rat plantaris muscle. *J Sports Sci Med*. 2009;8(1):51-7.

12. Wehling-Henricks M, Li Z, Lindsey C, et al. Klotho gene silencing promotes pathology in the mdx mouse model of Duchenne muscular dystrophy. *Hum Mol Genet*. 2016;25(12):2465–2482. doi:10.1093/hmg/ddw111

13. Bachman JF, Blanc RS, Paris ND, et al. Radiation-Induced Damage to Prepubertal Pax7+ Skeletal Muscle Stem Cells Drives Lifelong Deficits in Myofiber Size and Nuclear Number. *iScience*. Nov 20 2020;23(11):101760. doi:10.1016/j.isci.2020.101760

14. Bachman JF, Chakkalakal JV. Insights into muscle stem cell dynamics during postnatal development. *FEBS J*. 2021;10.1111/febs.15856. doi:10.1111/febs.15856

15. Fry CS, Lee JD, Mula J, et al. Inducible depletion of satellite cells in adult, sedentary mice impairs muscle regenerative capacity without affecting sarcopenia. *Nat Med*. Jan 2015;21(1):76-80. doi:10.1038/nm.3710

16. Tapscott SJ, Davis RL, Thayer MJ, Cheng PF, Weintraub H, Lassar AB. MyoD1: a nuclear phosphoprotein requiring a Myc homology region to convert fibroblasts to myoblasts. *Science*. Oct 1988;242(4877):405-11. doi:10.1126/science.3175662

17. Rudnicki MA, Schnegelsberg PN, Stead RH, Braun T, Arnold HH, Jaenisch R. MyoD or Myf-5 is required for the formation of skeletal muscle. *Cell*. Dec 1993;75(7):1351-9. doi:10.1016/0092-8674(93)90621-v

18. Yablonka-Reuveni Z, Rudnicki MA, Rivera AJ, Primig M, Anderson JE, Natanson P. The transition from proliferation to differentiation is delayed in satellite cells from mice lacking MyoD. *Dev Biol*. Jun 1999;210(2):440-55. doi:10.1006/dbio.1999.9284

19. Kuang S, Gillespie MA, Rudnicki MA. Niche regulation of muscle satellite cell self-renewal and differentiation. *Cell Stem Cell*. Jan 2008;2(1):22-31. doi:10.1016/j.stem.2007.12.012

20. Rawls A, Valdez MR, Zhang W, Richardson J, Klein WH, Olson EN. Overlapping functions of the myogenic bHLH genes MRF4 and MyoD revealed in double mutant mice. *Development*. Jul 1998;125(13):2349-58. doi.org/10.1242/dev.125.13.2349

21. Vivian JL, Olson EN, Klein WH. Thoracic skeletal defects in myogenin- and MRF4-deficient mice correlate with early defects in myotome and intercostal musculature. *Dev Biol*. Aug 2000;224(1):29-41. doi:10.1006/dbio.2000.9788

22. Ahrens HE, Huettemeister J, Schmidt M, Kaether C, von Maltzahn J. Klotho expression is a prerequisite for proper muscle stem cell function and regeneration of skeletal muscle. *Skelet Muscle*. 07 2018;8(1):20. doi:10.1186/s13395-018-0166-x

23. Caretti G, Di Padova M, Micales B, Lyons GE, Sartorelli V. The Polycomb Ezh2 methyltransferase regulates muscle gene expression and skeletal muscle differentiation. *Genes Dev*. Nov 2004;18(21):2627-38. doi:10.1101/gad.1241904

24. Juan AH, Derfoul A, Feng X, et al. Polycomb EZH2 controls self-renewal and safeguards the transcriptional identity of skeletal muscle stem cells. *Genes Dev*. Apr 2011;25(8):789-94. doi:10.1101/gad.2027911

25. Adhikari A, Davie J. JARID2 and the PRC2 complex regulate skeletal muscle differentiation through regulation of canonical Wnt signaling. *Epigenetics Chromatin*. 08 2018;11(1):46. doi:10.1186/s13072-018-0217-x

26. Hong S, Cho YW, Yu LR, Yu H, Veenstra TD, Ge K. Identification of JmjC domain-containing UTX and JMJD3 as histone H3 lysine 27 demethylases. *Proc Natl Acad Sci U S A*. Nov 2007;104(47):18439-44. doi:10.1073/pnas.0707292104

27. Agger K, Cloos PA, Christensen J, et al. UTX and JMJD3 are histone H3K27 demethylases involved in HOX gene regulation and development. *Nature*. Oct 2007;449(7163):731-4. doi:10.1038/nature06145

28. Seenundun S, Rampalli S, Liu QC, et al. UTX mediates demethylation of H3K27me3 at muscle-specific genes during myogenesis. *EMBO J*. Apr 2010;29(8):1401-11. doi:10.1038/emboj.2010.37

29. Faralli H, Wang C, Nakka K, et al. UTX demethylase activity is required for satellite cell-mediated muscle regeneration. *J Clin Invest*. Apr 2016;126(4):1555-65. doi:10.1172/JCI83239

30. Akiyama T, Wakabayashi S, Soma A, et al. Transient ectopic expression of the histone demethylase JMJD3 accelerates the differentiation of human pluripotent stem cells. *Development*. Oct 2016;143(20):3674-3685. doi:10.1242/dev.139360

31. Akiyama T, Wakabayashi S, Soma A, et al. Epigenetic Manipulation Facilitates the Generation of Skeletal Muscle Cells from Pluripotent Stem Cells. *Stem Cells Int*. 2017;2017:7215010. doi:10.1155/2017/7215010

32. Schindelin J, Arganda-Carreras I, Frise E, et al. Fiji: an open-source platform for biological-image analysis. *Nat Methods*. Jun 2012;9(7):676-82. doi:10.1038/nmeth.2019

33. Schneider CA, Rasband WS, Eliceiri KW. NIH Image to ImageJ: 25 years of image analysis. *Nat Methods*. Jul 2012;9(7):671-5. doi:10.1038/nmeth.2089

34. White JP, Baltgalvis KA, Sato S, Wilson LB, Carson JA. Effect of nandrolone decanoate administration on recovery from bupivacaine-induced muscle injury. *J Appl Physiol (1985)*. Nov 2009;107(5):1420-30. doi:10.1152/japplphysiol.00668.2009

35. Welc SS, Wehling-Henricks M, Kuro-O M, Thomas KA, Tidball JG. Modulation of Klotho expression in injured muscle perturbs Wnt signalling and influences the rate of muscle growth. *Exp Physiol*. Jan 2020;105(1):132-147. doi:10.1113/EP088142

36. Vandesompele J, De Preter K, Pattyn F, et al. Accurate normalization of real-time quantitative RT-PCR data by geometric averaging of multiple internal control genes. *Genome Biol*. Jun 2002;3(7):RESEARCH0034. doi:10.1186/gb-2002-3-7-research0034

37. Thomas KC, Zheng XF, Garces Suarez F, et al. Evidence based selection of commonly used RT-qPCR reference genes for the analysis of mouse skeletal muscle. *PLoS One*. 2014;9(2):e88653. doi:10.1371/journal.pone.0088653

38. Hildyard JCW, Finch AM, Wells DJ. Identification of qPCR reference genes suitable for normalizing gene expression in the mdx mouse model of Duchenne muscular dystrophy. *PLoS One*. 2019;14(1):e0211384. doi:10.1371/journal.pone.0211384

39. Villalta SA, Rinaldi C, Deng B, Liu G, Fedor B, Tidball JG. Interleukin-10 reduces the pathology of mdx muscular dystrophy by deactivating M1 macrophages and modulating macrophage phenotype. *Hum Mol Genet*. Feb 2011;20(4):790-805. doi:10.1093/hmg/ddq523

40. Kruidenier L, Chung CW, Cheng Z, et al. A selective jumonji H3K27 demethylase inhibitor modulates the proinflammatory macrophage response. *Nature*. Aug 2012;488(7411):404-8. doi:10.1038/nature11262

41. Heinemann B, Nielsen JM, Hudlebusch HR, et al. Inhibition of demethylases by GSK-J1/J4. *Nature*. Oct 2014;514(7520):E1-2. doi:10.1038/nature13688

42. Langmead B, Salzberg SL. Fast gapped-read alignment with Bowtie 2. *Nat Methods*. Mar 04 2012;9(4):357-9. doi:10.1038/nmeth.1923

43. Li H, Handsaker B, Wysoker A, et al. The Sequence Alignment/Map format and SAMtools. *Bioinformatics*. Aug 15 2009;25(16):2078-9. doi:10.1093/bioinformatics/btp352

44. Zhang Y, Liu T, Meyer CA, et al. Model-based analysis of ChIP-Seq (MACS). *Genome Biol*. 2008;9(9):R137. doi:10.1186/gb-2008-9-9-r137

45. Ramírez F, Ryan DP, Grüning B, et al. deepTools2: a next generation web server for deep-sequencing data analysis. *Nucleic Acids Res*. 07 08 2016;44(W1):W160-5. doi:10.1093/nar/gkw257

46. Gentleman RC, Carey VJ, Bates DM, et al. Bioconductor: open software development for computational biology and bioinformatics. *Genome Biol*. 2004;5(10):R80. doi:10.1186/gb-2004-5-10-r80

47. Huber W, Carey VJ, Gentleman R, et al. Orchestrating high-throughput genomic analysis with Bioconductor. *Nat Methods*. Feb 2015;12(2):115-21. doi:10.1038/nmeth.3252

48. Team BC, Maintainer BP. *TxDb.Mmusculus.UCSC.mm10.ensGene: Annotation package for TxDb object(s) . R package version 3.4.0.* 2016.

49. Kanehisa M, Sato Y, Kawashima M, Furumichi M, Tanabe M. KEGG as a reference resource for gene and protein annotation. *Nucleic Acids Res*. Jan 2016;44(D1):D457-62. doi:10.1093/nar/gkv1070

50. Huang dW, Sherman BT, Lempicki RA. Bioinformatics enrichment tools: paths toward the comprehensive functional analysis of large gene lists. *Nucleic Acids Res*. Jan 2009;37(1):1-13. doi:10.1093/nar/gkn923

51. Huang dW, Sherman BT, Lempicki RA. Systematic and integrative analysis of large gene lists using DAVID bioinformatics resources. *Nat Protoc*. 2009;4(1):44-57. doi:10.1038/nprot.2008.211

52. Palacios D, Mozzetta C, Consalvi S, et al. TNF/p38α/polycomb signaling to Pax7 locus in satellite cells links inflammation to the epigenetic control of muscle regeneration. *Cell Stem Cell*. Oct 2010;7(4):455-69. doi:10.1016/j.stem.2010.08.013

53. Dilworth FJ, Blais A. Epigenetic regulation of satellite cell activation during muscle regeneration. *Stem Cell Res Ther*. 2011;2(2):18. doi:10.1186/scrt59

54. Brack AS, Conboy IM, Conboy MJ, Shen J, Rando TA. A temporal switch from notch to Wnt signaling in muscle stem cells is necessary for normal adult myogenesis. *Cell Stem Cell*. Jan 2008;2(1):50-9. doi:10.1016/j.stem.2007.10.006

55. Le Grand F, Jones AE, Seale V, Scimè A, Rudnicki MA. Wnt7a activates the planar cell polarity pathway to drive the symmetric expansion of satellite stem cells. *Cell Stem Cell*. Jun 2009;4(6):535-47. doi:10.1016/j.stem.2009.03.013

56. Bernardi H, Gay S, Fedon Y, Vernus B, Bonnieu A, Bacou F. Wnt4 activates the canonical β-catenin pathway and regulates negatively myostatin: functional implication in

myogenesis. *Am J Physiol Cell Physiol*. May 2011;300(5):C1122-38. doi:10.1152/ajpcell.00214.2010

57. Tanaka S, Terada K, Nohno T. Canonical Wnt signaling is involved in switching from cell proliferation to myogenic differentiation of mouse myoblast cells. *J Mol Signal*. Oct 2011;6:12. doi:10.1186/1750-2187-6-12

58. Lustig B, Jerchow B, Sachs M, et al. Negative feedback loop of Wnt signaling through upregulation of conductin/axin2 in colorectal and liver tumors. *Mol Cell Biol*. Feb 2002;22(4):1184-93. doi:10.1128/mcb.22.4.1184-1193.2002

59. Baldin V, Lukas J, Marcote MJ, Pagano M, Draetta G. Cyclin D1 is a nuclear protein required for cell cycle progression in G1. *Genes Dev*. May 1993;7(5):812-21. doi:10.1101/gad.7.5.812

60. Sherr CJ. The Pezcoller lecture: cancer cell cycles revisited. *Cancer Res*. Jul 2000;60(14):3689-95.

61. Cadigan KM, Nusse R. Wnt signaling: a common theme in animal development. *Genes Dev*. Dec 1997;11(24):3286-305. doi:10.1101/gad.11.24.3286

62. Sakanaka C. Phosphorylation and regulation of beta-catenin by casein kinase I epsilon. *J Biochem*. Nov 2002;132(5):697-703. doi:10.1093/oxfordjournals.jbchem.a003276

63. Sahu A, Mamiya H, Shinde SN, et al. Age-related declines in α-Klotho drive progenitor cell mitochondrial dysfunction and impaired muscle regeneration. *Nat Commun*. 11 2018;9(1):4859. doi:10.1038/s41467-018-07253-3

64. Ohtani K, Zhao C, Dobreva G, et al. Jmjd3 controls mesodermal and cardiovascular differentiation of embryonic stem cells. *Circ Res*. Sep 2013;113(7):856-62. doi:10.1161/CIRCRESAHA.113.302035

65. Polesskaya A, Seale P, Rudnicki MA. Wnt signaling induces the myogenic specification of resident CD45+ adult stem cells during muscle regeneration. *Cell*. Jun 2003;113(7):841-52. doi:10.1016/s0092-8674(03)00437-9

66. Rochat A, Fernandez A, Vandromme M, et al. Insulin and wnt1 pathways cooperate to induce reserve cell activation in differentiation and myotube hypertrophy. *Mol Biol Cell*. Oct 2004;15(10):4544-55. doi:10.1091/mbc.e03-11-0816

67. van der Velden JLJ, Schols AMWJ, Willems J, Kelders MCJM, Langen RCJ. Glycogen synthase kinase 3 suppresses myogenic differentiation through negative regulation of NFATc3. *J Biol Chem*. Jan 2008;283(1):358-366. doi:10.1074/jbc.M707812200

68. Narita T, Sasaoka S, Udagawa K, et al. Wnt10a is involved in AER formation during chick limb development. *Dev Dyn*. Jun 2005;233(2):282-7. doi:10.1002/dvdy.20321

69. Carron C, Pascal A, Djiane A, Boucaut JC, Shi DL, Umbhauer M. Frizzled receptor dimerization is sufficient to activate the Wnt/beta-catenin pathway. *J Cell Sci*. Jun 2003;116(Pt 12):2541-50. doi:10.1242/jcs.00451

70. Später D, Hill TP, O'sullivan RJ, Gruber M, Conner DA, Hartmann C. Wnt9a signaling is required for joint integrity and regulation of Ihh during chondrogenesis. *Development*. Aug 2006;133(15):3039-49. doi:10.1242/dev.02471

71. Cawthorn WP, Bree AJ, Yao Y, et al. Wnt6, Wnt10a and Wnt10b inhibit adipogenesis and stimulate osteoblastogenesis through a β-catenin-dependent mechanism. *Bone*. Feb 2012;50(2):477-89. doi:10.1016/j.bone.2011.08.010

72. Ring L, Neth P, Weber C, Steffens S, Faussner A. β-Catenin-dependent pathway activation by both promiscuous "canonical" WNT3a-, and specific "noncanonical" WNT4- and WNT5a-FZD receptor combinations with strong differences in LRP5 and LRP6 dependency. *Cell Signal*. Feb 2014;26(2):260-7. doi:10.1016/j.cellsig.2013.11.021

73. Zhang B, Wu X, Zhang X, et al. Human umbilical cord mesenchymal stem cell exosomes enhance angiogenesis through the Wnt4/β-catenin pathway. *Stem Cells Transl Med*. May 2015;4(5):513-22. doi:10.5966/sctm.2014-0267

74. Umbhauer M, Djiane A, Goisset C, et al. The C-terminal cytoplasmic Lys-thr-X-X-X-Trp motif in frizzled receptors mediates Wnt/beta-catenin signalling. *EMBO J*. Sep 2000;19(18):4944-54. doi:10.1093/emboj/19.18.4944

75. Karasawa T, Yokokura H, Kitajewski J, Lombroso PJ. Frizzled-9 is activated by Wnt-2 and functions in Wnt/beta -catenin signaling. *J Biol Chem*. Oct 2002;277(40):37479-86. doi:10.1074/jbc.M205658200

76. Winn RA, Marek L, Han SY, et al. Restoration of Wnt-7a expression reverses non-small cell lung cancer cellular transformation through frizzled-9-mediated growth inhibition and promotion of cell differentiation. *J Biol Chem*. May 2005;280(20):19625-34. doi:10.1074/jbc.M409392200

77. Liu H, Fergusson MM, Castilho RM, et al. Augmented Wnt signaling in a mammalian model of accelerated aging. *Science*. Aug 2007;317(5839):803-6. doi:10.1126/science.1143578

78. Zhou L, Li Y, Zhou D, Tan RJ, Liu Y. Loss of Klotho contributes to kidney injury by derepression of Wnt/β-catenin signaling. *J Am Soc Nephrol*. Apr 2013;24(5):771-85. doi:10.1681/ASN.2012080865

CHAPTER III:

“Muscle-specific Jmjd3 is essential for development and neonatal survival”

ABSTRACT

Changes in epigenetic regulation have impacts on skeletal muscle growth, development and regeneration throughout life. We previously showed Klotho promotes the expansion of the satellite cell population during early postnatal development. We also showed that treating muscle cells with Klotho *in vitro* or genetically increasing Klotho *in vivo* reduced the expression of canonical Wnts, downstream Wnt target genes, and active β-catenin in satellite cells. Additionally, Klotho treatments promoted the accumulation of repressive H3K27me2/3 marks at the promotor regions of *Wnt* genes and reduced the expression of the H3K27 demethylase Jmjd3. Because we showed Klotho may influence canonical Wnt signaling and myogenesis by modulating the epigenetic mechanisms regulating H3K27 methylation, we hypothesize that reducing Jmjd3 in satellite cells of developing muscle will promote the expansion of the satellite cell pool in vivo by downregulating canonical Wnt signaling required for myogenic differentiation. Our findings show reducing Jmjd3 in Pax7-expressing cells promotes the accumulation of H3K27me3 repressive marks in Pax7+ cells but does not expand the Pax7+ cell population or promote myogenesis during development. The satellite cells-specific mutation in *Jmjd3* caused significant muscle abnormalities and early postnatal death. Our findings show adequate expression of *Jmjd3* is required for the expression of key myogenic transcription factors *Pax7*, *Myod1* and *Myog* and in the absence of Jmjd3, Wnt expression and canonical Wnt signaling are greatly impaired. These findings suggest muscle-specific Jmjd3 is required for muscle development, canonical Wnt signaling and neonatal survival.

INTRODUCTION

The formation of skeletal muscle happens in three, tightly regulated steps. [1] Muscle cell lineage commitment, progenitor cell proliferation and myogenic differentiation each require unique genetic and epigenetic changes that promote or repress gene expression. [1,2] Embryonic genome mapping suggests histone methylation controls lineage designation. [2,3] Although, changes in histone methylation affect the gene expression of key promyogenic genes during embryonic development and adult muscle regeneration, less is known about the epigenetic changes required during early postnatal muscle growth and development. [2,4-9]

Expression of Pax3 and Pax7 are essential for embryonic muscle progenitor cell designation but have differing roles during later stages of development. [10] For example, Pax7 but not Pax3 is the myogenic transcription factor responsible for promoting the self-renewal capacity in postnatal satellite cells. [10-14] Under conditions promoting growth or regeneration Pax7 is downregulated in satellite cells following the upregulation of terminal myogenic transcription factor myogenin. The temporal switch in gene expression is controlled by changes in epigenetic regulatory mechanisms promoting gene transcription or gene repression like the methylation state of histone 3 lysine 27 (H3K27me). [5-8,15-18] Repressive dimethyl and trimethyl groups on H3K27 (H3K27me2/3) are maintained at the promotor region of myogenin by the polycomb repressive complex 2 (PRC2) and the histone methyl transferase catalytic subunit Ezh2. [18] In response to differentiation cues H3K27me2/3 is removed from the promotor region of *Myog* permitting gene transcription and added to *Pax7* causing gene repression. [7,17]

Functionally opposite of the PRC2 complex and the H3K27 methyltransferase Ezh2 are the H3K27 demethylases Utx (KDM6A) and Jmjd3 (KDM6B) which permit transcriptional activation that is essential for differentiation. [19,20] The importance of demethylating H3K27 during muscle regeneration was established using a satellite cells-specific Utx knockdown. [8] In the absence of

Utx expression in satellite cells following acute injury, muscle was unable to completely regenerate because *Myog* expression was repressed. [8] The role of Utx in muscle growth and development appears to be stage-dependent. For example, Utx plays a key role in embryonic development and is a key regulator of myogenin *in vitro* but others suggest Utx is not required for muscle development *in vivo*. [7,8,21,22]

Despite the known contributions of Utx to myogenesis, less is known about the role of Jmjd3 in developmental myogenesis although *Jmjd3* germline mutants do not survive suggesting Jmjd3 is required for postnatal development. [23] Recent work has shed new light on different effects of Utx and Jmjd3 in stem cell development. Overexpression of the H3K27 demethylase catalytic domain of Jmjd3 (Jmjd3c) upregulated *Pax7* expression in pluripotent stem cells and overexpressing Jmjd3c before overexpressing *Myod1* induced the expression of several myogenic factors including *Myog*. [24] These findings suggest Jmjd3 may contribute to myogenesis during multiple stages in the myogenic pathway. We previously showed that the age-related protein Klotho reduced Jmjd3 which slows the progression of early postnatal myogenesis by affecting key myogenic transcription factors and the canonical Wnt pathway; a pathway that is required for satellite cells to terminally differentiate and contribute to developmental muscle growth. [25-27] Although satellite cell-specific Jmjd3 is not required for adequate adult muscle regeneration, [8] it is plausible that Jmjd3 and but not Utx regulates developmental myogenesis because forced expression of *Jmjd3* in pluripotent cells facilitates differentiation and induction of the myogenic pathway but changes in Utx did not affect myogenesis in healthy tissue. [24,28]

In the present investigation we tested the hypothesis that a satellite cell-specific mutation in *Jmjd3* would cause H3K27 methylation to accumulate in Pax7+ calls and promote satellite cell population expansion in developing muscle. We also tested whether reductions of muscle-

specific Jmjd3 would reflect changes in *Wnt*-family genes and β-catenin-mediated canonical Wnt signaling. In addition to the accumulation of H3K27me3 in Pax7+ cells, our data show that a ~50% reduction of Jmjd3 in Pax7-expressing cells causes significant muscle deformities and neonatal death. Our findings also show Jmjd3 is required for normal expression of key myogenic transcription factors and the expansion of myogenic cell populations. Finally, we show decreasing Jmjd3 in developing muscle reduces *Wnt* gene expression and canonical Wnt signaling.

METHODS

Ethical Approval

All experiments involving the use of animals were performed according to the National Institutes of Health Guide for the Care and Use of Laboratory Animals. All protocols were approved by the Chancellor's Animal Research Committee at the University of California, Los Angeles (Animal Welfare Assurance number A-3196).

Generating the Pax7^{cre}/Jmjd3^{flox} mouse model.

Mice with a satellite cell-targeted deletion of Jmjd3 were generated by outcrossing loxP-Jmjd3-loxP$^{+/+}$ mice (Jax Labs, B6.Cg-*Kdm6b*$^{tm1.1Rbo}$/J) and Pax7/cre$^{+/+}$ mice (Jax Labs, *Pax7*$^{tm1(cre)Mrc}$/J) to generate loxP-Jmjd3-loxP$^{+/-}$, Pax7/cre$^{+/-}$ hemizygous mice. Hemizygous mice were backcrossed with loxP-Jmjd3-loxP$^{+/+}$ mice producing four genotypes: loxP-Jmjd3-loxP$^{+/+}$, Pax7/cre$^{-/-}$ (*Jmjd3* floxed controls); loxP-Jmjd3-loxP$^{+/+}$, Pax7/cre$^{+/-}$ mice (*Jmjd3* floxed); loxP-Jmjd3-loxP$^{+/-}$, Pax7/cre$^{-/-}$ mice (*Jmjd3* hemi controls) and loxP-Jmjd3-loxP$^{+/-}$, Pax7/cre$^{+/-}$ mice (*Jmjd3* hemi). Mice were genotyped at P0 or at weening to validate the presence of floxed alleles and were housed in a specific pathogen-free facility under 12-hour light and dark cycles. For experiments using P0 neonatal muscle, pups and tissue were collected and weighed within 12-hours of birth. All other Pax7^{cre}/Jmjd3^{flox} experimental tissue was weighed at time of dissection and collected 3-months postnatal. Only male mice were used in these studies of 3-months old muscle.

Muscle fiber cross-sectional area

Quadriceps muscles from each mouse were dissected, weighed, and rapidly frozen in isopentane cooled in liquid nitrogen. Frozen muscles were cut at the midbelly in 10 μm thick cross-sections. Quadriceps muscles cross-sections were stained for 10 minutes with hematoxylin followed by three, double-distilled H_2O rinses. Cross-sectional areas (CSA) for no

fewer than 500 fibers in each section were measured. Fibers were sampled from five or more separate locations within the muscle cross-section and digitally measured using ImageJ. [29,30] Classification of small and large fibers was determined by setting three standard deviations from the mean CSA for the control group and quantifying the percent of fibers that fell within those ranges. [31,32]

Production of Pax7 antibody and immunohistochemistry.

Hybridoma cells expressing antibodies to Pax7 were purchased from the Developmental Studies Hybridoma Bank (DSHB, University of Iowa). Cells were cultured in ventilated T-75 flasks with complete medium consisting of Iscove's Modified Dulbecco's Medium (IMDM, Sigma) supplemented with sodium bicarbonate, 1% penicillin-streptomycin (Gibco), and 20% fetal bovine serum (FBS). Complete culture medium containing 20% FBS was added every other day until day 6 in culture at which time serum-free complete medium was added to cultures to maintain a cell density between $5x10^5$ to $1x10^6$ cells/ml. After 14 days in culture, the cells were divided evenly into non-ventilated flasks and diluted with equal volumes serum-free IMDM. After 14-days of non-ventilated culturing conditions, anti-Pax7 conditioned medium was collected and sterile filtered for antibody isolation. Anti-Pax7 was affinity purified from conditioned medium and eluted with 0.1 M glycine. The antibody concentration was determined by A280 absorbance reading with a spectrophotometer using a UV lamp. Antibody specificity was determined by western blot and immunohistochemistry.

Immunofluorescence

Double-labeling for Pax7 and Jmjd3, H3K27me3 or β-catenin.

Frozen sections were air-dried for 30 minutes and fixed with paraformaldehyde (PFA) for 10 minutes, washed for 15 minutes in phosphate-buffered saline (PBS), followed by 40 minutes of antigen retrieval in sodium citrate buffer containing 0.05% Tween-20 (pH = 6.0) and heated in a

water bath to 95 - 100°C. Following a cooling period of 30 minutes, sections were treated with blocking buffer from a mouse-on-mouse immunohistochemistry kit (M.O.M Kit; Vector Laboratories, Burlingame, CA, USA) supplemented with 0.3 M glycine for 1 hour. Sections were co-labeled with anti-Pax7 (1:500; DSHB) or anti-Pax7 (1:50, SCBT #SC-81648, RRID:AB_2159836) and rabbit anti-Jmjd3 (1:200, LifeSpan #LS-C144473, RRID:AB_10987745), rabbit anti-H3K27me3 (1:1000, Cell Signaling #9733, RRID:AB_2616029), or rabbit antibodies to active, non-phosphorylated (Ser45) β-catenin (1:1500, Cell Signaling #19807, RRID:AB_2650576) and incubated with primary antibodies overnight in a humidified chamber at 4°C. Sections were subsequently washed and incubated for 30 minutes with horse anti-mouse Dylight-594 (1:200 Vector #DI-2594, RRID:AB_2336412) and horse anti-rabbit Dylight-488 (1:100 Vector #DI-1088, RRID:AB_2336403). Sections were mounted with Prolong Gold Antifade Mountant containing blue DNA stain DAPI (Invitrogen #P36931). For data expressed as percent co-labeled, cells were determined to be Pax7 and DAPI positive then determined to be Jmjd3, H3K27me3 or β-catenin positive. Data are expressed as the percentage of total Pax7+ satellite cells that also express Jmjd3, H3K27me3 or active β-catenin (Jmjd3+ Pax7+, H3K27me3+ Pax7+ or β-catenin+ Pax7+/ Total Pax7+).

RNA Isolation and quantitative PCR

Whole muscle tissue was mechanically homogenized (Dupont) in Trizol reagent (Invitrogen). RNA was extracted with chloroform, precipitated with isopropanol, and purified using a RNeasy Mini Kit (Qiagen) according to manufacturer's protocol. Total RNA was quantified by the A260 absorbance reading with a spectrophotometer (Beckman). RNA samples isolated from P0 and 3-months old tissue had a concentration greater than or equal to 0.2 µg/µl and an absorbance ratio of 1.8 or higher. RNA quality was determined by the clear separation of 28S and 18S ribosomal RNA by electrophoresis. 2 µg of total RNA were reverse transcribed with Super Script

Reverse Transcriptase II (Invitrogen) using Oligo(dT)$_{12-18}$ Primers (Invitrogen) for product extension. cDNA was used to measure the expression for the genes of interest using SYBR green qPCR master mix (Bio-Rad). Real-time PCR was performed on an iQ5 thermocycler system with optical system software (Bio-Rad). Because genes used to normalize qPCR data can vary with age, disease or treatments, [33-35] we empirically identified *SRP14* and *TBP* as suitable reference genes based on methods previously described. [36] The normalization factor for each sample was calculated using the geometric mean of the Ct-values measured from the two reference genes. The highest relative expression value for each gene was set to 1 and all other expression values were scaled accordingly. QPCR primer sequences are listed in Table 3.1.

Table 3.1.

Gene	Forward	Reverse
Axin2	GACGCACTGACCGACGATTC	CTGCGATGCATCTCTCTCTGG
Ccnd1	CGAGGAGCTGCTGCAAATG	GGGTTGGAAATGAACTTCACATC
Fzd3	GGAACGCTGCAGAGAGTATCAC	GGAATCCCAACTATGAGAGCC
Fzd9	TGTGTTGGTACCCCTATCTTGC	CTTCTCCAGCTTCTCCGTATTG
Jmjd3	AGTGAGGAAGCCGTATGCTG	AGCCCCATAGTTCCGTTTGTG
Myod1	GAGCGCATCTCCACAGACAG	AAATCGCATTGGGGTTTGAG
Myog	CCAGTACATTGAGCGCCTAC	ACCGACTCCAGTGCATTGC
Pax7	CTCAGTGAGTTCGATTAGCCG	AACGGTTCCCTTTGTCGC
Tbp	TCCCCCTCTGCACTGAAATC	AGTGCCGCCCAAGTAGCA
Srp14	AGAGCGAGCAGTTCCTGAC	CGGYGCTGATCTTCCTTTTC
Wnt4	GAGAAGTTTGACGGTGCCAC	GTCCTCATCTGTATGTGGCTTG
Wnt9a	GACTTCCACAACAACCTCGTG	AGGAGCCAGACACACCATG
Wnt10a	CGAATGAGACTCCACAACAACCG	CGTGGCATTTGCACTTACGC

Table 3.1. Primers sequences used for PCR.

Immunohistochemistry

Frozen sections were air-dried for 30 minutes. Sections labeled with antibodies to Pax7 or myogenin were fixed with PFA for 10 minutes, washed for 15 minutes in PBS, followed by 40 minutes of antigen retrieval in sodium citrate buffer containing 0.05% Tween-20 (pH = 6.0) and heated in a water bath to 95 - 100°C. Sections that would be labeled with antibodies to developmental myosin heavy chain (dMHC) were fixed in ice-cold acetone for 10 minutes, dried for 10 minutes, and washed for 10 minutes in PBS. Endogenous peroxidases were quenched for 10 minutes with 0.3% H_2O_2. Sections were treated with blocking buffer from a mouse-on-mouse immunohistochemistry kit (M.O.M Kit; Vector) supplemented with 0.3 M glycine for 1 hour and immunolabeled with anti-Pax7 (1:500), mouse anti-myogenin (1:50, BD Biosciences #556358, RRID:AM_396383), or anti-dMHC (1:100; Leica Biosystems #NCL-MHCd, RRID:AM_563901), and incubated in a humidified chamber, overnight at 4°C. Sections were subsequently incubated with the M.O.M. kit biotin-conjugated anti-mouse IgG (1:200) for 30 minutes, followed by 15 minutes of PBS washes and a 30 minute incubation with M.O.M. kit ABC reagents. Immunolabeling was visualized with the peroxidase substrate 3-amino-9-ethylcarbazole (AEC kit; Vector), causing a dark red reaction product. The number of immunolabeled cells per 100 fibers was determined by counting the number of immunolabeled cells and total fibers within a field of view. The number of immunolabeled fibers per total fibers was determined by counting the number of immunolabeled fibers and total fibers within a field of view.

Statistics

Data are presented as the mean ± SEM. Non-parametric Student's t-test was used when determining differences between two groups. Groups were determined to be significantly different at $p < 0.05$.

RESULTS

Modulating Jmjd3 in Pax7-expressing cells affects muscle morphology and causes early neonatal death.

Our findings show that genetically decreasing *Jmjd3* expression in Pax7+ cells prior to birth have minor effects on the ratio of expected genotypes when tested within the first hours following birth (P0) (Fig. 3.1A). However, all *Jmjd3* floxed mice died prior to weening at 21-days following birth (P21) but all other expected genotypes (*Jmjd3* floxed control, *Jmjd3* hemi control and *Jmjd3* hemi) mice survived as expected (Fig. 3.1B). The body masses of P0 *Jmjd3* floxed and P0 *Jmjd3* hemi mice did not differ from the respective controls (Fig. 3.1C). Next, we measured individual quadriceps muscle masses to determine if the muscle-specific mutation in *Jmjd3* affects developmental skeletal muscle growth (Fig. 3.1D-H). Although there were no differences in the total body masses, P0 *Jmjd3* floxed mice have significantly less quadriceps mass compared to controls and P0 *Jmjd3* hemi mice have significantly larger muscles compared to controls (Fig. 3.1D, E). Regardless of changes in muscle mass, observational analysis shows large gaps between muscle fibers and substantial disorganization in developing muscle in P0 *Jmjd3* floxed and P0 *Jmjd3* hemi quadriceps muscles compared to control cross-sections (Fig. 3.1F-H).

Jmjd3 hemizygous mutation in satellite cells delays postnatal muscle growth.

Despite the increase of *Jmjd3* hemi quadriceps muscle mass at P0 (Fig. 3.1D, E), we measured a significant decrease in mean cross-sectional area of quadriceps muscle fibers from 3-months old *Jmjd3* hemi mice (Fig. 3.2A-C). Because we measured an unexpected reduction in mean cross-sectional area of quadriceps muscle fibers, we confirmed those data by stratifying the proportion of fiber areas into small, mean, and large groups to determine if the changes in mean cross-sectional area reflected a change in fiber size distribution (Fig. 3.2D, E). Our data confirm that muscles of 3-months old *Jmjd3* hemi mice had a 28.5% increase in small fibers compared

to controls and a 55.6% decrease in large fibers compared to control fibers (Fig. 3.2D, E), indicating that a muscle-specific reduction in *Jmjd3* expression alters muscle growth throughout developmental myogenesis.

Reductions in satellite cell-specific Jmjd3 promotes H3K27 methylation in floxed mice but not hemizygous mice.

We next tested whether manipulating the levels of Jmjd3 in Pax7+ cells of developing muscle would influence the total transcripts of *Jmjd3* in whole muscle and the methylation state of H3K27 in Pax7+ cells. Although QPCR data show that *Jmjd3* transcripts are reduced in whole quadriceps muscles of P0 *Jmjd3* floxed (Fig. 3.3A), *Jmjd3* expression was unchanged in whole quadriceps of P0 and 3-months old *Jmjd3* hemi mice (Fig. 3.3B, C). Despite there being no difference in *Jmjd3* transcript levels in whole muscle of *Jmjd3* hemi mice, a smaller proportion of Pax7+ cells were Jmjd3+ in the quadriceps of P0 *Jmjd3* floxed, P0 *Jmjd3* hemi, and 3-months old *Jmjd3* hemi mice compared to their age-matched controls (Fig. 3.3D-F). Because a primary function of Jmjd3 is to remove di and tri methyl groups from H3K27 [19] and our data indicate Klotho-mediated reductions in Jmjd3 influence the methylation state of myogenic genes, we tested whether the decrease in Jmjd3 would reflect an increase in H3K27 methylation in Pax7+ cells. Our data indicate the proportion of Pax7+ cells that showed detectible levels of H3K27me3+ was greater in P0 *Jmjd3* floxed quadriceps muscles than in controls (Fig. 3.3G). However, the proportion of Pax7+ cells that were H3K27me3+ did not differ between *Jmjd3* hemi mice and controls regardless of age (Fig. 3.3H-I), suggesting the hemizygous mutation in male mice was not effective in altering the overall methylation state of H3K27 in developmental myoblasts and satellite cells.

Jmjd3 modulates myogenesis during neonatal muscle growth.

Our work shows that *Jmjd3* is upregulated during muscle differentiation (Chapter 2) and others show that overexpression of the Jmjd3 catalytic domain promoted Pax7 expression in pluripotent stem cells. [24] Those findings suggest that Jmjd3 could regulate the expression of myogenic transcription factors during muscle development. To test this, we assayed for *Pax7*, *Myod1*, and *Myog* transcript levels in P0 *Jmjd3* floxed quadriceps muscles by QPCR. The data show *Pax7*, *Myod1* and *Myog* (Fig. 3.4A-C) are reduced in *Jmjd3* floxed muscles at P0. In addition, the number of Pax7+ cells (Fig. 3.4D-F) and myogenin+ cells (Fig. 3.4G-I) per 100 fibers are reduced in the absence of Jmjd3.

Because Pax7 is required for the self-renewal of developmental myoblasts and myogenin is required for developmental muscle growth, and our observational analysis indicated reductions of Jmjd3 in developing muscle negatively affect myofiber orientation (Fig. 3.1F-H), we tested the hypothesis that muscle development could be delayed when Jmjd3 was not adequately expressed. To address this question, we assayed for developmental myosin heavy chain positive (dMHC+) fibers in P0 *Jmjd3* floxed quadriceps muscle cross-sections. Our findings show muscle-specific reductions of Jmjd3 cause a ~20% increase in newly formed dMHC+ myofibers (Fig. 3.4J-L), indicating normal muscle development is delayed in the absence of adequate Jmjd3.

Jmjd3 affects Wnt ligand and Wnt target expression in neonatal muscle.

Our findings in Chapter 2 showed Klotho reduced Jmjd3 and active β-catenin but increased H3K27me3 in Pax7+ cells during development. Our data further showed treating myogenic cells *in vitro* with Klotho increased the accumulation of methyl groups on H3K27 associated with the promotor regions of Wnt-family genes and expressing KL Tg+ in vivo decreased Wnt-family transcripts in whole quadriceps muscles. These data suggest Klotho's effects on Wnt signaling could be mediated by Jmjd3. To test this, we assayed for changes in transcript levels of *Wnt*-

family genes of interest in P0 *Jmjd3* floxed muscles (Fig. 3.5). These data show reductions of *Wnt4*, *Wnt9a*, *Wnt10a*, *Fzd9*, and Wnt target gene *Axin2* in P0 *Jmjd3* floxed whole muscle (Fig. 3.5A-C, E, F). Whereas, *Fzd3* and *Ccnd1* were reduced but not significantly (Fig. 3.5D, G), suggesting Klotho's effects on *Wnt* expression could be mediated by Jmjd3 or through Jmjd3-independent mechanisms.

Loss of Jmjd3 reduces Wnt signaling in Pax7+ cells during neonatal muscle development. Collectively, our findings suggest Klotho's effects on Wnt signaling may be downstream of Klotho's effects on Jmjd3 and H3K27 methylation, suggesting Jmjd3 may promote canonical Wnt-signaling during developmental myogenesis. Because myogenesis is driven in-part by canonical Wnt-signaling, [27] we assayed for activated β-catenin in Pax7+ cells as an indicator for changes of canonical Wnt-signaling in neonatal muscle. Our findings show a 38.2% decrease in the proportion of Pax7+ cells that also expressed the functionally active form of β-catenin in *Jmjd3* floxed muscle at P0 (Fig. 3.6A-C). These data solidify the influence of Jmjd3 on canonical Wnt signaling in myogenic cells during early neonatal muscle growth and development.

Figure 3.1.

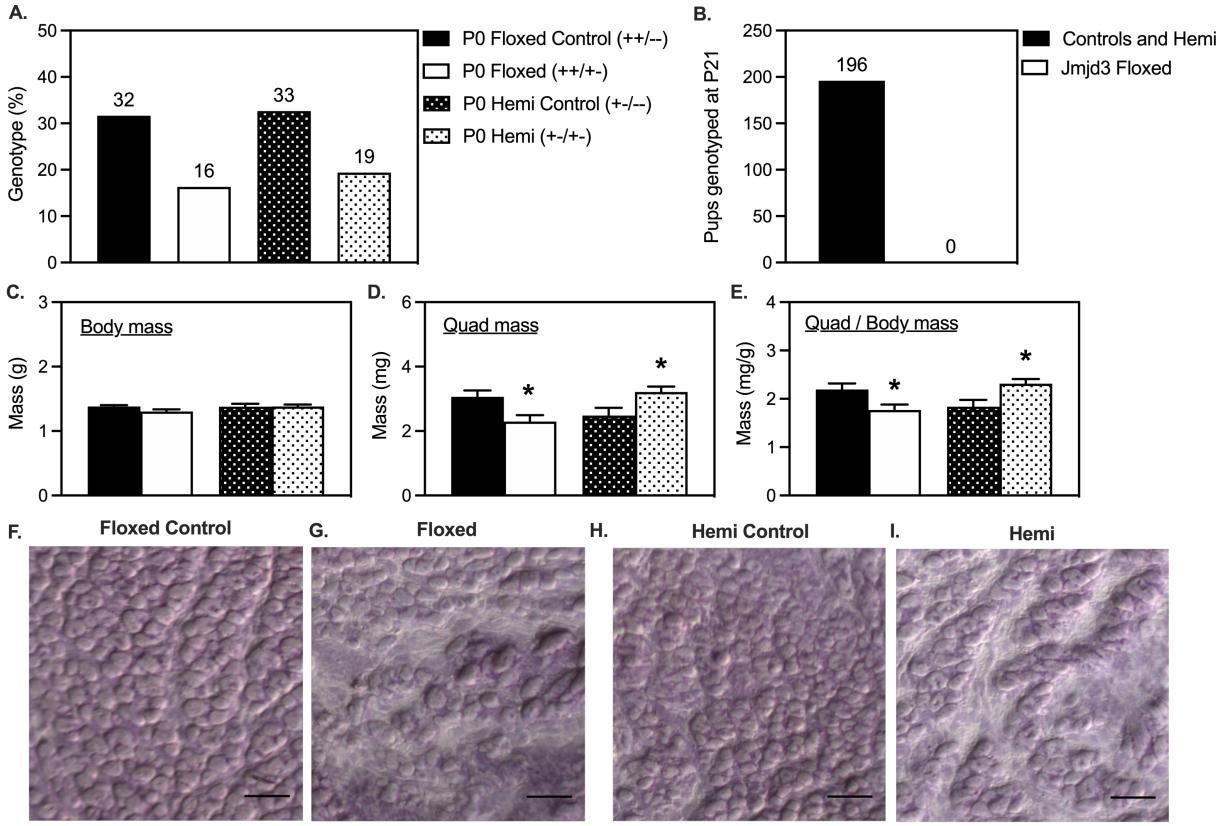

Figure 3.1. Modulating Jmjd3 in satellite cells affects muscle morphology and causes early neonatal death. (A) Percent of mice that were genotyped within 12-hours following birth that were *Jmjd3* floxed control, *Jmjd3* floxed, *Jmjd3* hemi control or *Jmjd3* hemi. N = 98 pups in 11 total litters. (B) Numbers of control and hemi mice (floxed control, hemi control and hemi) and *Jmjd3* floxed genotyped at P21. N = 196 (controls and hemi) and N = 0 (*Jmjd3* floxed). (C) Body mass (g) of P0 *Jmjd3* floxed control vs. *Jmjd3* floxed mice and P0 *Jmjd3* hemi control vs. *Jmjd3* hemi mice. (D) Quadriceps mass (mg) of P0 *Jmjd3* floxed control vs. *Jmjd3* floxed mice and P0 *Jmjd3* hemi control vs. *Jmjd3* hemi mice. (E) Ratio of quadriceps mass normalized to body mass (mg/g) of P0 *Jmjd3* floxed control vs. *Jmjd3* floxed mice and P0 *Jmjd3* hemi control vs. *Jmjd3* hemi mice. * indicates significantly different from age-matched control at $P < 0.05$ analyzed by *t*-test. Error bar represents SEM. N = 10 (*Jmjd3* floxed control); N = 9 (*Jmjd3* floxed); N = 8 (*Jmjd3* hemi control); N = 10 (*Jmjd3* hemi). (F-H) Representative images of *Jmjd3* floxed control (F), *Jmjd3* floxed (G), Jmjd3 hemi control (H), and *Jmjd3* hemi (I) quadriceps at P0 stained with hematoxylin. Bar = 50 μm.

Figure 3.2.

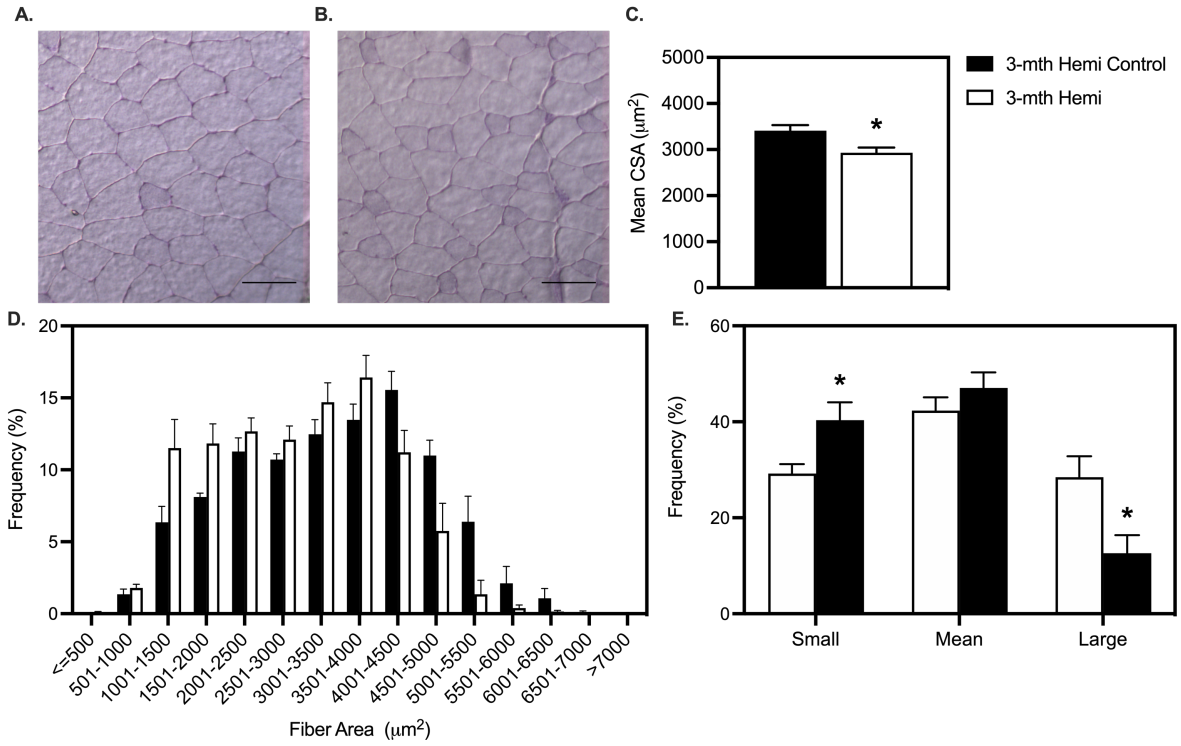

Figure 3.2. ***Jmjd3*** **hemizygous mutation in satellite cells delays postnatal muscle growth.** (A, B) Representative images of *Jmjd3* hemi control (A) and *Jmjd3* hemi (B) quadriceps at 3-months old stained with hematoxylin. Bar = 100 μm. (C) Mean cross-sectional area for quadriceps muscle fibers from *Jmjd3* hemi control and *Jmjd3* hemi mice at 3-months old. * indicates significantly different from age-matched control at $P < 0.05$ analyzed by *t*-test. (D) Frequency distribution of fiber cross-sectional areas for quadriceps muscles from 3-months old *Jmjd3* hemi control and *Jmjd3* hemi mice. (E) Proportion of small, mean, and large fibers. Small and large fibers are 3 standard deviations below or above the average cross-sectional area of control fibers. * indicates significantly different from control at $P < 0.05$ analyzed by *t*-test. N = 5.

Figure 3.3.

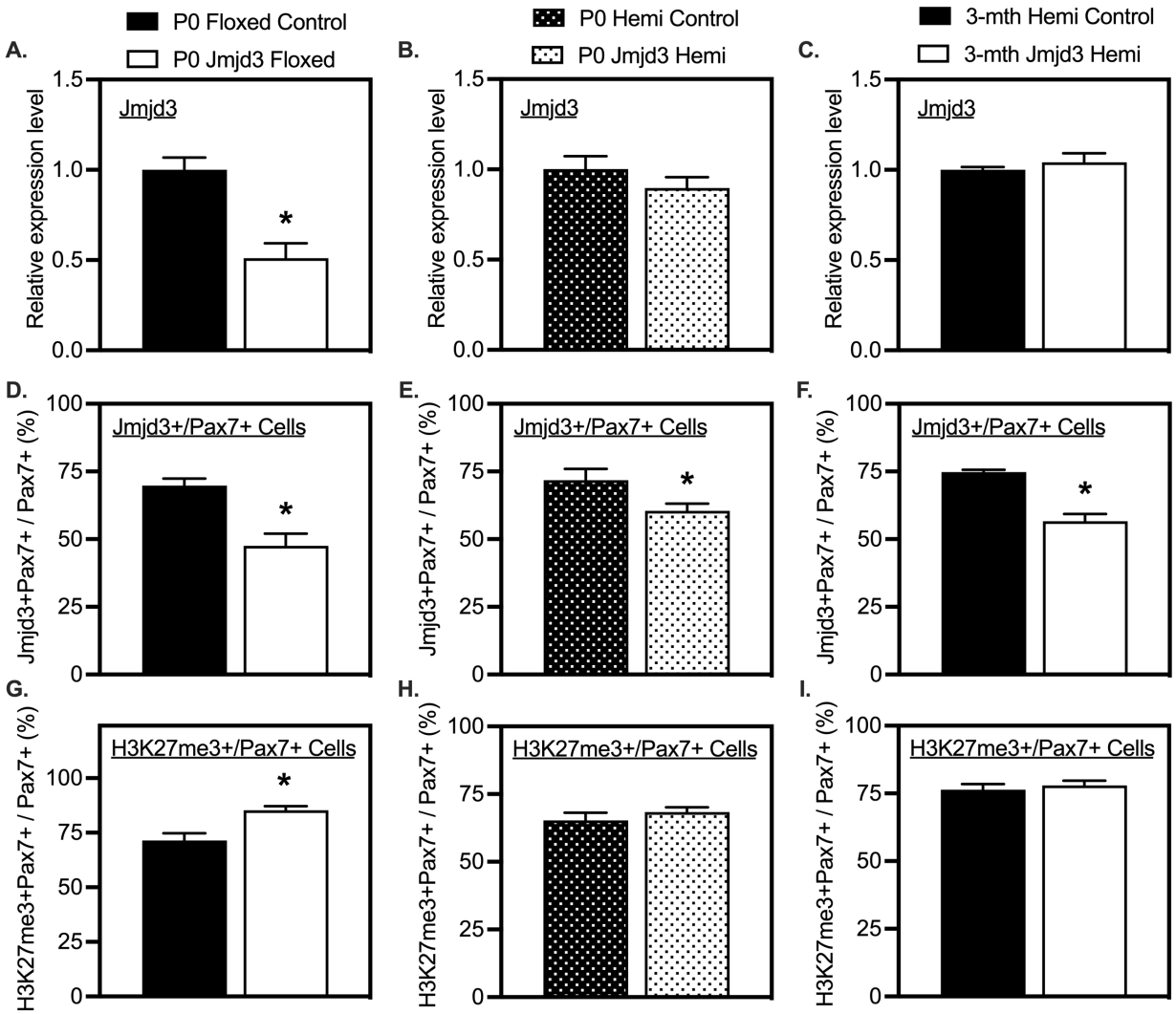

Figure 3.3. Reductions in satellite cell-specific Jmjd3 promotes H3K27 methylation in *Jmjd3* floxed mice but not *Jmjd3* hemizygous mice. (A) QPCR data showing relative expression of *Jmjd3* in quadriceps muscle from *Jmjd3* floxed control and *Jmjd3* floxed mice at P0. (B, C) QPCR data showing relative expression of *Jmjd3* in quadriceps muscle from *Jmjd3* hemi control and *Jmjd3* hemi mice at P0 (B) and 3-months old (C). (D) Ratio of Jmjd3+/Pax7+ cells to total Pax7+ cells in sections of quadriceps muscles from *Jmjd3* floxed control and *Jmjd3* floxed mice at P0. (E, F) Ratio of Jmjd3+/Pax7+ cells to total Pax7+ cells in sections of quadriceps muscles from *Jmjd3* hemi control and *Jmjd3* hemi mice at P0 (E) and 3-months old (F). (G) Ratio of H3K27me3+/Pax7+ cells to total Pax7+ cells in sections of quadriceps muscles from *Jmjd3* floxed control and *Jmjd3* floxed mice at P0. (H, I) Ratio of H3K27me3+/Pax7+ cells to total Pax7+ cells in sections of quadriceps muscles from *Jmjd3* hemi control and *Jmjd3* hemi mice at P0 (H) and 3-months old (I). * indicates significantly different from age-matched control at $P < 0.05$ analyzed by *t*-test. Error bar represents SEM. N = 5.

Figure 3.4.

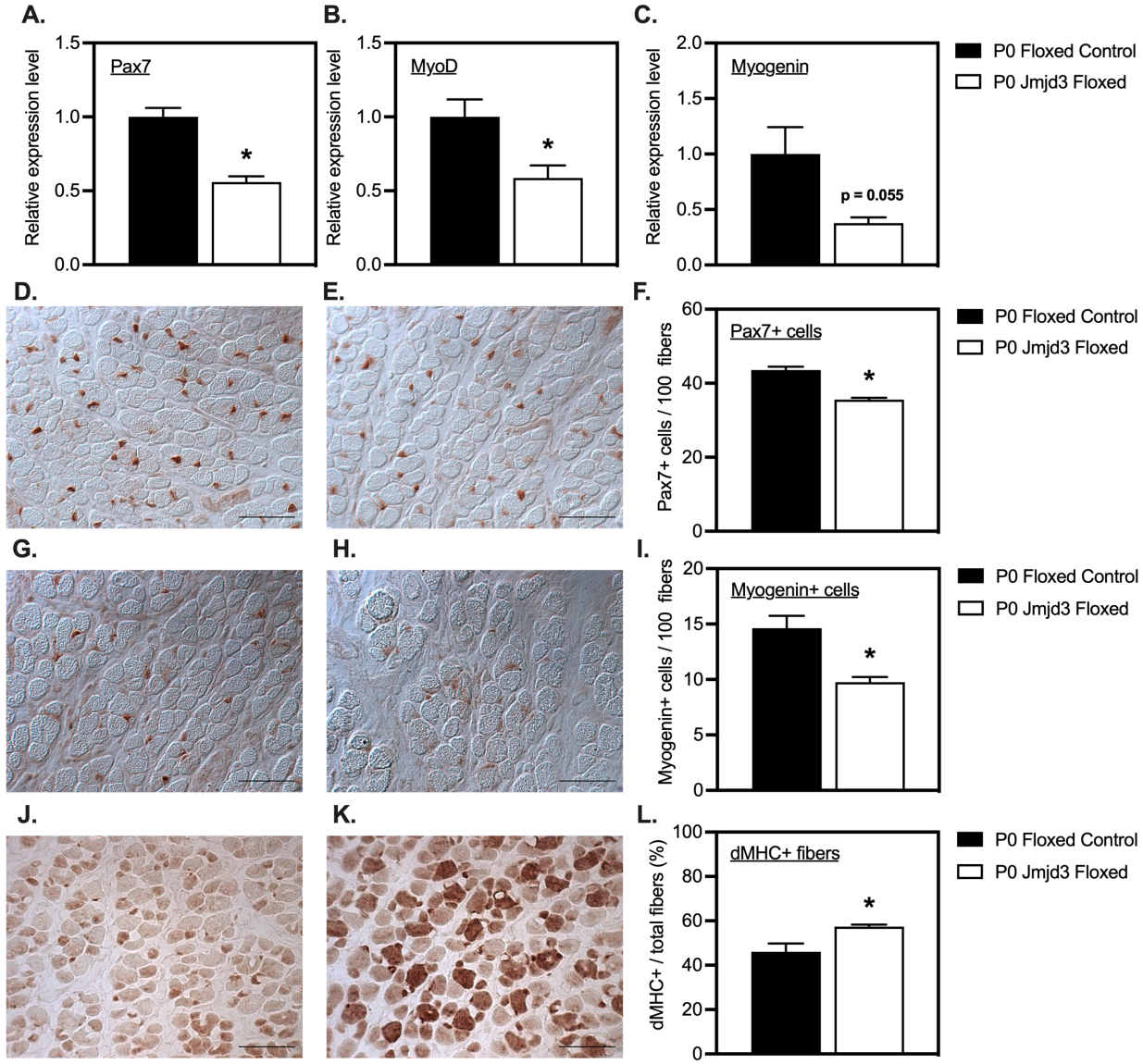

Figure 3.4. Jmjd3 modulates myogenesis during neonatal muscle growth. (A-C) QPCR data showing relative expression of *Pax7* (A), *Myod1* (B), and *Myog* (C) in quadriceps muscle from *Jmjd3* floxed control and *Jmjd3* floxed mice at P0. (D, E) Representative images of *Jmjd3* floxed control (D), *Jmjd3* floxed (E) quadriceps cross-sections at P0 immunolabeled for Pax7 (reddish-brown nuclei). (F) Numbers of Pax7+ cells per 100 fibers in quadriceps from *Jmjd3* floxed control and *Jmjd3* floxed mice at P0. (G, H) Representative images of *Jmjd3* floxed control (G), *Jmjd3* floxed (H) quadriceps cross-sections at P0 immunolabeled for myogenin (reddish-brown nuclei). (I) Numbers of myogenin+ cells per 100 fibers in quadriceps from *Jmjd3* floxed control and *Jmjd3* floxed mice at P0. (J, K) Representative images of *Jmjd3* floxed control (J), *Jmjd3* floxed (K) quadriceps cross-sections at P0 immunolabeled for dMHC (reddish-brown fibers). (L) Ratio of dMHC+ fibers to total fibers in quadriceps from *Jmjd3* floxed control and *Jmjd3* floxed mice at P0. For D and E, G and H, and J and K open arrow head (>) indicates Pax7+ (D, E), myogenin+ (G, H) or dMHC+ (J, K) labeled cells. Bar = 50 μm. For A-C, F, I, and L, * indicates significantly different from control at $P < 0.05$ analyzed by *t*-test. Error bar represents SEM. N = 4 or 5.

Figure 3.5.

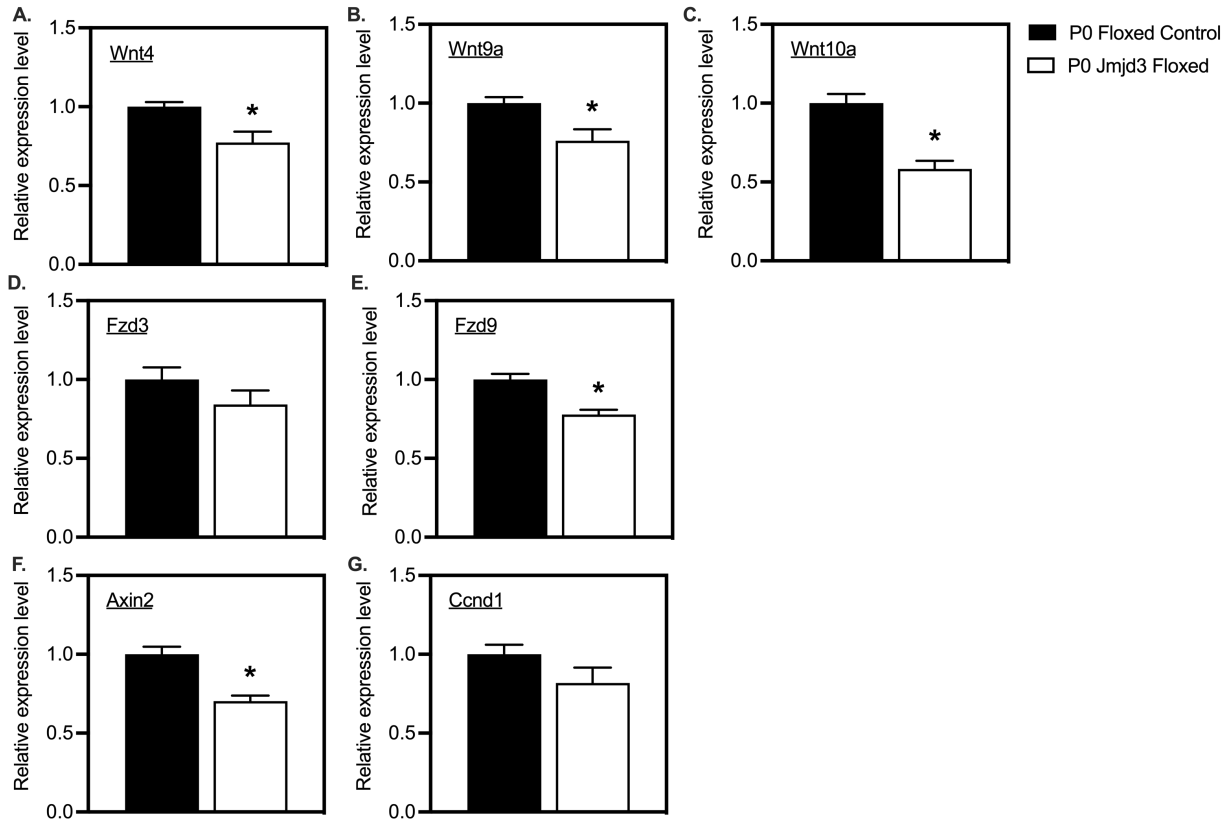

Figure 3.5. Jmjd3 affects Wnt ligand and Wnt target expression in neonatal muscle. (A-G) QPCR data showing relative expression of *Wnt4* (A), *Wnt9a* (B), *Wnt10a* (C), *Fzd3* (D), *Fzd9* (E), *Axin2* (F), and *Ccnd1* (G) in quadriceps muscle from *Jmjd3* floxed control and *Jmjd3* floxed mice at P0. * indicates significantly different from control at $P < 0.05$ analyzed by *t*-test. Error bar represents SEM. N = 4 or 5.

Figure 3.6.

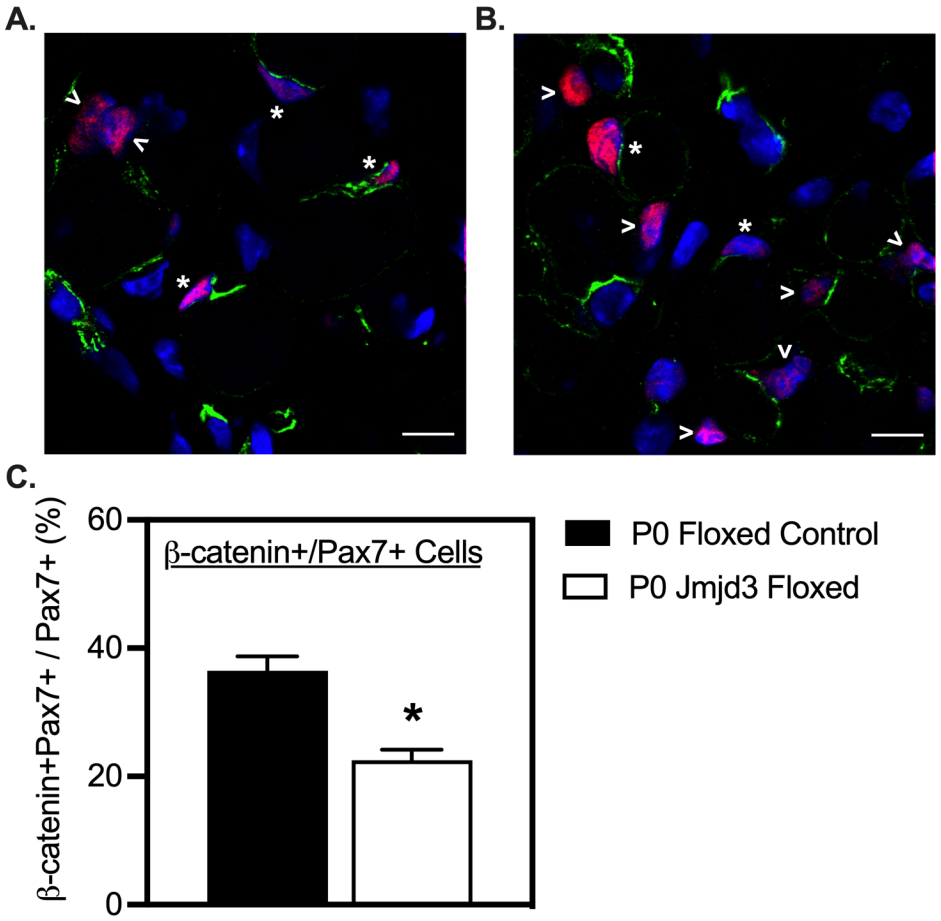

Figure 3.6. Loss of Jmjd3 reduces Wnt signaling in Pax7+ cells during neonatal muscle development. (A, B) Sections of *Jmjd3* floxed control (A) and *Jmjd3* floxed (B) quadriceps muscle at P0 labeled with anti-Pax7 (red), anti-β-catenin (green) and DNA labeled with DAPI (blue). * indicates Pax7+ cells also active β-catenin+. Open arrow head (>) indicates Pax7+ single labeled cells. Bar = 10 μm. (C) Ratio of Pax7+ cells that showed activated β-catenin relative to total Pax7+ cells in *Jmjd3* floxed control and *Jmjd3* floxed quadriceps muscles. * indicates significantly different from age-matched Wt at $P < 0.05$ analyzed by *t*-test. Error bar represents SEM. N = 5.

DISCUSSION

In the present study, we tested whether a muscle-specific mutation in the gene coding for the histone 3 lysine 27 (H3K27) demethylase Jmjd3 would have the same effects on developmental myogenesis and the Wnt-signaling pathway as the age-related protein Klotho. Although we showed Klotho decreased Jmjd3 and increased H3K27 methylation affecting myogenesis and the canonical Wnt pathway, here we show that directly inactivating *Jmjd3* in Pax7-expressing cells drastically impacts muscle morphology, inhibits developmental myoblast population expansion, and causes neonatal death in 100% of the *Jmjd3* floxed neonatal mice. Consistent with our Klotho-related findings and the hypothesis that Jmjd3 is a key regulatory factor of the Wnt pathway during muscle development, *Jmjd3* floxed mice have impaired expression of *Wnt*-family genes, Wnt targets, and active β-catenin in quadriceps muscles collected immediately following birth on postnatal day 0 (P0). These novel findings identify a necessary epigenetic regulatory mechanism mediated by Jmjd3 and H3K27 methylation that influences developmental myogenesis and neonatal survival.

Many have reported dynamic changes in posttranslational modifications that impact myogenesis. [8,22,37-39] Although systemic mutations in *Jmjd3* cause neonatal death, [23] we were surprised to discover mutations in muscle-specific *Jmjd3* are neonatally lethal solidifying Jmjd3 as an indispensable epigenetic regulator in developmental myogenesis and postnatal survival. Other investigators have shown increased expression of the Jmjd3 catalytic domain promoted myogenic programming and transcription factor expression in pluripotent stem cells. [24] Inversely, our data show a ~50% decrease in muscle-specific Jmjd3 is enough to reduce the gene expression of key myogenic transcription factors *Pax7*, *Myod1*, and *Myog* and the number of Pax7+ and myogenin+ cells in P0 quadriceps. We previously showed that elevated Klotho increased the population of developmental myoblasts during a timepoint when the majority of

mononuclear myogenic cells are actively proliferating, therefore Klotho and Jmjd3 may affect myogenesis in the same, but also different pathways.

There are at least two possible explanations for the differences between the data from the KL Tg+ model and the *Jmjd3* floxed model. First, the dynamic effects of Klotho on myogenesis may be upstream or independent of the effects of Klotho on Jmjd3. Pax7 is widely accepted as the master regulator promoting the propagation of developmental myoblasts and the self-renewal capacity of adult muscle satellite cells. [10-12,40-44] Pax7+ cells undergo a robust amplification between P0 and P28 in wild-type muscle and are the primary cell population contributing to myonuclear accretion and developmental muscle growth. [45,46] Our data show elevated Klotho increased Pax7+ cells, decreased the proportion of Pax7+ cells under laminin and extended the period of developmental fiber growth (Chapter 2). Others show that overexpression of *Jmjd3* in pluripotent stem cells promoted *Pax7* expression and when *Jmjd3* and *Myod1* were sequentially overexpressed, *Myog* was upregulated. [24] In agreeance, our data indicate a ~50% reduction in Jmjd3 inhibits the expansion of the Pax7-expressing cell population and causes abnormalities in muscle morphology likely because of reductions in the terminal differentiation factor myogenin. The previously reported findings together with our data suggests Jmjd3 regulates myogenesis but the effects of Klotho on Jmjd3 are independent of Klotho's influence on myogenesis.

Second, Klotho and Jmjd3 may influence the canonical Wnt pathway through different mechanisms. To our knowledge there are no published data showing Klotho binds directly to gene regulatory elements or to protein complexes that influence chromatin remodeling like the PRC2 complex. Previous investigations have shown that Klotho can bind directly to Wnt proteins, inhibiting downstream activity of at least one Wnt ligand and the canonical Wnt pathway. [47-49] Treating myogenic cells with canonical Wnt3a reduced the number of myogenic cell clusters on cultured fibers suggesting Wnt3a promoted differentiation. [49] In the same

system, Klotho treatments increased the number of clusters per fiber but when cells were treated concurrently with Wnt3a and Klotho, the Klotho-mediated increase in myogenic cell clusters was diminished suggesting Klotho bound Wnt3a and inhibited downstream β-catenin signaling, [49] as previously reported. [47,48] Alternatively, Jmjd3 does have direct influence on gene expression because Jmjd3 removes trimethyl and dimethyl groups from H3K27 allowing for gene accessibility. [9,19] Inhibitory studies showed reductions in Jmjd3 increased the repressive trimethyl marks on H3K27 at the β-catenin promotor and decreased downstream β-catenin-mediated gene activation. [50] Furthermore, Jmjd3 can also recruit β-catenin to the promotor region of the Brachyury gene which is required for the differentiation of pre-muscle tissue during embryonic development. [51] Therefore, the different modes of influence between Klotho and Jmjd3 on the canonical Wnt pathway suggest they are independent of each other, particularly because Klotho antagonizes canonical Wnt signaling by directly binding to canonical Wnt proteins, whereas Jmjd3 directly regulates β-catenin by demethylating H3K27 at the β-catenin gene promotor and recruits β-catenin to β-catenin target genes.

β-catenin-dependent canonical Wnt signaling is the rate limiting step in adult myogenesis and there is a wealth of literature supporting incremental changes in β-catenin signaling can have adverse repercussions on satellite cell-mediated adult myogenesis. [27,52-56] Wnt4, Wnt9a, Wnt10a, and Fzd9 Wnt-family molecules promote β-catenin accumulation leading to increased canonical Wnt signaling and Wnt target activation. [57-65] Therefore, our analysis on whole muscle from P0 Jmjd3 floxed mice suggests decreases in Wnt4, Wnt9a, Wnt10a, and Fzd9 reduce levels of activated β-catenin. Because Axin2 is a negative regulator of the Wnt pathway, [66] we speculated that *Axin2* may be upregulated in the Jmjd3 floxed model. However, our data show reduced *Axin2* expression in P0 *Jmjd3* floxed muscle. These findings can be explained through the regulatory relationship between *Axin2*, β-catenin, and Jmjd3. First, although Axin2 protein is

a negative regulator of Wnt signaling, the *Axin2* gene is activated by β-catenin-mediated signaling. [66] Also, investigations into neonatal cardiac cells indicate the promotor region of *Ctnnb1*, the gene coding for β-catenin is repressed by Jmjd3-mediated H3K27me3 silencing. [50] Furthermore, our immunohistological data show the proportion of Pax7+ cells also Jmjd3+ is reduced by ~32% compared to control muscle. Similarly, the proportion of Pax7+ cells also β-catenin+ show an ~38% reduction compared to controls. Together those data suggest the reduction in Jmjd3 causes a proportionally similar reduction in activated β-catenin.

The activation and localization of β-catenin in satellite cells appears to be dependent on the stage of myogenesis and the Wnt ligand initiating the Wnt/β-catenin cascade. [27,40,53] For example, overexpression of *Wnt4* in chick embryos promoted *Pax7* expression, *Myod1* expression, the formation of fast-twitch muscle fibers, and increased the total muscle mass. [67] In acute injury models loss of Wnt4 promoted satellite cell activation and muscle regeneration but the overexpression of Wnt4 inhibited muscle repair by delaying the onset of satellite cell activation. [68] Wnt4-expressing cells cocultured with myofibers and intact satellite cells reduced satellite cell proliferation while promoting the activation of β-catenin but not the nuclear translocation. [53] Others showed that overexpression of Wnt4 in cultured C2C12 myoblasts or primary adult satellite cells promoted differentiation although β-catenin translocation was not always required for the expression of terminal differentiation factors. [69,70] Our results suggest in the absence of Jmjd3 and the accumulation of H3K27me3 in Pax7+ cells silence *Wnt4*, *Wnt9a*, and Wnt10a causing a loss of activated β-catenin. Although, previous reports show Jmjd3 demethylase activity stimulates β-catenin expression, [50] our ChIP-seq experiments did not indicate Klotho mediated reductions in Jmjd3 promoted the accumulation of H3K27me2/3 at the promotor region of *Ctnnb1* gene.

While it is tempting to draw conclusive parallels between the effects of canonical Wnt signaling in adult muscle and our characterization of *Jmjd3* floxed muscle at P0, previous investigations showed the requirements of Wnt-mediated β-catenin signaling in developmental myogenesis differ from adult myogenesis. [27,40,53] For example, β-catenin signaling is required for the formation of the dermomyotome and the myotome but not during axial myogenesis. [40] Once progenitor cells have migrated to the limb, β-catenin is critical in fetal myogenesis and the shift between slow primary fibers that are formed during embryonic development and fast secondary fibers formed in fetal development. Mice with inactive β-catenin in Pax7+ cells die immediately following birth, have significantly fewer myofibers, and myofibers are disproportionately fast-twitch, [40] suggesting the inactivation of β-catenin blocks Pax7+ cells from expanding and fusing to established primary, slow-twitch fibers. [1,40] P0 *Jmjd3* floxed muscle has similar characteristics. P0 Jmjd3 floxed muscle is significantly smaller in mass compared to controls and has more dMHC+ fibers suggesting a delay in incremental muscle growth and development. Furthermore, elevated levels of Jmjd3 upregulate *Pax7* in pluripotent stem cells but increased Jmjd3 and MyoD promote *Myog* expression [24] suggesting Jmjd3 can affect different developmental stages in the myogenic pathway that are mediated by β-catenin. Together, these observations illuminate a novel epigenetic regulatory mechanism required for developmental myogenesis in which Jmjd3-medated demethylation of H3K27me2/3 at the promotors of canonical Wnts ligands is necessary for β-catenin activation and normal muscle growth.

REFERENCES

1. Biressi S, Molinaro M, Cossu G. Cellular heterogeneity during vertebrate skeletal muscle development. *Dev Biol*. Aug 2007;308(2):281-93. doi:10.1016/j.ydbio.2007.06.006

2. Bharathy N, Ling BM, Taneja R. Epigenetic regulation of skeletal muscle development and differentiation. *Subcell Biochem*. 2013;61:139-50. doi:10.1007/978-94-007-4525-4_7

3. Vastenhouw NL, Schier AF. Bivalent histone modifications in early embryogenesis. *Curr Opin Cell Biol*. Jun 2012;24(3):374-86. doi:10.1016/j.ceb.2012.03.009

4. Byrne K, McWilliam S, Vuocolo T, Gondro C, Cockett NE, Tellam RL. Genomic architecture of histone 3 lysine 27 trimethylation during late ovine skeletal muscle development. *Anim Genet*. Jun 2014;45(3):427-38. doi:10.1111/age.12145

5. Caretti G, Di Padova M, Micales B, Lyons GE, Sartorelli V. The Polycomb Ezh2 methyltransferase regulates muscle gene expression and skeletal muscle differentiation. *Genes Dev*. Nov 2004;18(21):2627-38. doi:10.1101/gad.1241904

6. Woodhouse S, Pugazhendhi D, Brien P, Pell JM. Ezh2 maintains a key phase of muscle satellite cell expansion but does not regulate terminal differentiation. *J Cell Sci*. Jan 2013;126(Pt 2):565-79. doi:10.1242/jcs.114843

7. Seenundun S, Rampalli S, Liu QC, et al. UTX mediates demethylation of H3K27me3 at muscle-specific genes during myogenesis. *EMBO J*. Apr 2010;29(8):1401-11. doi:10.1038/emboj.2010.37

8. Faralli H, Wang C, Nakka K, et al. UTX demethylase activity is required for satellite cell-mediated muscle regeneration. *J Clin Invest*. Apr 2016;126(4):1555-65. doi:10.1172/JCI83239

9. Burchfield JS, Li Q, Wang HY, Wang RF. JMJD3 as an epigenetic regulator in development and disease. *Int J Biochem Cell Biol*. Oct 2015;67:148-57. doi:10.1016/j.biocel.2015.07.006

10. Relaix F, Rocancourt D, Mansouri A, Buckingham M. A Pax3/Pax7-dependent population of skeletal muscle progenitor cells. *Nature*. Jun 2005;435(7044):948-53. doi:10.1038/nature03594

11. Seale P, Sabourin LA, Girgis-Gabardo A, Mansouri A, Gruss P, Rudnicki MA. Pax7 is required for the specification of myogenic satellite cells. *Cell*. Sep 2000;102(6):777-86. doi:10.1016/s0092-8674(00)00066-0

12. Oustanina S, Hause G, Braun T. Pax7 directs postnatal renewal and propagation of myogenic satellite cells but not their specification. *EMBO J*. Aug 2004;23(16):3430-9. doi:10.1038/sj.emboj.7600346

13. Kuang S, Kuroda K, Le Grand F, Rudnicki MA. Asymmetric self-renewal and commitment of satellite stem cells in muscle. *Cell*. Jun 2007;129(5):999-1010. doi:10.1016/j.cell.2007.03.044

14. Relaix F, Montarras D, Zaffran S, et al. Pax3 and Pax7 have distinct and overlapping functions in adult muscle progenitor cells. *J Cell Biol*. Jan 02 2006;172(1):91-102. doi:10.1083/jcb.200508044

15. Juan AH, Derfoul A, Feng X, et al. Polycomb EZH2 controls self-renewal and safeguards the transcriptional identity of skeletal muscle stem cells. *Genes Dev*. Apr 2011;25(8):789-94. doi:10.1101/gad.2027911

16. Hulin JA, Nguyen TD, Cui S, et al. Barx2 and Pax7 regulate Axin2 expression in myoblasts by interaction with β-catenin and chromatin remodelling. *Stem Cells*. 2016;34(8):2169-2182. doi:10.1002/stem.2396

17. Palacios D, Mozzetta C, Consalvi S, et al. TNF/p38α/polycomb signaling to Pax7 locus in satellite cells links inflammation to the epigenetic control of muscle regeneration. *Cell Stem Cell*. Oct 2010;7(4):455-69. doi:10.1016/j.stem.2010.08.013

18. Stojic L, Jasencakova Z, Prezioso C, et al. Chromatin regulated interchange between polycomb repressive complex 2 (PRC2)-Ezh2 and PRC2-Ezh1 complexes controls myogenin

activation in skeletal muscle cells. *Epigenetics Chromatin*. Sep 05 2011;4:16. doi:10.1186/1756-8935-4-16

19. Hong S, Cho YW, Yu LR, Yu H, Veenstra TD, Ge K. Identification of JmjC domain-containing UTX and JMJD3 as histone H3 lysine 27 demethylases. *Proc Natl Acad Sci U S A*. Nov 2007;104(47):18439-44. doi:10.1073/pnas.0707292104

20. Agger K, Cloos PA, Christensen J, et al. UTX and JMJD3 are histone H3K27 demethylases involved in HOX gene regulation and development. *Nature*. Oct 2007;449(7163):731-4. doi:10.1038/nature06145

21. Welstead GG, Creyghton MP, Bilodeau S, et al. X-linked H3K27me3 demethylase Utx is required for embryonic development in a sex-specific manner. *Proc Natl Acad Sci U S A*. Aug 2012;109(32):13004-9. doi:10.1073/pnas.1210787109

22. Wang C, Lee JE, Cho YW, et al. UTX regulates mesoderm differentiation of embryonic stem cells independent of H3K27 demethylase activity. *Proc Natl Acad Sci U S A*. Sep 2012;109(38):15324-9. doi:10.1073/pnas.1204166109

23. Burgold T, Voituron N, Caganova M, et al. The H3K27 demethylase JMJD3 is required for maintenance of the embryonic respiratory neuronal network, neonatal breathing, and survival. *Cell Rep*. Nov 2012;2(5):1244-58. doi:10.1016/j.celrep.2012.09.013

24. Akiyama T, Wakabayashi S, Soma A, et al. Epigenetic Manipulation Facilitates the Generation of Skeletal Muscle Cells from Pluripotent Stem Cells. *Stem Cells Int*. 2017;2017:7215010. doi:10.1155/2017/7215010

25. Cossu G, Borello U. Wnt signaling and the activation of myogenesis in mammals. *EMBO J*. Dec 1999;18(24):6867-72. doi:10.1093/emboj/18.24.6867

26. Girardi F, Le Grand F. Wnt Signaling in Skeletal Muscle Development and Regeneration. *Prog Mol Biol Transl Sci*. 01 2018;153:157-179. doi:10.1016/bs.pmbts.2017.11.026

27. Brack AS, Conboy IM, Conboy MJ, Shen J, Rando TA. A temporal switch from notch to Wnt signaling in muscle stem cells is necessary for normal adult myogenesis. *Cell Stem Cell*. Jan 2008;2(1):50-9. doi:10.1016/j.stem.2007.10.006

28. Akiyama T, Wakabayashi S, Soma A, et al. Transient ectopic expression of the histone demethylase JMJD3 accelerates the differentiation of human pluripotent stem cells. *Development*. Oct 2016;143(20):3674-3685. doi:10.1242/dev.139360

29. Schneider CA, Rasband WS, Eliceiri KW. NIH Image to ImageJ: 25 years of image analysis. *Nat Methods*. Jul 2012;9(7):671-5. doi:10.1038/nmeth.2089

30. Schindelin J, Arganda-Carreras I, Frise E, et al. Fiji: an open-source platform for biological-image analysis. *Nat Methods*. Jun 2012;9(7):676-82. doi:10.1038/nmeth.2019

31. White JP, Baltgalvis KA, Sato S, Wilson LB, Carson JA. Effect of nandrolone decanoate administration on recovery from bupivacaine-induced muscle injury. *J Appl Physiol (1985)*. Nov 2009;107(5):1420-30. doi:10.1152/japplphysiol.00668.2009

32. Welc SS, Wehling-Henricks M, Kuro-O M, Thomas KA, Tidball JG. Modulation of Klotho expression in injured muscle perturbs Wnt signalling and influences the rate of muscle growth. *Exp Physiol*. Jan 2020;105(1):132-147. doi:10.1113/EP088142

33. Vandesompele J, De Preter K, Pattyn F, et al. Accurate normalization of real-time quantitative RT-PCR data by geometric averaging of multiple internal control genes. *Genome Biol*. Jun 2002;3(7):RESEARCH0034. doi:10.1186/gb-2002-3-7-research0034

34. Thomas KC, Zheng XF, Garces Suarez F, et al. Evidence based selection of commonly used RT-qPCR reference genes for the analysis of mouse skeletal muscle. *PLoS One*. 2014;9(2):e88653. doi:10.1371/journal.pone.0088653

35. Hildyard JCW, Finch AM, Wells DJ. Identification of qPCR reference genes suitable for normalizing gene expression in the mdx mouse model of Duchenne muscular dystrophy. *PLoS One*. 2019;14(1):e0211384. doi:10.1371/journal.pone.0211384

36. Villalta SA, Rinaldi C, Deng B, Liu G, Fedor B, Tidball JG. Interleukin-10 reduces the pathology of mdx muscular dystrophy by deactivating M1 macrophages and modulating macrophage phenotype. *Hum Mol Genet*. Feb 2011;20(4):790-805. doi:10.1093/hmg/ddq523

37. Jin W, Peng J, Jiang S. The epigenetic regulation of embryonic myogenesis and adult muscle regeneration by histone methylation modification. *Biochem Biophys Rep*. Jul 2016;6:209-219. doi:10.1016/j.bbrep.2016.04.009

38. Lan F, Bayliss PE, Rinn JL, et al. A histone H3 lysine 27 demethylase regulates animal posterior development. *Nature*. Oct 2007;449(7163):689-94. doi:10.1038/nature06192

39. Wehling-Henricks M, Li Z, Lindsey C, et al. Klotho gene silencing promotes pathology in the mdx mouse model of Duchenne muscular dystrophy. *Hum Mol Genet*. May 2016;25(12):2465-2482. doi:10.1093/hmg/ddw111

40. Hutcheson DA, Zhao J, Merrell A, Haldar M, Kardon G. Embryonic and fetal limb myogenic cells are derived from developmentally distinct progenitors and have different requirements for beta-catenin. *Genes Dev*. Apr 2009;23(8):997-1013. doi:10.1101/gad.1769009

41. Buckingham M, Bajard L, Chang T, et al. The formation of skeletal muscle: from somite to limb. *J Anat*. Jan 2003;202(1):59-68.

42. Seale P, Ishibashi J, Scimè A, Rudnicki MA. Pax7 is necessary and sufficient for the myogenic specification of CD45+:Sca1+ stem cells from injured muscle. *PLoS Biol*. May 2004;2(5):E130. doi:10.1371/journal.pbio.0020130

43. Kuang S, Chargé SB, Seale P, Huh M, Rudnicki MA. Distinct roles for Pax7 and Pax3 in adult regenerative myogenesis. *J Cell Biol*. Jan 2006;172(1):103-13. doi:10.1083/jcb.200508001

44. Lepper C, Conway SJ, Fan CM. Adult satellite cells and embryonic muscle progenitors have distinct genetic requirements. *Nature*. Jul 2009;460(7255):627-31. doi:10.1038/nature08209

45. Bachman JF, Klose A, Liu W, et al. Prepubertal skeletal muscle growth requires Pax7-expressing satellite cell-derived myonuclear contribution. *Development*. 2018;145(20):dev167197. doi:10.1242/dev.167197

46. Gattazzo F, Laurent B, Relaix F, Rouard H, Didier N. Distinct Phases of Postnatal Skeletal Muscle Growth Govern the Progressive Establishment of Muscle Stem Cell Quiescence. *Stem Cell Reports*. 09 08 2020;15(3):597-611. doi:10.1016/j.stemcr.2020.07.011

47. Liu H, Fergusson MM, Castilho RM, et al. Augmented Wnt signaling in a mammalian model of accelerated aging. *Science*. Aug 2007;317(5839):803-6. doi:10.1126/science.1143578

48. Zhou L, Li Y, Zhou D, Tan RJ, Liu Y. Loss of Klotho contributes to kidney injury by derepression of Wnt/β-catenin signaling. *J Am Soc Nephrol*. Apr 2013;24(5):771-85. doi:10.1681/ASN.2012080865

49. Ahrens HE, Huettemeister J, Schmidt M, Kaether C, von Maltzahn J. Klotho expression is a prerequisite for proper muscle stem cell function and regeneration of skeletal muscle. *Skelet Muscle*. 07 2018;8(1):20. doi:10.1186/s13395-018-0166-x

50. Long F, Wang Q, Yang D, et al. Targeting JMJD3 histone demethylase mediates cardiac fibrosis and cardiac function following myocardial infarction. *Biochem Biophys Res Commun*. 08 06 2020;528(4):671-677. doi:10.1016/j.bbrc.2020.05.115

51. Ohtani K, Zhao C, Dobreva G, et al. Jmjd3 controls mesodermal and cardiovascular differentiation of embryonic stem cells. *Circ Res*. Sep 2013;113(7):856-62. doi:10.1161/CIRCRESAHA.113.302035

52. Brack AS, Conboy MJ, Roy S, et al. Increased Wnt Signaling During Aging Alters Muscle Stem Cell Fate and Increases Fibrosis. *Science*. 2007;317(5839):807-810. doi:10.1126/science.1144090

53. Otto A, Schmidt C, Luke G, et al. Canonical Wnt signalling induces satellite-cell proliferation during adult skeletal muscle regeneration. *J Cell Sci*. Sep 2008;121(Pt 17):2939-50. doi:10.1242/jcs.026534

54. von Maltzahn J, Chang NC, Bentzinger CF, Rudnicki MA. Wnt signaling in myogenesis. *Trends Cell Biol*. Nov 2012;22(11):602-9. doi:10.1016/j.tcb.2012.07.008

55. Figeac N, Zammit PS. Coordinated action of Axin1 and Axin2 suppresses β-catenin to regulate muscle stem cell function. *Cell Signal*. Aug 2015;27(8):1652-65. doi:10.1016/j.cellsig.2015.03.025

56. Murphy MM, Keefe AC, Lawson JA, Flygare SD, Yandell M, Kardon G. Transiently active Wnt/β-catenin signaling is not required but must be silenced for stem cell function during muscle regeneration. *Stem Cell Reports*. Sep 09 2014;3(3):475-88. doi:10.1016/j.stemcr.2014.06.019

57. Zhang B, Wu X, Zhang X, et al. Human umbilical cord mesenchymal stem cell exosomes enhance angiogenesis through the Wnt4/β-catenin pathway. *Stem Cells Transl Med*. May 2015;4(5):513-22. doi:10.5966/sctm.2014-0267

58. Ring L, Neth P, Weber C, Steffens S, Faussner A. β-Catenin-dependent pathway activation by both promiscuous "canonical" WNT3a-, and specific "noncanonical" WNT4- and WNT5a-FZD receptor combinations with strong differences in LRP5 and LRP6 dependency. *Cell Signal*. Feb 2014;26(2):260-7. doi:10.1016/j.cellsig.2013.11.021

59. Später D, Hill TP, O'sullivan RJ, Gruber M, Conner DA, Hartmann C. Wnt9a signaling is required for joint integrity and regulation of Ihh during chondrogenesis. *Development*. Aug 2006;133(15):3039-49. doi:10.1242/dev.02471

60. Narita T, Sasaoka S, Udagawa K, et al. Wnt10a is involved in AER formation during chick limb development. *Dev Dyn*. Jun 2005;233(2):282-7. doi:10.1002/dvdy.20321

61. Winn RA, Marek L, Han SY, et al. Restoration of Wnt-7a expression reverses non-small cell lung cancer cellular transformation through frizzled-9-mediated growth inhibition and promotion of cell differentiation. *J Biol Chem*. May 2005;280(20):19625-34. doi:10.1074/jbc.M409392200

62. Cawthorn WP, Bree AJ, Yao Y, et al. Wnt6, Wnt10a and Wnt10b inhibit adipogenesis and stimulate osteoblastogenesis through a β-catenin-dependent mechanism. *Bone*. Feb 2012;50(2):477-89. doi:10.1016/j.bone.2011.08.010

63. Carron C, Pascal A, Djiane A, Boucaut JC, Shi DL, Umbhauer M. Frizzled receptor dimerization is sufficient to activate the Wnt/beta-catenin pathway. *J Cell Sci*. Jun 2003;116(Pt 12):2541-50. doi:10.1242/jcs.00451

64. Umbhauer M, Djiane A, Goisset C, et al. The C-terminal cytoplasmic Lys-thr-X-X-X-Trp motif in frizzled receptors mediates Wnt/beta-catenin signalling. *EMBO J*. Sep 2000;19(18):4944-54. doi:10.1093/emboj/19.18.4944

65. Karasawa T, Yokokura H, Kitajewski J, Lombroso PJ. Frizzled-9 is activated by Wnt-2 and functions in Wnt/beta -catenin signaling. *J Biol Chem*. Oct 2002;277(40):37479-86. doi:10.1074/jbc.M205658200

66. Lustig B, Jerchow B, Sachs M, et al. Negative feedback loop of Wnt signaling through upregulation of conductin/axin2 in colorectal and liver tumors. *Mol Cell Biol*. Feb 2002;22(4):1184-93. doi:10.1128/mcb.22.4.1184-1193.2002

67. Takata H, Terada K, Oka H, Sunada Y, Moriguchi T, Nohno T. Involvement of Wnt4 signaling during myogenic proliferation and differentiation of skeletal muscle. *Dev Dyn*. Oct 2007;236(10):2800-7. doi:10.1002/dvdy.21327

68. Eliazer S, Muncie JM, Christensen J, et al. Wnt4 from the Niche Controls the Mechano-Properties and Quiescent State of Muscle Stem Cells. *Cell Stem Cell*. 11 2019;25(5):654-665.e4. doi:10.1016/j.stem.2019.08.007

69. Bernardi H, Gay S, Fedon Y, Vernus B, Bonnieu A, Bacou F. Wnt4 activates the canonical β-catenin pathway and regulates negatively myostatin: functional implication in myogenesis. *Am J Physiol Cell Physiol*. May 2011;300(5):C1122-38. doi:10.1152/ajpcell.00214.2010

70. Tanaka S, Terada K, Nohno T. Canonical Wnt signaling is involved in switching from cell proliferation to myogenic differentiation of mouse myoblast cells. *J Mol Signal*. Oct 2011;6:12. doi:10.1186/1750-2187-6-12

CHAPTER IV:

Conclusions

In this study we investigated the effects of the age-related molecule Klotho on muscle during developmental myogenesis and Klotho's influence on the epigenetic state of muscle stem cells called satellite cells. The significant results of this work revealed a novel pathway through which Klotho decreased the histone 3 lysine 27 (H3K27) demethylase Jmjd3 and increased the gene-repressive dimethyl and trimethyl groups on H3K27 (H3K27me2/3) in myogenic cells. Additionally, we showed the accumulation of H3K27 methylation was associated with reduced expression of key Wnt pathway molecules known to affect satellite cell activation, proliferation and differentiation. Furthermore, we determined that elevated *klotho* expression increased the total number of Pax7+, reduced the proportion of Pax7+ cells also Jmjd3+ and increased repressive methyl groups on H3K27 in satellite cells during early postnatal development but not in young adult muscle. We showed that Klotho's effects on canonical Wnt signaling are mediated by a Jmjd3-dependent mechanism because similar to Klotho transgenic mice *Jmjd3* floxed mice had fewer β-catenin+/Pax7+ cells and lower expression of Wnt-family genes. However, unlike Klotho transgenic mice, *Jmjd3* floxed mice die within hours following birth which revealed Jmjd3 as an essential factor for developmental myogenesis. Together, these data show that Klotho modulates canonical Wnt signaling in a Jmjd3-dependent mechanism which influences early postnatal muscle development.

Klotho increased myoblast cell numbers but delayed muscle growth and myonuclear accretion during early postnatal development.

We previously showed that *klotho* expression was highest in muscle during early postnatal development but sharply declined in early adulthood, [1] which was confirmed in this study. Our data indicated that Klotho colocalized with Pax7+ cells, Pax7- nuclei and on the surface of myofibers during early postnatal development but not in muscle that was close to maturity. Those observations suggested Klotho contributed to early postnatal myogenesis by regulating muscle-related pathways in Pax7+ cells. To determine if sustained levels of *klotho* affected

normal developmental myogenesis, we utilized *klotho* transgenic (KL Tg+) mice that continuously express elevated levels of *klotho*, after endogenous *klotho* decreased. Our findings showed Klotho delayed myofiber growth at two-weeks following birth (P14), however Klotho did not affect fiber growth at P28 and accelerated growth at 3-months of age after endogenous *klotho* was downregulated in control muscles. Previous investigations indicated that a contributing factor of postnatal muscle growth was myonuclear accretion, or the addition of myonuclei to established myofibers. [2,3] In developing muscle, myonuclear accretion occurs when Pax7+ cells undergo terminal differentiation and fuse to previously formed muscle fibers. Our data showed KL Tg+ mice had less myonuclear accretion at P14 and more myonuclei at 3-months of age which supported the observation that Klotho delayed early postnatal developmental muscle growth and accelerated muscle hypertrophy in young adult muscle.

Another characteristic of maturing skeletal muscle is the positioning of Pax7+ cells beneath laminin, [3] a basement membrane protein that is part of the extracellular matrix of myofibers. Our data showed KL Tg+ mice had more Pax7+ cells above laminin outside of the myofiber, which indicated cell activation or delayed satellite cell quiescence. Together, our data strongly supported the interpretation that Klotho delayed developmental myogenesis by maintaining the activation of myoblasts that are resistant to terminal differentiation. Our analysis agreed with previously published work that showed Klotho promoted proliferative pathways in cultured myoblasts and decreased terminal differentiation factors in differentiated muscle cells *in vitro*. [1,4]

Elevated Klotho and reduced Jmjd3 have similar effects on the Wnt pathway but differ in perinatal survival.

Our data strongly indicated that a muscle-specific mutation in *Jmjd3* does not exactly mimic the effects of Klotho during early postnatal muscle development. Previous findings showed Klotho increased the lifespan in otherwise healthy mice [5,6] and elevated Klotho reduced the

pathological severity and extended the life of *mdx* mice, a model for Duchenne muscular dystrophy. [1,7] Others showed that Klotho deficiency reduced stem cells populations and impaired myogenesis [8-10] but *in vitro* ablation of *Jmjd3* in embryonic stem cells did not influence self-renewal capacity or pluripotency. [11] Although our recently published work showed Klotho affected the canonical Wnt pathway through a similar mechanism as Jmjd3, our unpublished work showed *Jmjd3* floxed mice died within hours following birth (P0) which suggested that the muscle-specific mutation in the *Jmjd3* gene diverged from KL Tg+ mice during development which had severe consequences on survival.

However, like KL Tg+ mice, *Jmjd3* floxed mice had increased H3K27me3 in Pax7+ cells which indicated that a significant proportion of the satellite cell population had elevated gene repression in the absence of Jmjd3 and agreed with our published work. Others showed demethylation of H3K27 is required for myogenesis [12] and ectopic expression of *Jmjd3* in pluripotent stem cells upregulated *Pax7* and overexpression of *Jmjd3* followed by overexpression of *Myod1* increased *Myog* expression. [13] Similarly, our *in vitro* data showed that *Jmjd3* overexpression increased *Myog* expression in differentiated muscle cells but did not change *Pax7* or *Myod1* expression, whereas the inhibition of *Jmjd3 in vitro* reduced *Myog* expression while *Pax7* and *Myod1* remained unchanged. Our *in vivo* data indicated that *Jmjd3* floxed whole quadriceps muscles had reduced expression of *Pax7*, *Myod1* and *Myog.* However, the number or Pax7+ cells and the number of myogenin+ cells were also reduced in *Jmjd3* floxed muscle, which may explain the divergence in *Pax7* and *Myod1* expression data between the *in vitro* and *in vivo* experiments because fewer cells could equivalate to lower whole muscle transcript levels. Together, our work and previous work from other groups strongly indicated that the effect of Klotho on stem cell self-renewal and myogenesis are directly related to the age-related susceptibility of myogenic cells to Klotho signaling. Furthermore, our data showed the

modulation of the Wnt pathway and downstream myogenesis are similar when Klotho is elevated or Jmjd3 is reduced.

Klotho modulates the epigenetic regulatory mechanisms required for myogenic differentiation and the activation of the canonical Wnt pathway.

Canonical Wnt signing drives myogenic differentiation. [14] Researchers have shown that Klotho modulated the canonical Wnt pathway, likely by binding extracellular Wnt ligands. [4,10,15] Additionally, the loss of *klotho* inhibits muscle regeneration, whereas elevated *klotho* boosted regeneration and fiber growth following muscle injury and in dystrophic muscle. [1,4,7,10,16,17] Although our data agree with previous reports that indicated Klotho modulates the canonical Wnt pathway, we identified a novel function of Klotho in the epigenetic regulation of Wnt genes. Elevated Klotho reduced the H3K27 demethylase Jmjd3 but had no effect on any other H3K27 regulatory genes we tested. Because no other H3K27-related genes were affected by Klotho, we attributed the elevated H3K27me2/3 marks at the promotor regions of Wnt genes *in vitro* and in Pax7+ cells *in vivo* to the inhibition of Jmjd3 by Klotho.

Our data showed Klotho treatment and Jmjd3 downregulation had similar but not additive effects on Wnt4, Wnt9a and Wnt10a which suggested that Klotho and Jmjd3 acted through similar mechanisms that affected the Wnt pathway. Furthermore, regardless of stage of development KL Tg+ mice had reduced canonical Wnt signaling in Pax7+ cells, as did P0 Jmjd3 floxed mice. Because the activation of the canonical Wnt pathway is required for muscle differentiation, and our published work showed Klotho delayed muscle growth and myonuclear accretion we speculated Klotho's effects on myogenesis were dependent on changes in Wnt signaling and Jmjd3.

Our data clearly showed that the Klotho-mediated reduction of Jmjd3 and the genetic inhibition of Jmjd3 act through similar pathways to inhibit β-catenin. First, Klotho increased H3K27me3, decreased Jmjd3 and inhibited active β-catenin in Pax7+ cells throughout early postnatal development. Second, myoblasts stimulated with Klotho *in vitro* had reduced *Jmjd3* gene expression and decreased Wnt-family gene expressed mediated by increased H3K27me2/3 at the promotor regions of Wnt-family genes known to activate the canonical Wnt pathway. Furthermore, neonatal Jmjd3 floxed muscles also had increased H3K27me3 and decreased activated β-catenin, although *klotho* expression was unchanged in P0 Jmjd3 floxed muscle (KL expression data not shown). Others showed increased *Jmjd3* expression *in vitro* upregulated the *Ctnnb1* gene that codes for β-catenin as well as increased the expression of β-catenin target genes. [18] Knockdown of *Jmjd3* in cancer cells blocked normal β-catenin activity and the activation of β-catenin target genes. [19] Additionally, gene activation mediated by β-catenin is associated with the recruitment of Jmjd3 to the promotor regions of at least two developmental genes [20] and others showed that Jmjd3 facilitated the recruitment of β-catenin to the Brachyury gene promotor, which is essential for embryonic stem cell differentiation. [11] Therefore, Jmjd3 likely regulates multiple steps in the canonical Wnt pathway including activation of genes coding for Wnt ligands and the *Ctnnb1* gene coding for a β-catenin, and Klotho's effects on canonical Wnt signaling are strongly associated with the negative regulatory effect of Klotho on Jmjd3.

Klotho and Jmjd3 may influence noncanonical Wnt signaling in the same or different pathways.

Although our data strongly indicate Klotho and Jmjd3 are operating in similar pathways affecting canonical Wnt activation, we cannot exclude the possibility that Klotho and Jmjd3 may influence the noncanonical, β-catenin-independent pathway. Noncanonical Wnt signaling influences cell proliferation, polarity, fate decisions and migration. [21] Some Wnt ligands, like Wnt1 and Wnt3a

have been identified as canonical Wnt ligands because of the receptor-ligand interactions and the downstream activation of β-catenin. [22] Alternativity, Wnt5a and Wnt11 are primarily associated with noncanonical Wnt signaling, [22] although one older study showed Wnt5a can bind to canonical Wnt receptors. [23] Additional research has indicated that both canonical and noncanonical Wnts can activate very early myogenic programming and some Wnts, like Wnt4 can activate both canonical and noncanonical signaling in muscle. [24-27] Others have shown that noncanonical Wnts are simultaneously expressed with canonical Wnts during development and suggested that noncanonical Wnts play a regulatory role in the Wnt/β-catenin pathway. [28] Therefore, we must consider the possibility that the inhibitory effects of Klotho and Jmjd3 on Wnt4 could affect the both β-catenin-dependent and β-catenin-independent pathways.

In conclusion, our work supports our hypothesis that Klotho influences the epigenetic regulation of muscle stem cells. Overexpression of Klotho during early postnatal muscle development delayed fiber growth and myonuclear accretion, increased the number of Pax7+ and MyoD+ myoblasts, decreased the colocalization of Jmjd3 in Pax7-expressing cells and increased the proportion of Pax7+ cells also H3K27me3+. Myogenic cells stimulation with Klotho expressed lower levels of Jmjd3 compared to controls and had more H3K27me2/3 associated with the promotor regions of *Wnt*-family genes known to activate or inhibit steps in the myogenic pathway. Manipulating Jmjd3 in myogenic cell cultures or genetically inhibiting *Jmjd3* in Pax7-expressing cells had similar effects on the Wnt pathway and on myogenesis, particularly in the downregulation of myogenin. Although our data strongly support the repressive effects of Klotho on Jmjd3 and both elevated Klotho and inhibited Jmjd3 repressed the canonical Wnt pathway, we were not able to investigate the effects of Jmjd3 on myogenesis at any time point beyond P0. While the certain neonatal lethality caused by a germline, muscle-specific mutation in Jmjd3 resulted in unfortunate limitations of the current project, the fact that a 50% reduction in muscle-

specific Jmjd3 caused certain perinatal death demonstrates the importance of further investigation of Jmjd3 in myogenesis.

References

1. Wehling-Henricks M, Li Z, Lindsey C, et al. Klotho gene silencing promotes pathology in the mdx mouse model of Duchenne muscular dystrophy. *Hum Mol Genet*. May 2016;25(12):2465-2482. doi:10.1093/hmg/ddw111

2. Bachman JF, Klose A, Liu W, et al. Prepubertal skeletal muscle growth requires Pax7-expressing satellite cell-derived myonuclear contribution. *Development*. 2018;145(20):dev167197. doi:10.1242/dev.167197

3. Gattazzo F, Laurent B, Relaix F, Rouard H, Didier N. Distinct Phases of Postnatal Skeletal Muscle Growth Govern the Progressive Establishment of Muscle Stem Cell Quiescence. *Stem Cell Reports*. 09 08 2020;15(3):597-611. doi:10.1016/j.stemcr.2020.07.011

4. Welc SS, Wehling-Henricks M, Kuro-O M, Thomas KA, Tidball JG. Modulation of Klotho expression in injured muscle perturbs Wnt signalling and influences the rate of muscle growth. *Exp Physiol*. Jan 2020;105(1):132-147. doi:10.1113/EP088142

5. Kuro-o M, Matsumura Y, Aizawa H, et al. Mutation of the mouse klotho gene leads to a syndrome resembling ageing. *Nature*. Nov 1997;390(6655):45-51. doi:10.1038/36285

6. Kurosu H, Yamamoto M, Clark JD, et al. Suppression of aging in mice by the hormone Klotho. *Science*. Sep 2005;309(5742):1829-33. doi:10.1126/science.1112766

7. Wehling-Henricks M, Welc SS, Samengo G, et al. Macrophages escape Klotho gene silencing in the mdx mouse model of Duchenne muscular dystrophy and promote muscle growth and increase satellite cell numbers through a Klotho-mediated pathway. *Hum Mol Genet*. Oct 2018;27(1):14-29. doi:10.1093/hmg/ddx380

8. Vadakke Madathil S, Coe LM, Casu C, Sitara D. Klotho deficiency disrupts hematopoietic stem cell development and erythropoiesis. *Am J Pathol*. Mar 2014;184(3):827-41. doi:10.1016/j.ajpath.2013.11.016

9. Fan J, Sun Z. The Anti-aging Gene Klotho Regulates Proliferation and Differentiation of Adipose-derived Stem Cells. *Stem Cells*. Feb 2016;34(6):1615-1625. doi:10.1002/stem.2305

10. Ahrens HE, Huettemeister J, Schmidt M, Kaether C, von Maltzahn J. Klotho expression is a prerequisite for proper muscle stem cell function and regeneration of skeletal muscle. *Skelet Muscle*. 07 2018;8(1):20. doi:10.1186/s13395-018-0166-x

11. Ohtani K, Zhao C, Dobreva G, et al. Jmjd3 controls mesodermal and cardiovascular differentiation of embryonic stem cells. *Circ Res*. Sep 2013;113(7):856-62. doi:10.1161/CIRCRESAHA.113.302035

12. Faralli H, Wang C, Nakka K, et al. UTX demethylase activity is required for satellite cell-mediated muscle regeneration. *J Clin Invest*. Apr 2016;126(4):1555-65. doi:10.1172/JCI83239

13. Akiyama T, Wakabayashi S, Soma A, et al. Epigenetic Manipulation Facilitates the Generation of Skeletal Muscle Cells from Pluripotent Stem Cells. *Stem Cells Int*. 2017;2017:7215010. doi:10.1155/2017/7215010

14. Brack AS, Conboy IM, Conboy MJ, Shen J, Rando TA. A temporal switch from notch to Wnt signaling in muscle stem cells is necessary for normal adult myogenesis. *Cell Stem Cell*. Jan 2008;2(1):50-9. doi:10.1016/j.stem.2007.10.006

15. Liu H, Fergusson MM, Castilho RM, et al. Augmented Wnt signaling in a mammalian model of accelerated aging. *Science*. Aug 2007;317(5839):803-6. doi:10.1126/science.1143578

16. Sahu A, Mamiya H, Shinde SN, et al. Age-related declines in α-Klotho drive progenitor cell mitochondrial dysfunction and impaired muscle regeneration. *Nat Commun*. 11 2018;9(1):4859. doi:10.1038/s41467-018-07253-3

17. Clemens Z, Sivakumar S, Pius A, et al. The biphasic and age-dependent impact of klotho on hallmarks of aging and skeletal muscle function. *Elife*. 04 20 2021;10doi:10.7554/eLife.61138

18. Akiyama T, Wakabayashi S, Soma A, et al. Transient ectopic expression of the histone demethylase JMJD3 accelerates the differentiation of human pluripotent stem cells. *Development*. Oct 2016;143(20):3674-3685. doi:10.1242/dev.139360

19. Pereira F, Barbáchano A, Silva J, et al. KDM6B/JMJD3 histone demethylase is induced by vitamin D and modulates its effects in colon cancer cells. *Hum Mol Genet*. Dec 2011;20(23):4655-65. doi:10.1093/hmg/ddr399

20. Dahle Ø, Kumar A, Kuehn MR. Nodal signaling recruits the histone demethylase Jmjd3 to counteract polycomb-mediated repression at target genes. *Sci Signal*. Jun 2010;3(127):ra48. doi:10.1126/scisignal.2000841

21. Gómez-Orte E, Sáenz-Narciso B, Moreno S, Cabello J. Multiple functions of the noncanonical Wnt pathway. *Trends Genet*. Sep 2013;29(9):545-53. doi:10.1016/j.tig.2013.06.003

22. Niehrs C. The complex world of WNT receptor signalling. *Nat Rev Mol Cell Biol*. Dec 2012;13(12):767-79. doi:10.1038/nrm3470

23. He X, Saint-Jeannet JP, Wang Y, Nathans J, Dawid I, Varmus H. A member of the Frizzled protein family mediating axis induction by Wnt-5A. *Science*. Mar 14 1997;275(5306):1652-4. doi:10.1126/science.275.5306.1652

24. Wagner J, Schmidt C, Nikowits W, Christ B. Compartmentalization of the somite and myogenesis in chick embryos are influenced by wnt expression. *Dev Biol*. Dec 01 2000;228(1):86-94. doi:10.1006/dbio.2000.9921

25. Otto A, Schmidt C, Patel K. Pax3 and Pax7 expression and regulation in the avian embryo. *Anat Embryol (Berl)*. Aug 2006;211(4):293-310. doi:10.1007/s00429-006-0083-3

26. Bernardi H, Gay S, Fedon Y, Vernus B, Bonnieu A, Bacou F. Wnt4 activates the canonical β-catenin pathway and regulates negatively myostatin: functional implication in myogenesis. *Am J Physiol Cell Physiol*. May 2011;300(5):C1122-38. doi:10.1152/ajpcell.00214.2010

27. Eliazer S, Muncie JM, Christensen J, et al. Wnt4 from the Niche Controls the Mechano-Properties and Quiescent State of Muscle Stem Cells. *Cell Stem Cell*. 11 2019;25(5):654-665.e4. doi:10.1016/j.stem.2019.08.007

28. Fan J, Wei Q, Liao J, et al. Noncanonical Wnt signaling plays an important role in modulating canonical Wnt-regulated stemness, proliferation and terminal differentiation of hepatic progenitors. *Oncotarget*. Apr 2017;8(16):27105-27119. doi:10.18632/oncotarget.15637